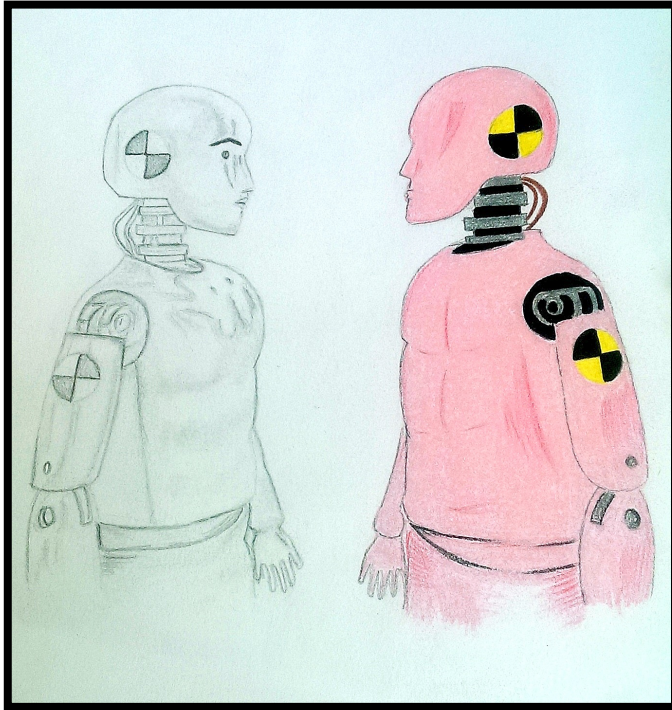




**CHALMERS**  
UNIVERSITY OF TECHNOLOGY

---



# **Evaluating biofidelity of Anthropometric Test Devices under the use of Pre-Pretensioners**

Evaluation of future Pre-Pretensioner system with respect to injury levels

*Master's thesis in the Programme of Automotive Engineering*

Pooja Umeshkumar, Alba Márquez Medina



MASTER'S THESIS IN PROGRAMME OF AUTOMOTIVE ENGINEERING

# Evaluating biofidelity of Anthropometric Test Devices under the use of Pre-Pretensioners

Evaluation of future Pre-Pretensioner system with respect to injury levels

Pooja Umeshkumar, Alba Márquez Medina

Department of Applied Mechanics  
Division of Vehicle Safety  
Injury prevention  
CHALMERS UNIVERSITY OF TECHNOLOGY  
Göteborg, Sweden 2015

Evaluating biofidelity of Anthropometric Test Devices under the use of Pre-Pretensioners

Pooja Umeshkumar, Alba Márquez Medina

© Pooja Umeshkumar, Alba Márquez Medina, 2015-01-01

Master's Thesis 2015:60

ISSN 1652-8557

Department of Applied Mechanics

Division of Vehicle Safety

Injury prevention

Chalmers University of Technology

SE-412 96 Göteborg

Sweden

Telephone: + 46 (0)31-772 1000

Cover:

Sketched and painted by the authors of this thesis.

Name of the printers / Department of Applied Mechanics

Göteborg, Sweden 2015-01-01



## Evaluating biofidelity of Anthropometric Test Devices under the use of Pre-Pretensioners

Evaluation of future Pre-Pretensioner system with respect to injury levels

Master's thesis in Master's programme of Automotive Engineering

Pooja Umeshkumar, Alba Márquez Medina

Department of Applied Mechanics

Division of Vehicle Safety

Injury prevention

Chalmers University of Technology

### Abstract

Pre-pretensioner (PPT) seatbelts are equipped with an electrical pretensioner that tightens the belt in safety critical situations and liberates some webbing if the driver is able to avoid the hazard. These PPT seatbelts introduce new loading scenarios, posing a requirement to evaluate the biofidelity of present-day Anthropometric Test Devices (ATDs). This study evaluates the biofidelity of ATDs of different sizes in four pre-defined positions under PPT seatbelt loading also considering the habituation effect. Data from 5<sup>th</sup> and 50<sup>th</sup> percentile females, and 95<sup>th</sup> percentile male volunteers and their corresponding ATDs- Hybrid III 5<sup>th</sup> and 95<sup>th</sup> percentile dummies, and a prototype BioRID 50 percentile female dummy were analyzed. Evaluation of the biofidelity was done by comparing the responses of volunteers and ATDs. Basic kinematics parameters were tracked with TEMA3.5-012 software and the seatbelt force, current and voltage signals were obtained from the transducer. Corridors were generated with the volunteer subjects' mean response  $\pm 1$  standard deviation. Hybrid III family does not reproduce human-like motion of the head-neck complex under PPT loading due to the stiffness of the neck and torso. The 50<sup>th</sup> percentile female BioRID dummy shows a reversed trend compared to the flexion-extension motion of the volunteers. Changes in stiffness and damping properties may lead to improvements in biofidelity of these dummies under low load conditions (PPT loading). In general, the small female volunteers are observed to have larger head-neck rotation amplitudes, which may contribute to higher whiplash risk in females. Large male volunteers show lower backset reduction and low T1 kinematics compared to other sizes of volunteers. Some volunteers exhibit limited range of head-neck motion compared to others, which may be a result of neck muscle tension.

Current studies about PPT seatbelts suggest that there is a scope to develop more powerful systems that may use higher forces to reposition the occupant before an impact. This study identifies injury assessment reference values for neck injuries and optimal force values for PPT development. Dynamic and static tests were conducted with H-III6C and the BioRID50F prototype. Two safe crash pulses, one with a maximum deceleration of 4g at 56ms and a delta V of 9km/h and another with a mean acceleration of 6g and a delta V of 28km/h were used in child and adult ATDs respectively. Neck injury assessment reference values ( $NIC_{protraction}$  and  $N_{IJ}$ ) were obtained from the dynamic tests and literature review. In static tests, neck injury criteria for higher seatbelt forces were obtained to compare them with the previous thresholds. Forces close to 600N might be critical in children when seated slightly leaning forward. Some test results were discarded due to technical limitations, hence for future testing it is recommended to use sensors and data acquisition systems according to the low loading scenario.

**Key words:** biofidelity, pre-pretensioners, ATDs, volunteers, corridor, kinematics, whiplash.

# Acknowledgements

We thank Anna Carlsson, Chalmers Industriteknik, who has patiently supported and guided us towards a better understanding of the field of biomechanics. Her constant guidance, constructive criticism and fruitful discussions have contributed to the development of this thesis work.

We thank our professor and examiner Mats Svensson, Chalmers University of Technology, for giving us this opportunity.

We are also grateful to Autoliv Research for accepting us as master thesis students and for provision of expertise, and technical support in the implementation of this work. We thank specially Dan Bråse for his help, constant support and dedication during this thesis. We are grateful to the rest of staff members at Autoliv Research, in particular Katarina Bohman for her valuable suggestions and ideas for the project.

We also thank the collaboration of Volvo Car Corporation in this thesis. We thank, in particular Annelie Ristoff and Bo Svanger. We would like to express our gratitude towards Jean Adrien Develet who devoted his time and guided us in the beginning of our project.

We also express our gratitude to all SAFER members for the nice work environment and all the master thesis students in the Vehicle Safety Division for the enriching cultural exchange. Ramiro García deserves a special thank you for all the nice moments during coffee breaks.

*Alba*

I give my sincere thanks and appreciation to my grandparents, parents and sister for always being there, for their continuous support and for being a source of love and strength in my life. My mom deserves special gratitude for always believing in me. Thank to Carlos, for his constant encouragement. I also thank my friends and classmates from the University of Oviedo for all the good memories during my engineering studies. Also, I would like to thank all my Erasmus friends who have made this experience in Sweden unforgettable. Thank you Pooja for being such an excellent thesis partner.

*Pooja*

I would like to thank my parents without whose never-failing encouragement and love I would not be what I am today. Thank you ma and pa for being my strength. I express my gratitude to all my mentors for always guiding me in the right path. Special thank you and love for being my constants – Ammu, Kane and Kappu. I would like to thank Riti; my best friend for listening to my stories and adventures every single day and not complaining. Also, thank you Gunddu for always being there and helping me keep my smile. And a big thank you to Alba for being the most amazing thesis partner.

# Contents

Abstract .....	I
Acknowledgements.....	II
Contents .....	III
Notations.....	VI
PART-I	
1 Introduction.....	1
1.1 Background.....	1
1.2 Pre-crash active seatbelt.....	1
1.3 Head restraint.....	3
1.4 Whiplash Associated Disorders .....	4
1.5 Gender and Size differences .....	6
2 Purpose.....	7
2.1 Limitations .....	7
3 Methodology.....	8
3.1 Previous study: data collection .....	8
3.2 Research subjects.....	9
3.2.1 Anthropometric Test Devices (ATDs) .....	9
3.2.2 Volunteers subjects .....	9
3.3 Test matrix (positions) .....	10
3.4 Data analysis.....	12
3.4.1 Parameters selection to study the biofidelity .....	12
3.4.2 Data processing.....	13
4 Results.....	15
4.1 Evaluation of biofidelity of ATDs.....	15
4.1.1 95 <sup>th</sup> percentile male (AM95) .....	15
4.1.2 50 <sup>th</sup> percentile female (AF50).....	22
4.1.3 5 <sup>th</sup> percentile female (AF05).....	30
4.2 Habituation effect in AM95 and AF50 .....	36
4.2.1 AM95.....	36
4.2.2 AF50 .....	36
4.3 Differences in kinematics of AM95, AM50, AF50 and AF05 .....	43
5 Discussions.....	49
5.1 Future work.....	54

6	Conclusion .....	55
PART-II		
7	Introduction .....	57
7.1	Background .....	57
7.2	Thorax .....	57
7.3	Neck .....	61
8	Purpose .....	63
9	Methodology .....	64
9.1	Research subjects .....	64
9.2	Dynamic tests .....	64
9.3	Static tests .....	64
9.4	Data Analysis .....	65
10	Results .....	66
10.1	Injury assessment reference values .....	66
10.2	Neck loading for different seatbelt forces .....	67
11	Discussions .....	68
11.1	Future work .....	69
12	Conclusion .....	70
13	References .....	71
14	Appendix .....	78
14.1	Initial test positions for all volunteer sizes .....	78
14.2	Locating the centre of T1 .....	80
14.3	Volunteers' corridor plots .....	84
14.3.1	95 <sup>th</sup> percentile male (AM95) .....	84
14.3.2	50 <sup>th</sup> percentile female (AF50) .....	88
14.3.3	5 <sup>th</sup> percentile female (AF05) .....	92
14.4	Tables corresponding to habituation effect .....	96
14.4.1	95 <sup>th</sup> percentile male (AM95) .....	96
14.4.2	50 <sup>th</sup> percentile female (AF50) .....	98
14.5	Tables corresponding to differences in kinematics of AM95, AM50, AF50 and AF05 .....	99
14.6	Differences in kinematics of Hybrid III 5 <sup>th</sup> percentile, BioRID50F, BioRID-II, THOR NT and Hybrid III 95 <sup>th</sup> percentile .....	101
14.7	Dynamic test setup .....	106
14.8	Static test setup .....	108
14.9	T1 x-acceleration and Head x-acceleration plots .....	108
14.9.1	Dynamic tests .....	108

14.9.2	Static tests .....	109
14.9.3	$F_x$ , $F_z$ and $MOC_y$ values from static tests .....	110

## Notations

GPD	Gross Domestic Product
ATD	Anthropometric Test Device
AEB	Autonomous Emergency Braking
PPT	Pre-Pretensioner
ESC	Electronic Stability Control
ECU	Electronic Control Unit
WAD	Whiplash Associated Disorders
PMHS	Post Mortem Human Surrogates
AF05	5 <sup>th</sup> Percentile Female (small female)
AF50	50 <sup>th</sup> Percentile Female (female of average size)
AM50	50 <sup>th</sup> Percentile Male (male of average size)
AM95	95 <sup>th</sup> Percentile Male (large male)
IIII	Hybrid III (A crash test dummy designed for high speed frontal impact tests)
AMVO	Anthropometry of Motor Vehicle Occupants
OC	Occipital Condyle
AM	Auditory Meatus
CFC	Channel Frequency Class
AIS	Abbreviated Injury Scale
AAAM	Association for the Advancement of Automotive Medicine
NIC	Neck Injury Criterion
NIJ	Normalized Neck Injury Criterion
IARV	Injury Assessment Reference Values

# PART - I





# 1 Introduction

## 1.1 Background

Approximately 1.24 million deaths occur every year on the world's roads and another 20 to 50 million suffer injuries as a consequence of traffic collisions. Road traffic accidents are the eighth leading cause of death worldwide and current tendencies suggest that in fifteen years road traffic accidents will become the fifth leading cause of death. Moreover, motor vehicle crashes are the leading cause of death for young people, aged 15-29 years. Road crashes cost USD \$ 518 billion globally and for each individual country, road traffic accidents cost from 1-2% of their annual GDP [1].

According to this, road traffic injury prevention must be included in a broad range of sectors, such as road infrastructure development, government policies, urban and environmental planning, the supply of hospital services and safer vehicles. Present day technological advancement in the automotive industry is supporting the development of active restraints. Pre-crash active seatbelts were developed with the goal of keeping occupants in a better position before the crash and optimizing the efficiency of passive safety restraints. The integrated safety offers the benefit of crash avoidance and reduction of crash severity [2].

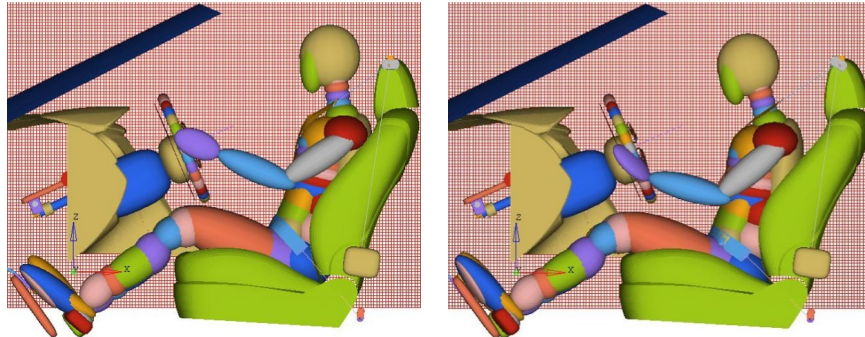
Injury mechanisms and drivers' behaviour are many times addressed in vehicle crash safety studies. Data obtained from crash tests with standard Anthropometric Test Devices (ATDs) in ideal seating postures is often assumed to be representative of a real road traffic accident. Nevertheless, age, gender and anthropometrics influence the drivers' posture. Moreover, in real life scenarios, the driver's posture can change before the collision because of body's inertial loading by Autonomous Emergency Braking (AEB) systems or crash avoidance maneuvers. According to a Japanese analysis of traffic accident data, around 60% of the drivers took crash avoidance maneuvers. The analysis also suggests that the injury degree is influenced by the pre-crash reaction. Consequently, restraint systems should consider posture changes and driver motion at the pre-crash phase [3].

## 1.2 Pre-crash active seatbelt

Pre-crash active seatbelts also known as pre-pretensioner seatbelts (PPT) use information available in active safety systems such as electronic stability control (ESC) system, cameras and/or radars to restrain the occupant in a pre-crash phase. Active seat belts have an electrical pretensioner that tightens the belt in safety critical situations and liberates some webbing if the driver is able to avoid the hazard. Motor torque is transmitted to seatbelt webbing via reduction gear and a clutch system. When the electronic control unit (ECU) detects an emergency situation, it supplies required current to the motor connected to the retractor. Seatbelt retractor withdraws the belt by producing tension in it.

Under a braking situation prior to an impact, the dummy in the crash test or the occupant in real life moves forward due to the deceleration causing a change in occupant posture that increases occupant injuries. Moreover, the distance between airbag and occupant is reduced. A direct impact of the airbag can produce head or neck injuries. Numerical simulations, considering that the brake was activated prior to

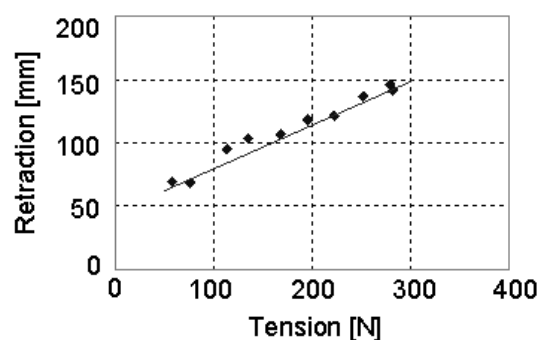
collision, show this change in body posture during the braking stage (*Figure 1.1*). Without pre-crash seatbelts, the body posture before the impact does not optimize the effectiveness of the occupant restraints.



*Figure 1.1: Posture change and movement due to braking at  $t=0s$  (left) and  $t=0.6s$  (right)[5]*

According to an observational study 10% of the drivers and 22 % of the passengers are poorly positioned for impact [8]. Motorized shoulder belt tensioning can reduce seatbelt slack and perform occupant repositioning in pre-crash situations if the impact is determined sufficiently early. Automotive manufactures have pre-crash active seatbelts in production or preproduction stages and are beginning to study the benefits of this system in vehicles.

Since pre-pretensioner seatbelt is operated by an electric motor a relation between the webbing retraction and the motor torque (seat belt webbing tension force) exists. The linear relation implies that the retraction length can be monitored based on the webbing tension of the pre-pretensioner seatbelt. (*Figure 1.2*)



*Figure 1.2: Retraction performance of motor retractor [6]*

Occupant forward movement is lowered with larger seatbelt retraction (*Figure 1.3*). Numerical simulations show that the more belt retraction, the lower the chest deceleration and displacement.

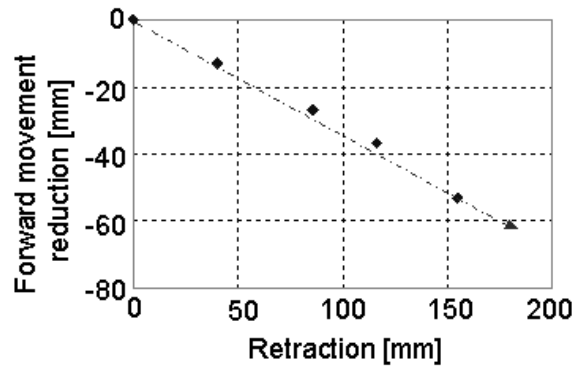


Figure 1.3: Forward chest movement reduction by seatbelt retraction [6]

Increasing seatbelt-webbing tension prior to a crash can reduce occupant injury risk. However, excessive retraction of seatbelt can produce an upward trend in chest deflection, owing to the initial deflection of the chest created by retraction. The upper limit of seat belt tension should be adjusted to occupants' tolerance limit [6]. Two main system design parameters for active seatbelts are the amount of tension or retraction to be activated and the timing at which the device activates the motor retractor. Occupant size has an important effect in retraction time. Larger car occupants require more time because of a slower retraction velocity [7].

### 1.3 Head restraint

In rear impacts, head restraint together with the seat is the main car interior component that contributes to internal load transfer. Head restraints prevent neck injuries in rear-end collisions hence head restraint positioning plays an important role in rear impacts. To protect the occupant, vehicle's head restraint should be tall enough such that the top of the restraint is above center of gravity of the head and close to the back of head. If the restraint is far from the head, less support is provided and head and torso will tend to move separately creating harmful forces on the neck. Height and backset are the basic geometric requirements, which are measured to produce a rating of good, acceptable, marginal or poor restraint. A procedure for Evaluating Motor Vehicle Head Restraints (RCAR 2008) states that a restraint to be rated as marginal should not be farther than 11 cm of the head and a good geometry implies a head restraint no farther than 7 cm behind it [4]. (Figure 1.4)

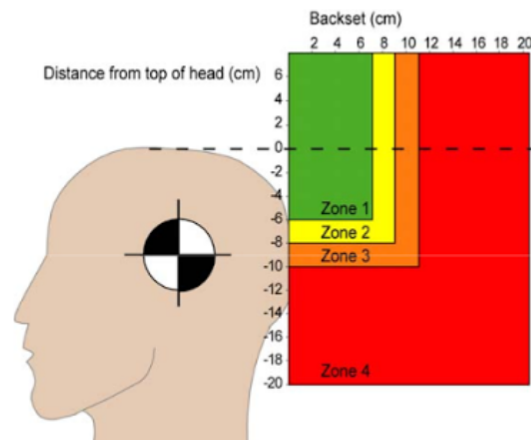


Figure 1.1: Diagram of geometric head restraint ratings [4]

## 1.4 Whiplash Associated Disorders

Whiplash Associated Disorders (WAD) can occur in impacts from all directions and at low velocity changes. The whiplash injury mechanism remains unclear but various factors may influence this neck injury. These factors are divided in three groups: seat factors, occupant factors and external factors [9]. Seat factors, for example are seat and head restraint geometry, occupant factors include gender or anthropometry while external factors are vehicle mass or stiffness [10]. Occupant factors have a direct link with the incidence and duration of WAD, consequently differences between world populations should be considered in order to optimize the performance of the restraints in vehicle design.

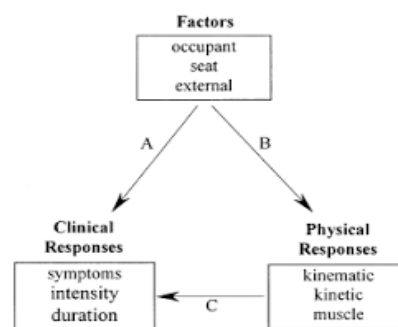


Figure 1.2: Relationships between potentially influential factors and physical and clinical responses [11].

According to statistics, rear impact induced whiplash injuries account for 50 % of the total injuries [12]. A study from Hanover, Germany states that males account for 58 % of the occupants involved in rear impacts, but in relation with neck injuries, females were involved 2.4 times more than males [9]. Another study of rear end collisions involving 1,147 occupants, presents that 52% of them had pain one year later and 62 % of females had remained symptoms two years after the impact [13]. The incidence of recovery is lower in female than male occupants [14]. Gender is an influential factor in rear impact induced injuries (Figure 1.6) [15]. Female upper body interaction with the head restraint and seatback varies in comparison with males due to difference in anthropometry and mass distribution.

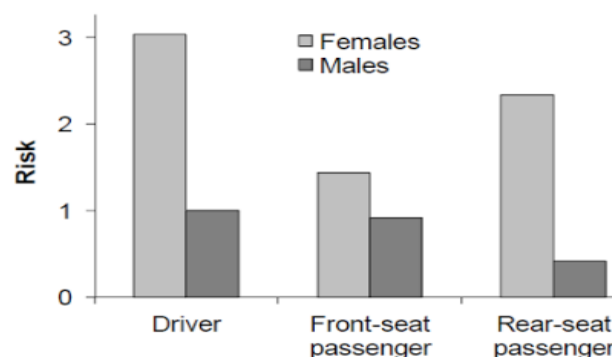
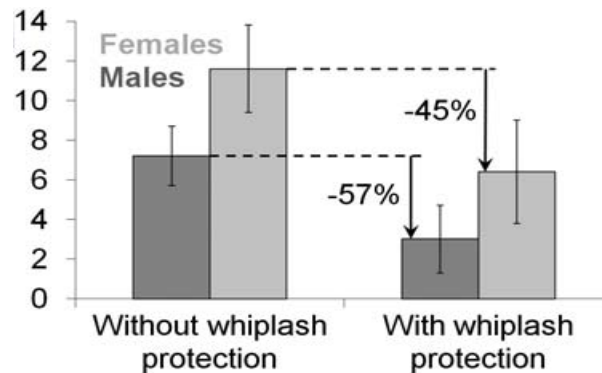


Figure 1.3: Risk of permanent whiplash injury in relation to male driver risk (normalized to 1) for different seating positions in rear impacts. Adopted from A. Carlsson [16]

According to insurance data, whiplash protections that already exist in the market have approximately 65 % higher effect for males than females [17]. Therefore, it is important to adapt the restraint systems by considering the female properties and the different anthropometric sizes of the population worldwide.



*Figure 1.4: Whiplash injury reduction for females and males including 95% CI.  
Adopted from Carlsson.A [16]*

Whiplash injuries are costly and the related socio-economic impact is approximately 10 billion euros annually in Europe [18]. They account for 70 % of all injuries leading to disability in Swedish automotive market [19].

According to statistics, between late 1960s and late 1990s, there was an increase in whiplash injuries [20]. Different factors have contributed to this raising level of WAD risk and number of injuries:

- Vehicle structure is stronger and stiffer [21].
- Seatbacks strength has increased to provide better retention in high-speed crashes [22]. This increase in strength has led to higher stiffness, which affects the interaction between the seatback and occupant. It can produce an increase in neck forces.
- Whiplash injury risk increases with the use of seatbelts [23]. The seatbelt restrains the torso in the rebound phase of the rear impact collision [24]. However, pretensioners, airbags and load limiters have the capability to reduce neck loads [77].
- Occupants in cars that are not equipped with advanced whiplash protection, have 50 % higher risk of suffering whiplash injuries compared with occupants in cars with whiplash protections systems installed [19].

## 1.5 Gender and Size differences

Head restraint positioning is not the only variable that affects the kinematics of human-neck complex. Other factors such as gender and occupant size are involved in biomechanics of rear-end collisions. Body mass and gender differences have significant physiological implications.

Higher whiplash injury risk may be explained due to anatomical differences between males and females. Males have smaller range of neck motion than females in extension [25]. Female occupants have greater S-curve motion. In rear-end collisions, they have greater head [26], segmental and facet joint motions than males [27]. In addition, the two cartilages on the juxtaposed subchondral bones of the articular pillars and the structure of the facet joints present differences between males and females specimens [28]. According to a study with post mortem human surrogates (PMHS) cervical spines, cartilage in male specimens was comparatively thicker [28]. There are also differences in anterior cruciate ligament strength (43% stronger in males) and stiffness (55% stiffer in males)[29].

There are anatomical differences in the location and size of neck muscles that may lead to differences in load distributions between male and female specimens. Female neck muscles have lower strength [30] and faster reaction (11%) than male neck muscles [31]. Moreover, they have smaller necks in relation to head size [32].

Gender difference is not the only variable that has an influence in vertebral size. Dimensions of C3-C7 vertebral bodies tend to increase with stature [33].

## 2 Purpose

Anthropometric test devices are mechanical surrogates of the humans, which are used in crash testing to determine effectiveness of restraint systems. These crash dummies are designed to be repeatable, reproducible, fulfill requirements of anthropometry and biofidelity and allow measurement of parameters that are related to injuries. On one hand, dummies should represent a human in terms of size, mass and mass distribution and on the other, it has to mimic human biomechanical response to an impact. Biofidelity is evaluated based on cadaver and volunteer studies. Since it is not possible to use human volunteers in crash tests that are conducted to replicate real accident scenarios, their replacement, ATDs, are required to be biofidelic.

New vehicle restraint systems such as pre-pretensioner seatbelts, introduce new loading scenarios, posing a requirement to evaluate the biofidelity of the current ATDs. Therefore, the aim of this study is to evaluate the biofidelity of crash dummies under pre-pretensioner seatbelts loading.

The results of this study can be used to improve the design of the current ATDs, contribute to the development of pre-pretensioner seatbelts in the automotive industry as well as reduce crash injuries worldwide in the future.

Research questions which are considered in this study:

- Evaluation of the kinematics and belt-occupant interaction between Hybrid III 5<sup>th</sup> percentile female dummy and AF05 volunteer subjects for different occupant positions.
- Evaluation of the kinematics and belt-occupant interaction between BioRID 50<sup>th</sup> percentile female dummy (BioRID50F) and AF50 volunteer subjects for different occupant positions.
- Evaluation of the kinematics and belt-occupant interaction between Hybrid III 95<sup>th</sup> percentile male dummy and AM95 volunteer subjects for different occupant positions.
- Evaluation of different volunteers' responses taking into account differences in gender and size.
- Evaluation of the differences between the first volunteer exposure and the second volunteer exposure under low loading scenario (habituation effect).

### 2.1 Limitations

- Unable to place HybridIII in some of the positions.
- Evaluation of PPT loading scenario in children, pregnant women, elderly or obese population. Only healthy and relatively young people were included in the study so the expected results are not representative of the whole population.
- Evaluation of subjective volunteers' impressions to the restraint system.
- Evaluation of different load cases.
- Evaluation of the PPT seatbelt under dynamic conditions.
- Evaluation of chest deflection under PPT loading.

## 3 Methodology

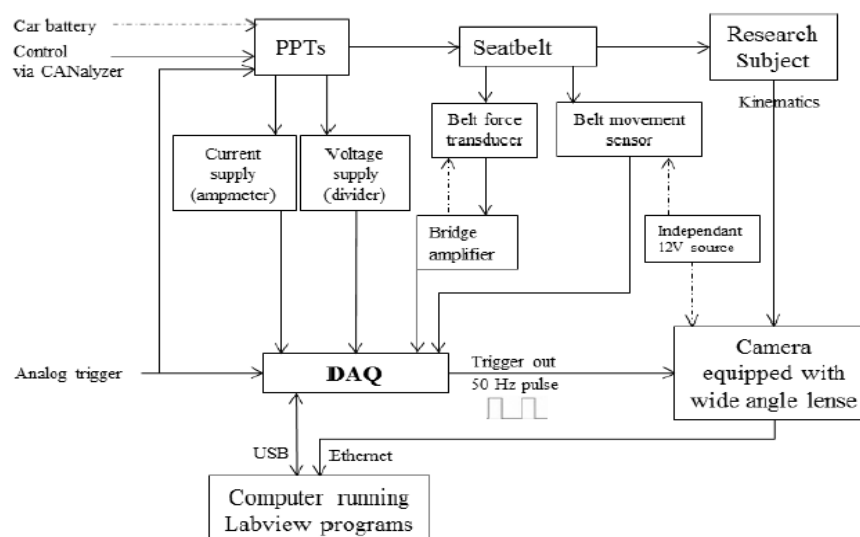
### 3.1 Previous study: data collection

Data collection to evaluate the biofidelity of ATDs under seatbelt pre-pretensioner loading was performed in a previous master thesis by Jean-Adrien Develet for Chalmers University of Technology (2013)[34].

Tests were conducted for ATDs and volunteers in a stationary environment after the regional ethical board in Göteborg approved them. The study was performed in a Volvo XC70 (MY2009) and car seats were set according to EuroNCAP 2011 testing protocol for neck injury protection. Coordinate systems were selected in agreement with SAE J211/ISO6487. Passenger vehicle for the experiment was equipped with a prototype unit including three pre-pretensioners, controller and power supply. Current and power supply data from the PPTs as well as tension in the seatbelt (acquired with a seatbelt transducer) were collected during the experiment. In addition, video cameras recorded the kinematics of research subjects ensuring anonymity of the volunteers (*Figure 3.1*). Skin landmarks were located on the research subjects with a goal of positioning important reference points for kinematics analysis during data processing.

Data from four different sizes of volunteers and their corresponding ATDs were collected in the preceding master thesis but the biofidelity evaluation was performed only for the 50th percentile male. Data that were already collected but not processed and analysed are the starting point of the present study.

In the previous study it was found that the BioRID-II reproduced the volunteer motion more aptly than the THOR-NT in front row positions. Also, the ATDs showed some limitations in reproducing the head-neck movement.



*Figure 3.1: Data acquisition system used in previous master thesis. Adopted from Adrien. J [34]*



## 3.2 Research subjects

Current restraint systems are primarily adapted for the 50<sup>th</sup> percentile male. However, occupant restraint system development should include anthropometric differences in the population worldwide to guarantee an optimal protection during vehicle accidents.

### 3.2.1 Anthropometric Test Devices (ATDs)

The Hybrid III 95<sup>th</sup> percentile (HIII AM95) was chosen to represent the 95<sup>th</sup> percentile male subjects and Hybrid III 5<sup>th</sup> percentile (HIII AF05) was chosen to represent the 5<sup>th</sup> percentile female subjects. These ATDs are designed for frontal loading. The thoracic spine of HIII is made of steel and does not allow bending [35]. The lack of bending in thoracic spine influences the motion of torso [36]. Moreover, chest properties of the dummy were adapted to non-belted situations, so the interaction with seatbelt restraint system is not very humanlike [37]. HIII does not have a movable clavicle and scapula, which affects the range of motion of the shoulder. The shoulder design is stiffer compared with human volunteers [36]. In low speed rear impacts, the HIII does not reproduce human's head motion, which is found to be more complex. The HIII is not very adequate for evaluating neck injuries in low speed rear-end collisions [38]. However, these dummies are the only ATDs, which are available to represent the small females and large males.

The BioRID50F, a 50<sup>th</sup> percentile female rear impact prototype crash test dummy, was chosen to represent the 50<sup>th</sup> percentile female subjects. This dummy was built by modifying the BioRID II dummy (50<sup>th</sup> percentile male dummy for low-speed rear-end impacts). The torso jacket was scaled and the length of the spine was reduced. In the female prototype, weaker springs substitute the neck muscles in comparison with the BioRID II. In addition, arms and legs were reduced and material was removed in order to have a more precise representation of the female body [39]. The prototype was built with the goal of testing the head restraint and seat back response in rear-end collisions.

### 3.2.2 Volunteers subjects

Volunteer subjects represent different size groups; 5<sup>th</sup> percentile female, 50<sup>th</sup> percentile female, 50<sup>th</sup> percentile male and 95<sup>th</sup> percentile male. Data from the 50<sup>th</sup> percentile male population was presented in the previous master thesis [34]. Selection criteria of volunteers were based on anthropometric specifications from the Anthropometry of Motor Vehicle Occupants (AMVO) study [40]. An interval of  $\pm 3\%$  on the stature values and  $\pm 13\%$  on the weight values was accepted in the recruitment of the volunteers [34].

Aging in both genders is associated with a decrease in neuromuscular performance due to the reduction in skeletal muscle mass and the loss of strength [41]. According to that, the age of the volunteers' subjects may influence the response of the volunteers so relatively young and only healthy subjects were part of the research study.

*Table 3.1: AF05 anthropometric specifications*

Subject	Weight [kg]	Stature [cm]
HIII AF05	49	150
Volunteer's recruitment criteria	47±6	151±4

*Table 3.2: AF50 anthropometric specifications*

Subject	Weight [kg]	Stature [cm]
BioRID50F AF50	62.3	161.8
Volunteer's recruitment criteria	62±8	162±5

*Table 3.3: AM50 anthropometric specifications*

Subject	Weight [kg]	Stature [cm]
BioRID-II AM50	78	178
THOR-NT AM50	78	180
Volunteer's recruitment criteria	77±8	175±5

*Table 3.4: AM95 anthropometric specifications*

Subject	Weight [kg]	Stature [cm]
HIII AM95	101	185
Volunteer's recruitment criteria	102.5±13.5	187±6

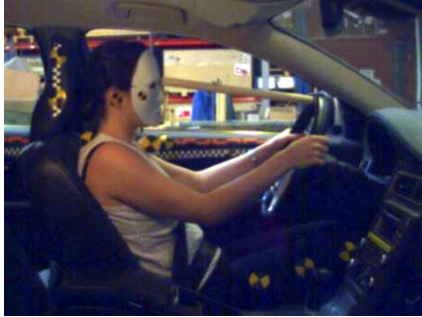

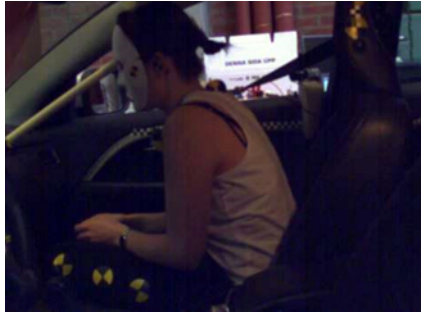
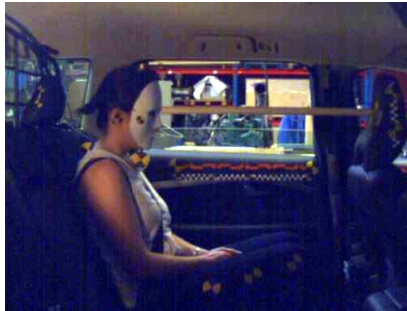
*Table 3.5: Number of volunteers in each research group*

Subject	Number of volunteers in the study
AF05	2
AF50	9
AM50	8
AM95	10

### 3.3 Test matrix (positions)

In the preceding master thesis, four testing positions were selected after a literature review to represent different driving scenarios [34]. Data in the four positions are available for evaluating the biofidelity. However, it was not possible to place the HIII 95<sup>th</sup> percentile in position 4 and the HIII 5<sup>th</sup> percentile in position 3 due to limitations in the range of motion of these ATDs. Consequently, there are no ATD data for these two cases to compare with the volunteer subjects' responses. Four different test scenarios were considered: a driver in a frequent driving posture, a driver in a leaning forward posture, a front passenger leaning forward and a rear occupant in a common posture which marginally exceeds the backset recommendations. In order to maintain the same positions in subsequent tests a support rod was used. All positions are described with more details and their explanations are accompanied with screenshots from the video analysis software (TEMA3.5-012) for a better understanding (*Table 3.5*).

Table 3.6: Test matrix with description of positions. Adapted from Adrien.J [34]

Position	Description	Picture
1. Real life normal driving	Person in driver seat with hands placed on the steering wheel. Normal driving position according to “the dynamic assessment of car seat for neck injury protection testing protocol (EuroNCAP 2011)”	
2. Attempting to increase the visibility at intersections	Person in driver seat, leaning forward with hands on steering wheel trying to increase the visibility at intersections	
3. Searching for the glove box	Forward passenger with hands on the lap, head position replicating the action of searching the glove box.	
4. Talking to the forward occupants	Occupant in the rear seat, hands on lap, head replicating the action of an occupant leaning forward to talk to the front row occupants	

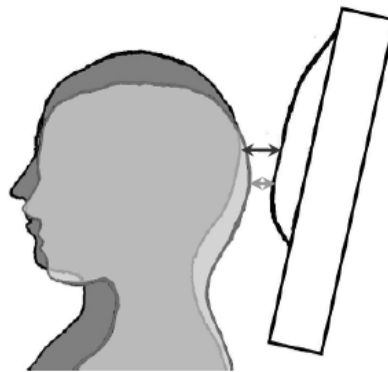
### 3.4 Data analysis

#### 3.4.1 Parameters selection to study the biofidelity

Evaluation of biofidelity was done by comparing the responses of volunteers and ATDs. Basic kinematics parameters were chosen to describe their motion. To obtain comparable results with the previous thesis work and have consistency in the analysis of the data the same two-link approach was used for the analysis of head-neck kinematics. Lower and upper pivots were located at the T1 and Auditory Meatus (AM) respectively.

Seating position of the research subjects, in relation to car head restraint was described by the backset (the horizontal gap between the back of the head and the front surface of the head restraint). Increased backset has been found to have a negative impact in neck symptom duration [42].

Backset depends on several factors. Initial head restraint distance may depend on seating position. In comparison with the occupant in the front passenger seat, the backset increases for male (37 mm) and female (26 mm) drivers with hands on the steering wheel. Increased kyphosis in the thoracic spine is the cause of this postural change depending on the seating position [43]. There is also a difference in the initial backset based on the gender; it is shorter for females compared to males (*Figure 3.2*). One possible explanation is that females have shorter stature and shorter arms (50-70 mm) than males [44].



*Figure 3.2: Different initial backset of a female (light grey) and a male (dark grey) volunteer. Adopted from Carlsson.A [16]*

The motion of T1 was described by T1 x-displacement, T1 x-velocity, T1 z-displacement and T1 angular rotation. T1 kinematics allows tracking the torso motion along the axis. The T1 position in volunteer's subjects and ATDs was calculated based on two skin landmarks (Clavicle Target and T1 Target) (*Appendix 14.2*).

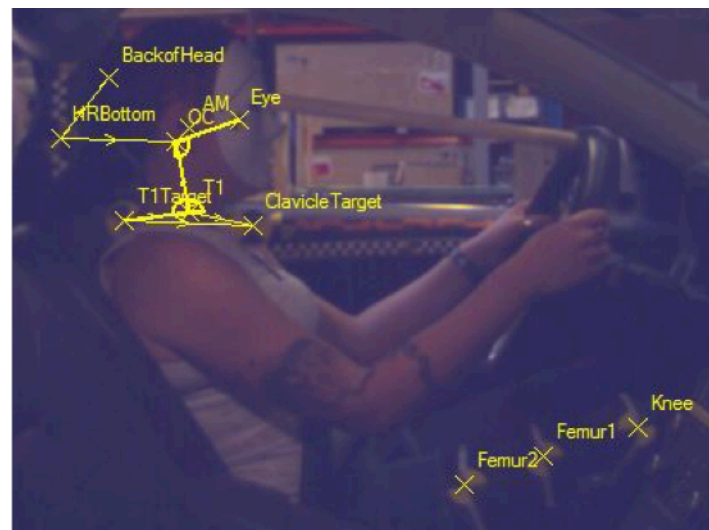
Neck and head motions are important in whiplash mitigation research. Therefore, neck and head rotations were described in order to study if ATDs provide a sufficiently biofidelic response of the flexion and extension motion of the volunteers neck.

Seatbelt force is the cause of the motion. It is influenced by different mechanical properties of the ATDs and the muscular tension of the volunteers during the experiment. A drop in the seatbelt force may be explained by the state of the battery.

### 3.4.2 Data processing

Videos of the volunteers and ATDs were taken during the test. A number of target points were marked on the subjects in order to be able to track these points on TEMA3.5-012. Two landmarks, one called T1 Target and the other Clavicle Target were marked to identify position of T1 (*Appendix 13.2*). The occipital condyle (OC) was drawn with a marker that was identified by palpating during the experiment. The other targets were Auditory Meatus (AM), eye, knee, femur and the back of head. The back of head was taken to be a point on the back of the head that makes the first contact with head restraint. Targets were also placed on the door of car to serve as markings for scaling. A target was placed on the centre of the head restraint and offset was accounted during the analysis.

The video recorded during the test was imported into TEMA3.5-012. A template, specifying the camera parameters, scaling factors and offsets to the reference plane was created. Each position had a different set of offsets and hence, one template for each position was created. The corresponding camera views were imported into these templates. Targets, distances and angles were tracked on TEMA3.5-012 (*Figure 3.3*).



*Figure 3.3: TEMA3.5-012 screenshot with targets, distances and angles*

T1 Angle is the angle between the T1 Target and T1. It gives a picture of motion of T1 in the sagittal plane. Neck angle is the angle between T1 and OC. It indicates the motion of neck with respect to T1 in sagittal plane. Head angle is the angle between the lines connecting the OC-Eye and OC-T1. It represents the movement of the head also in the sagittal plane. It is a clear representative of flexion or extension motion (*Figure 3.4*).

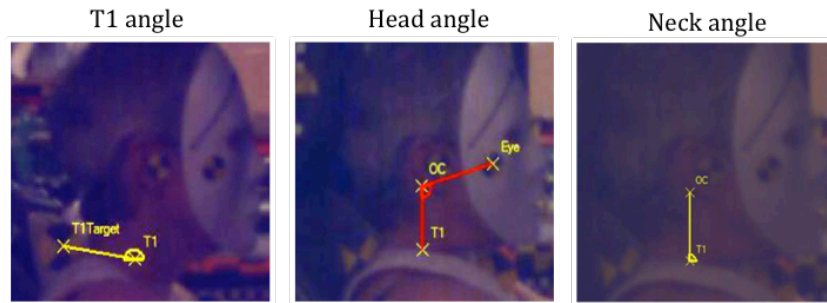


Figure 3.4: Screenshot from TEMA3.5-012 showing the different angles

A timetable was created with angles, distances and targets varying with time and was exported as a text file.

After tracking the kinematics with TEMA3.5-012, seatbelt force, current consumption and voltage data were imported to MATLAB along with the kinematics parameters for each test. Force and voltage signals were filtered with a Channel Frequency Class (CFC) filter of 30. Data was synchronized at the moment when the current supply started and the signals were cut at 1.5 s. An offset correction was made for the seatbelt force signal. Moreover, a sign correction was implemented for position 3 data to match the coordinate system (SAE J211/ISO6487), since the videos for the front passenger seat were filmed from a different side (*Table 3.5*).

Corridors were created with the volunteer subjects' mean response  $\pm 1$  standard deviation. However, corridors were not generated for 5<sup>th</sup> percentile female volunteers due to their limited number. Comparison between ATDs and volunteer responses was done to evaluate the biofidelity of dummies under PPT loading. Different kinematics responses for all research subjects were examined according to peak occurrences, amplitude and asymptote values for each subjects' data.

All the volunteer data could not be processed during analysis due to some issues like missing camera frames, extremely low or no current values.

## 4 Results

### 4.1 Evaluation of biofidelity of ATDs

#### 4.1.1 95<sup>th</sup> percentile male (AM95)

**Seatbelt force characteristics:** The seatbelt force response can be described in three stages; increase in force until 1<sup>st</sup> peak is reached, followed by a drop and then the 2<sup>nd</sup> peak, which is followed by a nearly constant force.

In the 1<sup>st</sup> stage, force increases continuously as the webbing is being retracted; there is a reduction in the initial belt slack until 1<sup>st</sup> peak is attained. In the 2<sup>nd</sup> stage, the occupants move at a constant T1 x-velocity, hence there is a drop in seatbelt force. The instance that the torso makes a contact with the seat, seatbelt force starts to increase again. After reaching the 2<sup>nd</sup> peak, power supply to the pre-pretensioner ends resulting in a decrease in force level. Subsequently, the pre-pretensioner maintains a constant force level.

In *position 1*, (*Figure 4.1*) it is observed that HIII reaches the 1<sup>st</sup> peak quicker than the volunteers (0.19s and 0.29s respectively). The initial slope of HIII is steeper than the slope of the volunteers. The ATD asymptote is between the volunteer subjects' mean and the inferior boundary of the corridor. However, the second peak occurs at the same instance (0.5s).

In *position 2*, (*Figure 4.2*) the dummy and the volunteers reach the first and the second peaks at the same time (0.2s and 0.49s respectively) and the seatbelt force values matches approximately. The initial slope is similar for both of them and the most significant difference can be appreciated in the seatbelt force drop that the HIII experiments after the first peak while volunteers do not experience this decline in the force value.

In *position 3*, (*Figure 4.3*) it can be observed that ATD reaches the first peak faster (0.16s) in comparison with the volunteers (0.28s). The initial slope of the HIII is steeper than the volunteers' one. After the first peak, force value decreases for the dummy, however the volunteers do not show this behavior. The second peak occurs at the same time (0.5s) and reaches a similar force level. The HIII asymptote exceeds the volunteers mean force by 20 N.

The results are summarized in *Tables 4.1-2*.

*Table 4.1: Peak occurrence and seatbelt force for 1<sup>st</sup> peak in positions 1,2,3,4*

Subject	Peak occurrence (s)				Force level (N)			
	1	2	3	4	1	2	3	4
AM95	0.29	0.2	0.28	/	245	174	195	/
HIII AM95	0.19	0.2	0.16	/	250	188	210	/

Table 4.2: Peak occurrence and seatbelt force for 2<sup>nd</sup> peak in positions 1,2,3,4

Subject	Peak occurrence (s)				Force level (N)			
	1	2	3	4	1	2	3	4
AM95	0.5	0.49	0.5	/	229	213	226	/
HIII AM95	0.5	0.49	0.5	/	207	212	232	/

**Backset:** In position 1, (Figure 4.1) backset reduction is not significant in volunteers and HIII. The peak amplitude and peak occurrence are not evident as there is no reduction in backset values. However, there is a difference in the initial backset for the volunteers (24mm) compared to HIII (33mm).

In position 2, (Figure 4.2) HIII and volunteers have similar initial backsets (230mm and 220mm respectively). Backset reduction is faster for HIII (0.36s) in comparison with volunteers (0.45s). Nonetheless, volunteers have greater backset amplitude (120mm) than the HIII (83mm).

In position 3, (Figure 4.3) the initial backset of HIII is greater (295mm) than the volunteer subjects mean (260mm). The peak occurs at the same instance (~ 0.4s). It is observed that both of them attain a similar asymptote value (~210mm).

The results are summarized in Table 4.3

Table 4.3: Amplitude, peak occurrence and asymptote of backset for positions 1,2,3,4

Subject	Amplitude (mm)				Peak occurrence (s)				Asymptote (mm)			
	1	2	3	4	1	2	3	4	1	2	3	4
AM95	/	120	48	/	/	0.45	0.45	/	23	100	209	/
HIII AM95	11	83	74	/	0.24	0.36	0.4	/	28	160	211	/

**T1 x-displacement and T1 x-velocity:** In position 1, (Figure 4.1) the HIII follows the same trend as volunteers in T1 x-displacement and T1x-velocity plots. There is a difference of 5mm in T1 x-displacement asymptotes of ATD and volunteers mean. It is seen that HIII responses are closer to the superior boundary of the volunteers' corridor.

In position 2, (Figure 4.2) the same trend is observed between the dummy and volunteers. The asymptote of T1 x-displacement is greater for volunteers (93mm) in comparison to HIII (58mm). T1 x-displacement of the dummy is closer to the superior boundary of the corridor. Also, T1 x-velocities have similar peak values (320mm/s for the volunteers and 344mm/s for the HIII) and HIII response is close to volunteers mean response.

In position 3, (Figure 4.3) HIII practically overlap the volunteer subjects mean responses. Both have similar peak values at same instances as well as close asymptote values.



The results are summarized in *Tables 4.4-5*

*Table 4.4: Amplitude, peak occurrence and asymptote of T1-x displacement for positions 1,2,3,4*

Subject	Amplitude (mm)				Peak occurrence (s)				Asymptote (mm)			
	1	2	3	4	1	2	3	4	1	2	3	4
AM95	13	93	49	/	0.25	0.48	0.4	/	10	93	49	/
HIII AM95	6	60	53	/	0.22	0.5	0.46	/	5	58	53	/

*Table 4.5: Amplitude, peak occurrence and asymptote of T1-x velocity for positions 1,2,3,4*

Subject	Amplitude (mm/s)				Peak occurrence (s)				Asymptote (mm/s)			
	1	2	3	4	1	2	3	4	1	2	3	4
AM95	115	320	245	/	0.16	0.2	0.17	/	2	2	1	/
HIII AM95	100	344	230	/	0.15	0.22	0.18	/	0	1	2	/

**Head and neck complex:** In *position 1*, (*Figure 4.1*) the amplitudes of neck and head rotations of volunteers and HIII are very close. It can be seen that HIII and volunteer mean overlap each other in head rotation, indicating that the dummy reproduces human head motion approximately. Neck angle however, shows that the HIII follows the superior boundary of the corridor. Asymptotes for the neck rotation have a difference of 4deg.

In *position 2*, (*Figure 4.2*) the volunteers experience a flexion followed by an extension while the dummies do not show any head motion. The HIII does not reproduce the neck motion of the volunteer subjects although they have the same amplitude values (~7deg). The neck of the HIII reproduces an extension motion instead of the flexion-extension motion shown by the volunteers.

In *position 3*, (*Figure 4.3*) the responses are similar to position 2. The dummy does not reproduce any head motion. The dummy also reproduces an extension motion of the neck instead of the flexion-extension motion as seen in the volunteers.

The results are summarized in *Table 4.6*

*Table 4.6: Amplitude of head and neck rotations*

Subject	Head rotation (deg)				Neck rotation (deg)			
	1	2	3	4	1	2	3	4
AM95	2	6	6	/	4	8	8	/
HIII AM95	4	1	1	/	3	7	7	/

***T1 z-displacement:*** In *all positions*, T1-z displacement shows that the trend followed by HIII and volunteer mean is similar. However, the HIII is close to the superior boundary of the volunteer corridor. These displacements do not bring any remarkable information since the amplitude is around only 5mm in all cases.

The results are summarized in *Table 4.7*

*Table 4.7: Amplitude of T1-z displacement for position 1,2,3,4*

Subject	T1- z displacement (mm)			
	1	2	3	4
AM95	2	1	8	/
HIII	4	5	1	/

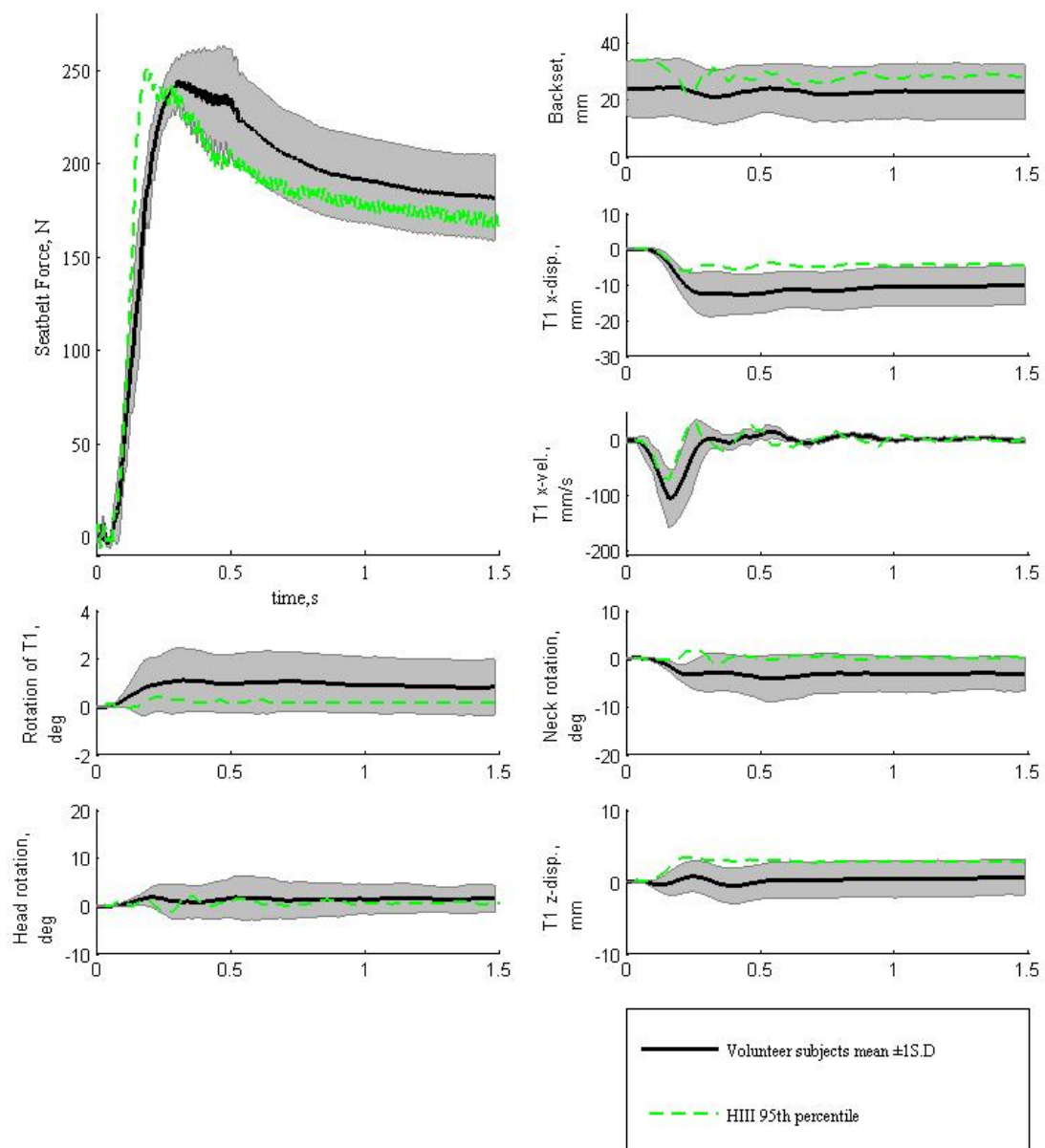


Figure 4.1: Corridors for the evaluation of AM95 ATDs in position 1

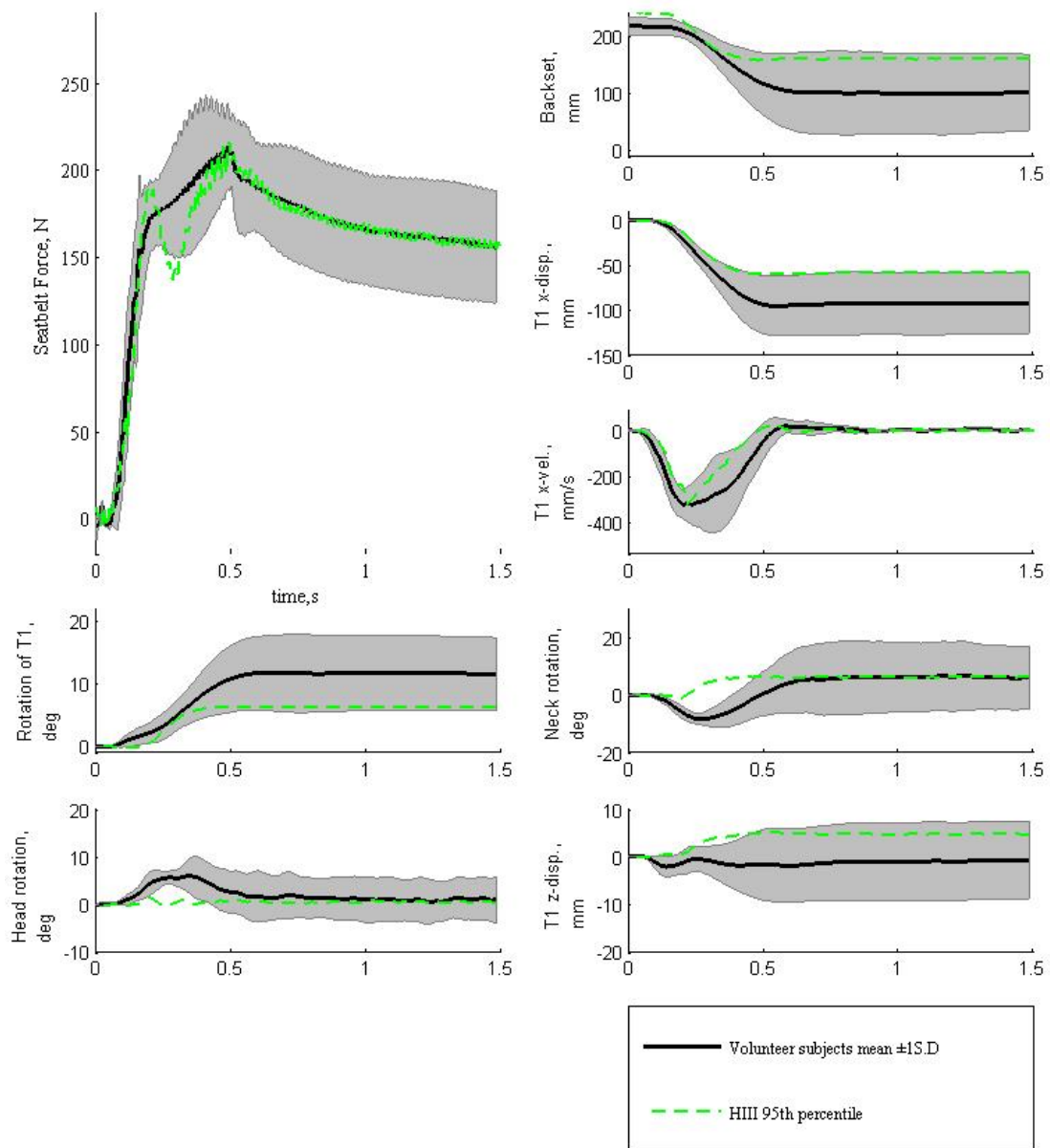


Figure 4.2: Corridors for the evaluation of AM95 ATDs in position 2

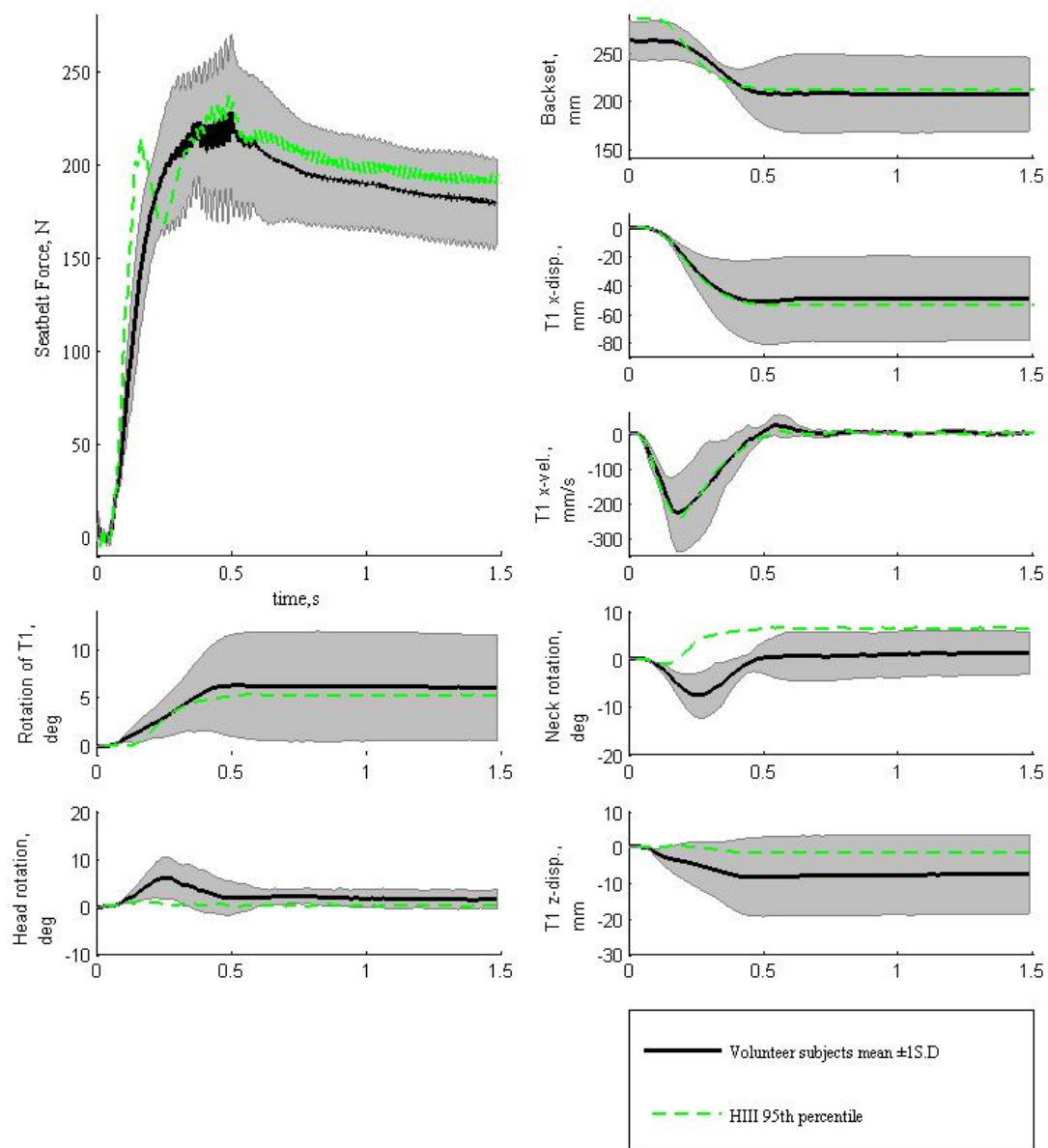


Figure 4.3: Corridors for the evaluation of AM95 ATDs in position 3

### 4.1.2 50<sup>th</sup> percentile female (AF50)

**Seatbelt force characteristics:** In *position 1*, (*Figure 4.4*) the initial slope of the BioRID50F is steeper and has a faster response (0.22s) compared to the volunteers (0.27s). The same trend is also observed in the second peak. ATD reaches the second peak before the volunteers' mean response (0.45 s and 0.5 s respectively). Force levels in BioRID50F are always higher than the volunteers' force levels. In the first part of the response, BioRID50F follows the upper boundary of the volunteers' corridor but in the later phases it has higher asymptote force value (40N). It can be observed that the female volunteers experience a drop in force level between the first and second peak that is reproduced by the dummy.

In *position 2*, (*Figure 4.5*) the first peak is attained at the same instance (0.2s) however they having varying force values (BioRID50F=220N, Volunteers=150N). Also, both reach the second peak at approximately the same time (0.52s) exhibiting differences in force values (BioRID50F=270N, Volunteers=222N). Asymptote value is greater for BioRID50F than for the volunteers (70N). At 0.8s an oscillation in the BioRID50F force can be observed due to a minor rebound.

In *position 3*, (*Figure 4.6*) the peak occurrences were synchronized for the BioRID50F and the volunteers (1<sup>st</sup> peak ~0.22s, 2<sup>nd</sup> peak ~0.51s) although the ATD showed higher peak values. The force value of the dummy was closer to the upper limit of the volunteers' corridor. After the second peak, some oscillations can be noticed for both of them.

In *position 4*, (*Figure 4.7*) BioRID50F reproduces the volunteers' response. The initial slope is the same for the ATD and the volunteers. The peaks occurred synchronously (1<sup>st</sup> peak ~0.22s, 2<sup>nd</sup> peak ~0.5s) although the BioRID50F has lower force values. The BioRID50F response is closer to the lower boundary of the corridor until the second peak and then is closer to the volunteers' mean response.

The results are summarized in *Tables 4.8-9*

*Table 4. 8: Peak occurrence and seatbelt force for 1<sup>st</sup> peak in positions 1,2,3,4*

Subject	Peak occurrence (s)				Force level (N)			
	1	2	3	4	1	2	3	4
AF50	0.22	0.22	0.21	0.22	250	150	102	244
BioRID50F	0.27	0.19	0.22	0.22	275	220	157	215

*Table 4.9: Peak occurrence and seatbelt force for 2<sup>nd</sup> peak in positions 1,2,3,4*

Subject	Peak occurrence (s)				Force level (N)			
	1	2	3	4	1	2	3	4
AF50	0.5	0.51	0.51	0.47	246	222	166	240
BioRID50F	0.45	0.53	0.51	0.48	270	270	195	210

**Backset:** In *position 1*, (Figure 4.4) the backset remains nearly constant in volunteers (~24mm). However, the BioRID50F has a greater initial backset (42mm) and it shows significant backset reduction (peak=0.34s). After the peak, ATD response matches the female volunteers' asymptote value (24mm).

In *position 2*, (Figure 4.5) the BioRID50F and the volunteers' mean have the same initial backset (200mm). They exhibit a backset reduction, although the BioRID50F reaches a comparatively low peak value (20mm) faster (0.42s) than the volunteers. After that they reach the same asymptote value (74mm).

In *position 3*, (Figure 4.6) the BioRID50F and the volunteers have the same initial backset (400mm) and they reach nearly the same peak value (~100mm, 0.6s). Subsequently, the BioRID50F shows an increment in backset value, as a result the final asymptote value is 65mm higher.

In *position 4*, (Figure 4.7) initial backset is higher for the ATD (~ 25mm) and it has a steeper and faster decline until it attains the peak value (50mm, 0.4s). However, after the peak BioRID50F shows an increment in the backset. Its asymptote value is 20mm higher than the volunteers.

The results are summarized in Table 4.10

Table 4.10: Amplitude, peak occurrence and asymptote of backset for positions 1,2,3,4

Subject	Amplitude (mm)				Peak occurrence (s)				Asymptote (mm)			
	1	2	3	4	1	2	3	4	1	2	3	4
AF50	/	120	325	40	/	0.58	0.6	0.6	24	74	95	68
BioRID50F	40	180	300	80	0.34	0.42	0.6	0.4	24	74	160	88

**T1 x-displacement and T1 x-velocity:** In *position 1*, (Figure 4.4) the BioRID50F follows nearly the same trend as the volunteers in both displacement and velocity. However, the peak value of BioRID50F's displacement is 4mm lower and velocity is 50mm/s lower.

In *position 2*, (Figure 4.5) although the ATD and volunteers attain peak displacement at the same instance (~0.5s), the BioRID50F has lower amplitude (90mm) than volunteers (110mm). In case of velocity, the BioRID50F has a greater peak value (602mm/s) and at a shorter time period (0.18s) compared to the volunteers (402 mm/s, 0.22s).

In *position 3*, (Figure 4.6) BioRID50F's T1 x-displacement has lower amplitude (160mm) in comparison with the volunteers (240mm). After the peak, the difference in displacement is nearly constant. T1 x-velocity of the dummy is closer to the upper boundary of the volunteers' corridor but it reaches the peak value faster (BioRID50F at 0.28s, volunteers at 0.38s).

In *position 4*, (Figure 4.7) BioRID50F's T1 x-displacement is closer to the lower boundary of the corridor and its initial slope is steeper. Although there is a difference

of 8 mm in the peak value, this distance is halved in the asymptote's value. The BioRID50F and the volunteers reach the peak velocity value at the same time ( $\sim 0.13$ s) however; ATD peak value is greater (373mm/s) than the volunteers' (180mm/s).

The results are summarized in *Tables 4.11-12*

*Table 4.11: Amplitude, peak occurrence and asymptote of T1-x displacement for positions 1,2,3,4*

Subject	Amplitude (mm)				Peak occurrence (s)				Asymptote (mm)			
	1	2	3	4	1	2	3	4	1	2	3	4
AF50	16	110	240	30	0.38	0.5	0.56	0.45	17	120	245	30
BioRID50F	20	90	160	38	0.34	0.46	0.54	0.3	17	78	145	34

*Table 4.12: Amplitude, peak occurrence and asymptote of T1-x velocity for positions 1,2,3,4*

Subject	Amplitude (mm/s)				Peak occurrence (s)				Asymptote (mm/s)			
	1	2	3	4	1	2	3	4	1	2	3	4
AF50	130	402	840	180	0.16	0.22	0.38	0.12	3	5	5	4
BioRID50F	181	602	700	373	0.14	0.18	0.28	0.14	4	5	5	5

**Head and neck complex:** In *position 1*, (*Figure 4.4*) BioRID50F does not reproduce the volunteers' head and neck motion. The female volunteers experience a small flexion while the BioRID50F experiences an initial extension followed by flexion.

In *position 2*, (*Figure 4.5*) the ATD reproduces a dual-motion. However, it shows an extension followed by a flexion while the volunteers show a flexion followed by an extension.

In *position 3*, (*Figure 4.6*) ATD and volunteers follow the same motion as in position 2.

In *position 4*, (*Figure 4.7*) the volunteers show a small flexion-extension motion while the BioRID50F experiences a larger extension-flexion motion.

The results are summarized in *Table 4.13*

*Table 4.13: Amplitude of head and neck rotations*

Subject	Head rotation (deg)				Neck rotation (deg)			
	1	2	3	4	1	2	3	4
AF50	6	10	9	6	8	15	13	6
BioRID50F	3	35	8	16	7.2	35	49	16



***T1 z-displacement:*** In *all positions*, the amplitude of T1 z-displacement is lower than 15 mm. The displacement values are small and not very significant. In position 2 and 4, it is observed that the BioRID50F values are close to the upper boundary of the volunteers' corridor.

The results are summarized in *Tables 4.14*

*Table 4.14: Amplitude of T1-z displacement for position 1,2,3,4*

Subject	T1- z displacement (mm)			
	1	2	3	4
AF50	6	5	14	4
BioRID50F	4	15	8	6

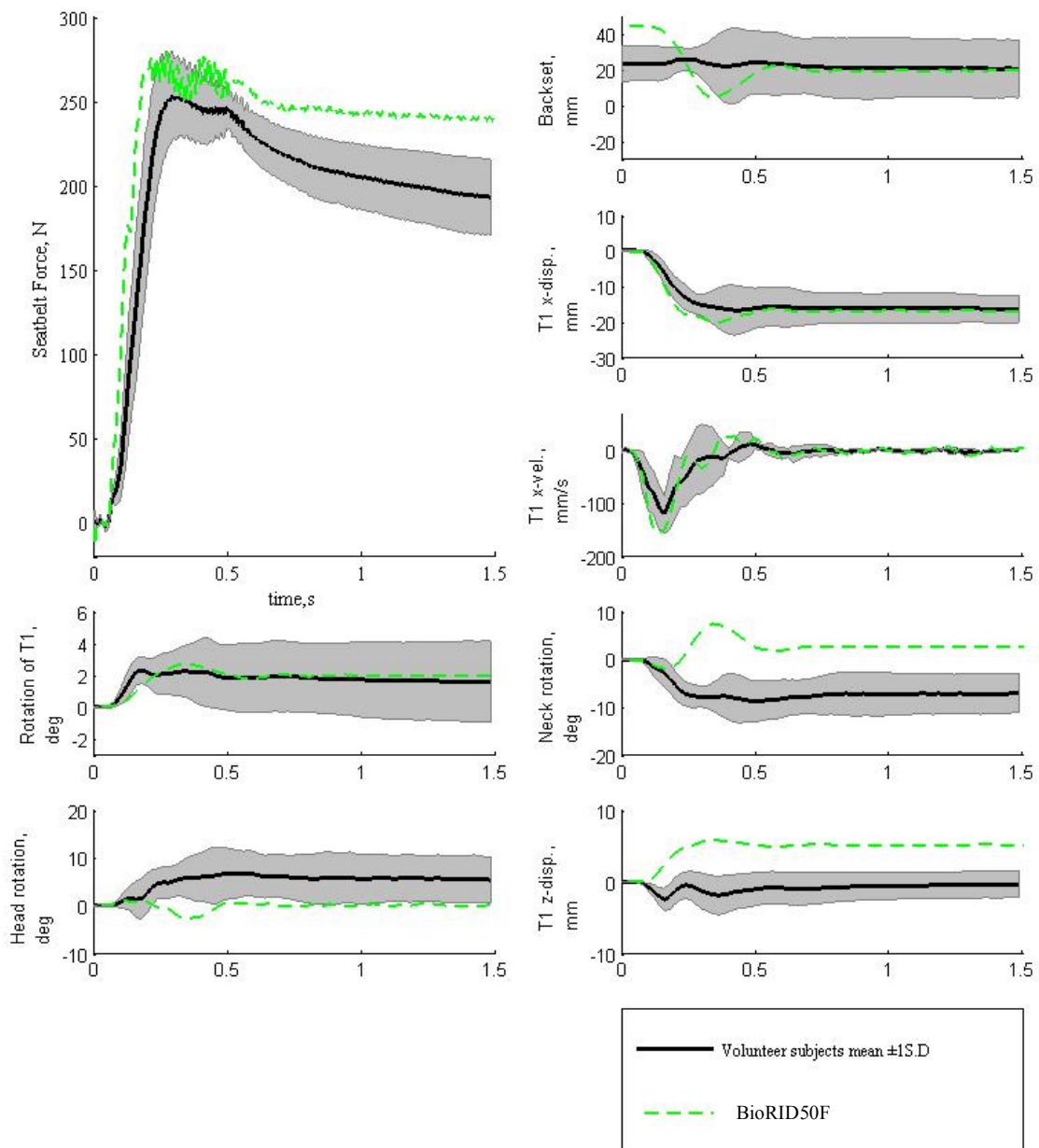


Figure 4.4: Corridors for the evaluation of AF50 ATD position 1

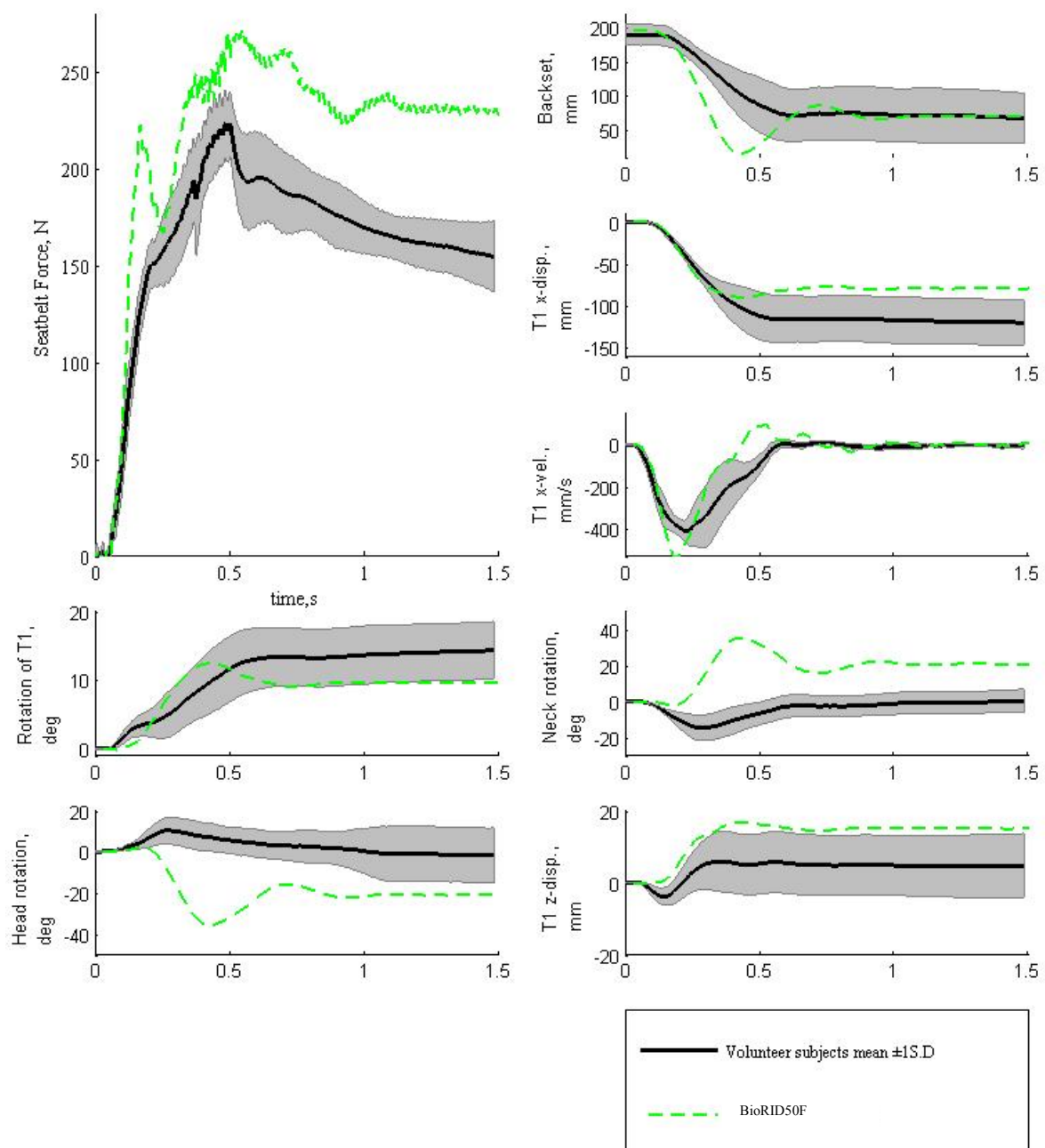


Figure 4.5: Corridors for the evaluation of AF50 ATD position 2

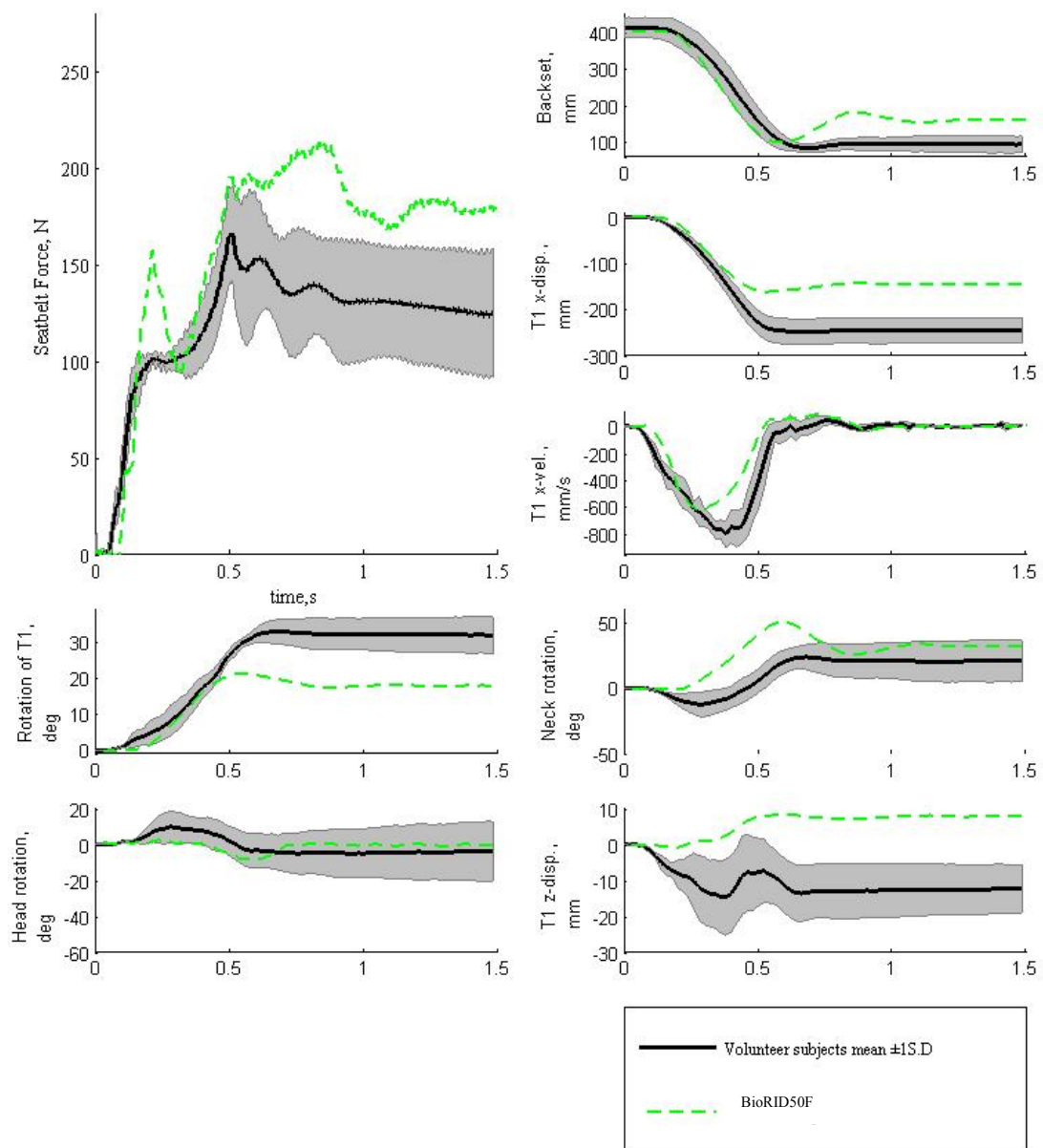


Figure 4.6: Corridors for the evaluation of AF50 ATD position 3

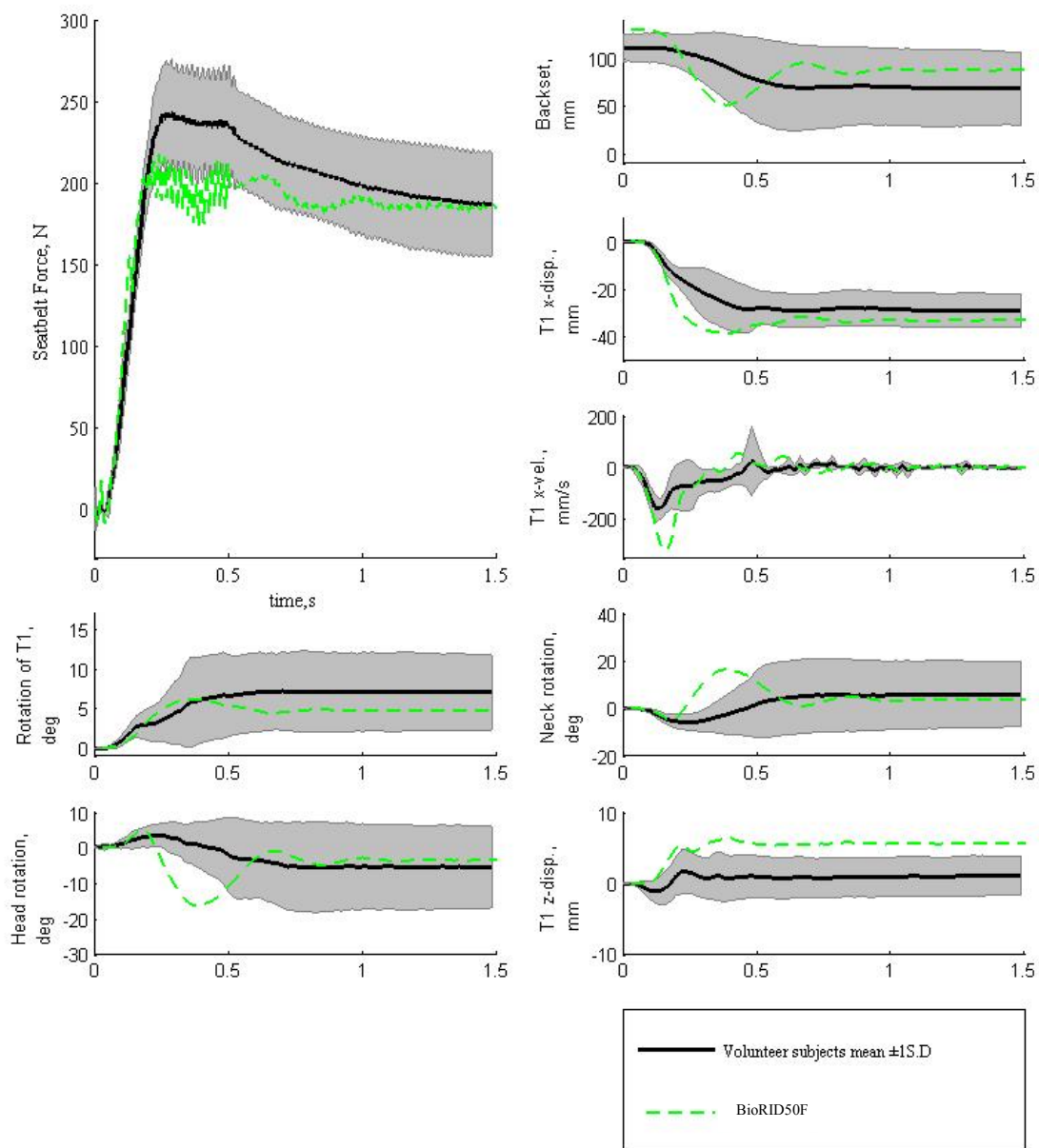


Figure 4.7: Corridors for the evaluation of AF50 ATD position 4

### 4.1.3 5<sup>th</sup> percentile female (AF05)

**Seat belt force characteristics:** In *position 1*, (Figure 4.8) it is seen that volunteer 1 follows the same trend as HIII, 1<sup>st</sup> peak occurs at 0.3sec for 1<sup>st</sup> volunteer and at 0.32s for the dummy. At the peak, values of force level differ by 35N. The 3<sup>rd</sup> volunteer however, shows a different trend. The 1<sup>st</sup> peak is observed at 0.22s followed by a drop in force level before attaining the 2<sup>nd</sup> peak. The difference in asymptote between the HIII and volunteer 1 is 30N while that between volunteer 3 and the dummy is 15N.

In *position 2*, (Figure 4.9) volunteers and the dummy responses overlap until the 1<sup>st</sup> peak is reached. Peak occurrences in volunteers and HIII are very close (0.22, 0.26 and 0.23 respectively). However, the asymptote of the HIII is 200N while that of the volunteers is 150N.

In *position 4*, (Figure 4.10) volunteers and the dummy follow the same trend with similar peak force values (257N, 225N, 250N respectively). The 2<sup>nd</sup> peak however is observed to occur earlier in the dummy than volunteers. The asymptotes of HIII and volunteer 1 overlap each other while volunteer three has a lower value.

The results are summarized in Tables 4.15-16

Table 4.15: Occurrence and seatbelt force for 1st peak in positions 1,2,3,4

Subject	Peak occurrence (s)				Force level (N)			
	1	2	3	4	1	2	3	4
AF05 01	0.30	0.22	/	0.28	245	167	/	257
AF05 03	0.22	0.26	/	0.27	110	181	/	225
HIII AF05	0.32	0.23	/	0.27	210	181	/	250

Table 4.16: Occurrence and seatbelt force for 2nd peak in positions 1,2,3,4

Subject	Peak occurrence (s)				Force level (N)			
	1	2	3	4	1	2	3	4
AF05 01	0.54	0.5	/	0.5	240	222	/	271
AF05 03	0.5	0.5	/	0.5	185	230	/	220
HIII AF05	/	0.53	/	0.4	/	244	/	249

**Backset:** In *position 1*, (Figure 4.8) backset reduction for the dummy lies between the two volunteers. Volunteer 1 and HIII show similar trend of backset reduction (peak at ~0.35s). The peak amplitude and peak occurrence are not evident in volunteer 3. There is also a difference in initial backset value for the volunteers (25mm and 60mm) compared to the HIII (40mm).

In *position 2*, (Figure 4.9) HIII and volunteers have a similar initial backset (110 mm, 120 mm respectively). The backset reduction is faster for the HIII and volunteer 1 in comparison with volunteer 3. HII reproduces the motion of volunteer 1 as their responses overlap each other. Volunteer 3 does not show a peak but has a gradual decrease in backset value. All three cases end with similar asymptote values.

In *position 4*, (Figure 4.10) the initial backsets of all three cases vary by approximately 20mm. However, they follow the same pattern. The HIII shows a faster backset reduction compared to the volunteers (HIII=0.28s, volunteer1=0.34s, volunteer3=0.42s). The backset reduction is evident in all three cases.

The results are summarized in Table 4.17

Table 4.17: Amplitude, peak occurrence and asymptote of backset for positions 1,2,3,4

Subject	Amplitude (mm)				Peak occurrence (s)				Asymptote (mm)			
	1	2	3	4	1	2	3	4	1	2	3	4
AF05 01	23	73	/	60	0.34	0.52	/	0.34	4.2	37	/	106
AF05 03	/	66	/	50	/	/	/	0.42	46	46	/	85
HIIIAF05	20	81	/	53	0.35	0.4	/	0.28	17.5	42	/	65

**T1 x-displacement and T1 x-velocity:** In *position 1*, (Figure 4.8) HIII follows the same trend as volunteer 1 in T1 x-displacement. However, volunteer 3 shows a rebound after the 1<sup>st</sup> peak. The asymptotes of T1 x- displacement also vary in all cases. (~10mm from each other). In T1 x-velocity volunteers exhibit similar responses until the 1<sup>st</sup> peak (~0.16s, ~200mm/s) after which volunteer 3 experiences a small rebound. The dummy has smaller amplitude and a slower response.

In *position 2*, (Figure 4.9) the volunteers and HIII follow similar trends in T1 x-velocity and T1 x-displacement. However, HIII has lower amplitude in T1 x-displacement (~15mm) and shows a slower T1 x-velocity response (~0.08s later).

In *position 4*, (Figure 4.10) HIII and volunteers follow a similar trend in T1 x-displacement. The volunteers have higher asymptote values than the HIII. The T1 x-velocities of all three cases are similar; particularly HIII and volunteer 3 overlap each other. Volunteer 1 has a greater peak T1 x-velocity compared to volunteer 1 and HIII (~50mm/s greater).

The results are summarized in Tables 4.18-19

Table 4.18: Amplitude, peak occurrence and asymptote of T1-x displacement for positions 1,2,3,4

Subject	Amplitude (mm)				Peak occurrence (s)				Asymptote (mm)			
	1	2	3	4	1	2	3	4	1	2	3	4
AF05 01	35	80	/	69	0.26	0.48	/	0.3	35	79	/	69
AF05 03	27	72	/	45	0.24	0.28	/	0.35	27	72	/	45
HIII AF05	16	59	/	32	0.34	0.42	/	0.3	16	58	/	32

Table 4.19: Amplitude, peak occurrence and asymptote of T1-x velocity for positions 1,2,3,4

Subject	Amplitude (mm/s)				Peak occurrence (s)				Asymptote (mm/s)			
	1	2	3	4	1	2	3	4	1	2	3	4
AF05 01	226	400	/	356	0.16	0.18	/	0.14	4	7	/	4
AF05 03	300	367	/	300	0.16	0.16	/	0.16	4	12	/	2
HIII AF05	124	328	/	316	0.24	0.24	/	0.16	0	3	/	8

**Head and neck complex:** In position 1, (Figure 4.8) amplitudes of neck and head rotations of volunteers and HIII show a large difference. The head rotation in volunteers has larger amplitude (10 and 18deg) while the dummy has a slight head movement (1.5deg). The volunteer neck shows a clear flexion followed by an extension while the dummy fails to show any motion. A similar trend is observed in head rotation also.

In position 2, (Figure 4.9) same trend as position 1 is observed, dummy does not reproduce the flexion-extension motion of the volunteers.

In position 4, (Figure 4.10) the dummy does not reproduce the head or the neck motion similar to the volunteers. Extension-flexion is observed in the dummy whereas the volunteers exhibit flexion-extension.

The results are summarized in Table 4.20

Table 4.20: Amplitude of head and neck rotations

Subject	Head rotation (deg)				Neck rotation (deg)			
	1	2	3	4	1	2	3	4
AF05 01	10	11	/	7	13	16	/	15
AF05 03	18	25	/	7	18	23	/	10
HIII AF05	1.5	3	/	11	1.6	10	/	12

**T1 z-displacement:** In all positions, the T1 z-displacement has amplitude less than 8mm for volunteers and the dummy indicating that displacement is not significant. The results are summarized in Tables 4.4-5

Table 4.21: Amplitude of T1 z-displacement for position 1,2,3,4

Subject	T1 z-displacement (mm)			
	1	2	3	4
AF05 01	3	6	/	5
AF05 03	4.5	7	/	3
HIII AF05	4	8	/	7



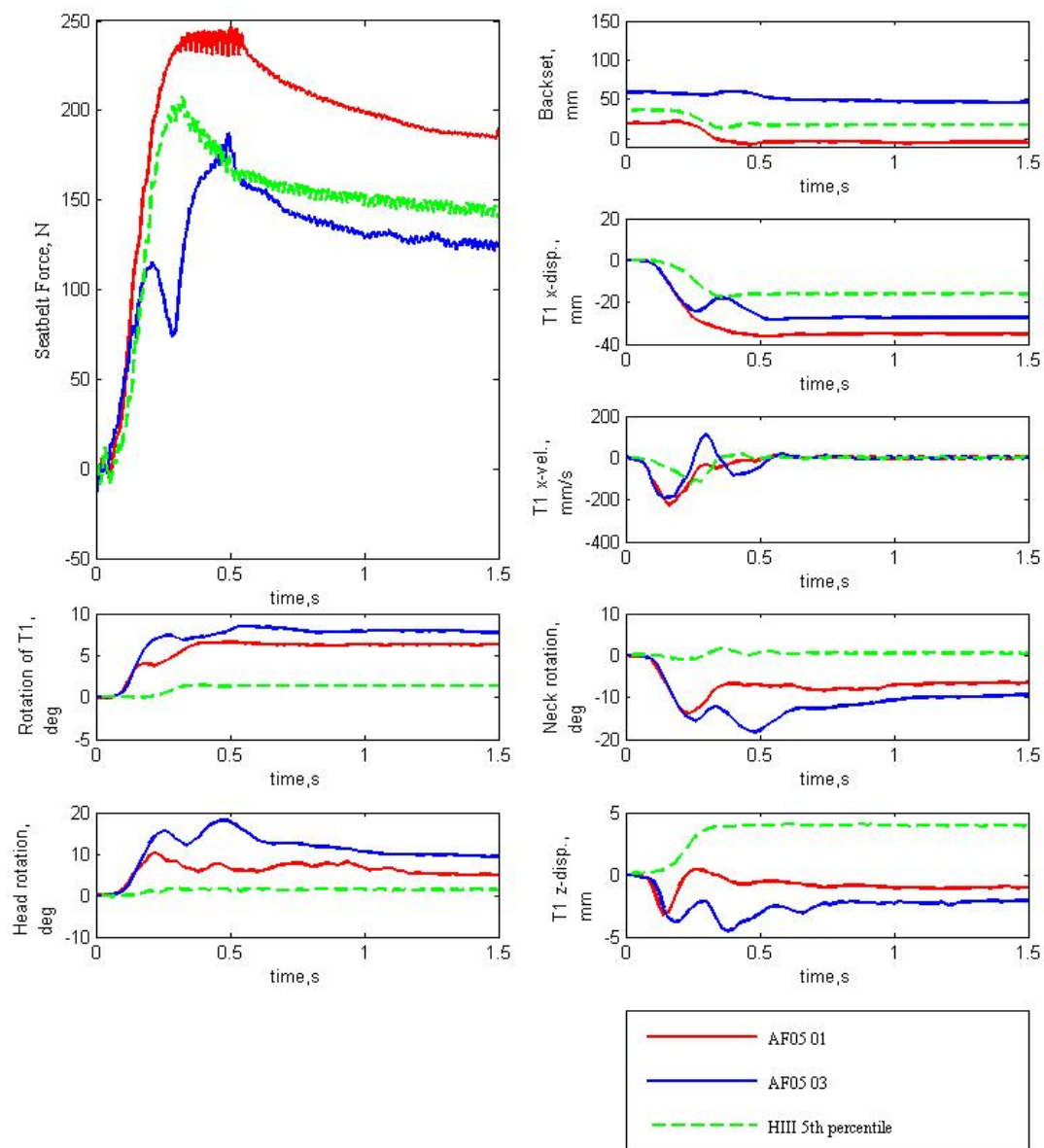


Figure 4.8: Evaluation of AF05 for position 1

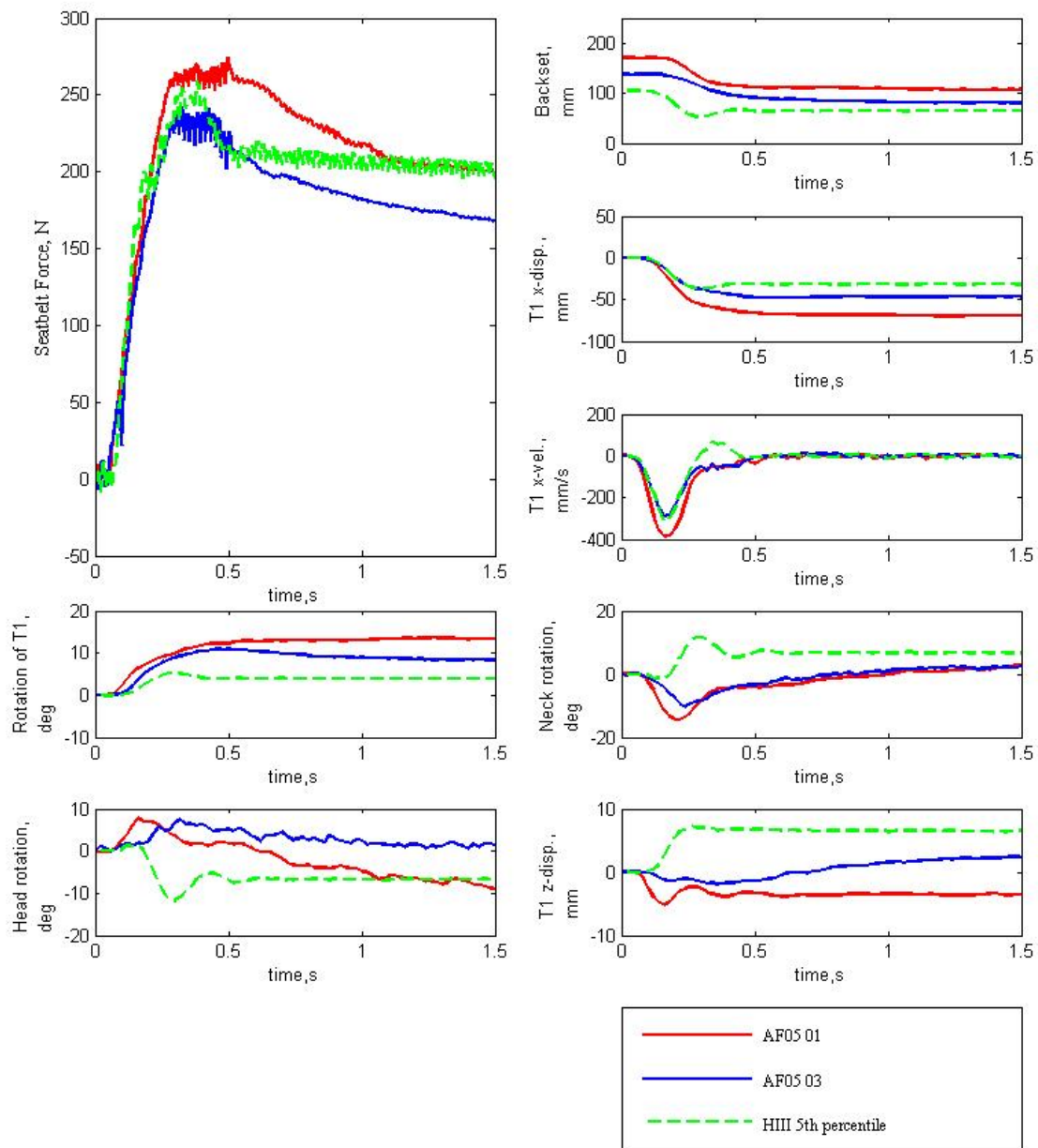


Figure 4.9: Evaluation of AF05 for position 2

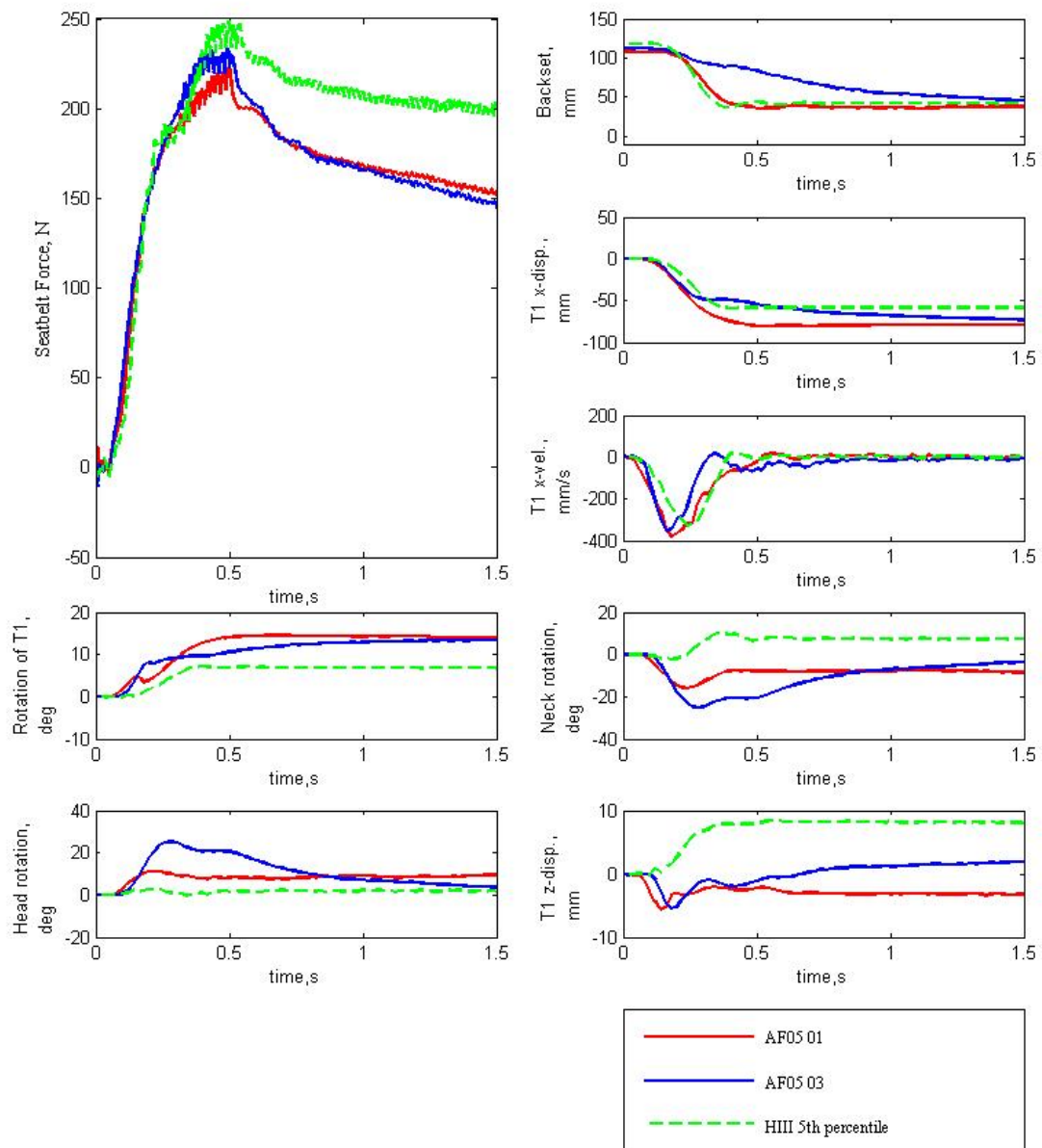


Figure 4.10: Evaluation of AF05 for position 4

## 4.2 Habituation effect in AM95 and AF50

Data for two AM95 volunteer subjects (AM95 01, AM95 05) and also data for two AF50 volunteer subjects (AF50 02, AF50 05) are presented. The first test (1<sup>st</sup> exposure to PPT loading) and the second test (2<sup>nd</sup> exposure to PPT loading) were plotted together in the same graph for each volunteer in order to compare the two responses. The volunteers were seated in the driver seat with hands on the lap.

### 4.2.1 AM95

No clear changes in the seatbelt force characteristics were observed between the 1<sup>st</sup> and 2<sup>nd</sup> exposure. The backset in AM95 subjects is constant in both of the exposures. In AM95 01, it is observed that the volunteer shows larger head-neck movement in the second exposure. It may be explained by the fact that the volunteer might have been relaxed and potentially helping after he was exposed to the 1<sup>st</sup> PPT loading. In AM95 05, the results show that the volunteer has different head-neck motion in the two tests. During the first test, the head-neck complex produces an extension followed by a flexion. However, during the second exposure; the volunteer experiences a flexion-extension movement. In AM95 06, the results of neck rotation show that the volunteer experiences only a flexion during the 2<sup>nd</sup> exposure while he exhibits a small extension in the 1<sup>st</sup> exposure. In AM95 07, all the parameters from both tests overlap each other, except the seatbelt force response. In the 2<sup>nd</sup> test, the seatbelt force is lower than in the 1<sup>st</sup> test.

### 4.2.2 AF50

The shape of the seatbelt force response is almost the same in the first and second exposure to PPT loading for both the volunteers. In AF50 05, the belt slack is reduced faster during the first exposure and there is no remarkable difference in the head-neck motion. However, the amplitude of the T1 kinematics is greater for the first test (~5mm for T1 x-displacement, ~50mm for T1 x-velocity). It can be observed that there is a slight change in backset value during the first exposure but it remains nearly constant during the second. Lower range of motion during the second test can be explained by a tense behavior of the female volunteer. In AF50 02, there is no evident variation in T1 kinematics or backset reduction. However, head-neck movement is larger and a greater flexion motion can be observed in the first test (~6deg in head rotation, ~5deg in neck rotation). One possible explanation is that the female volunteer could be more tensed during the second test resulting in a lower amplitude of the head-neck motion.

In conclusion, differences between the first and the second test may depend on the volunteer's behavior and individual differences between the subjects.

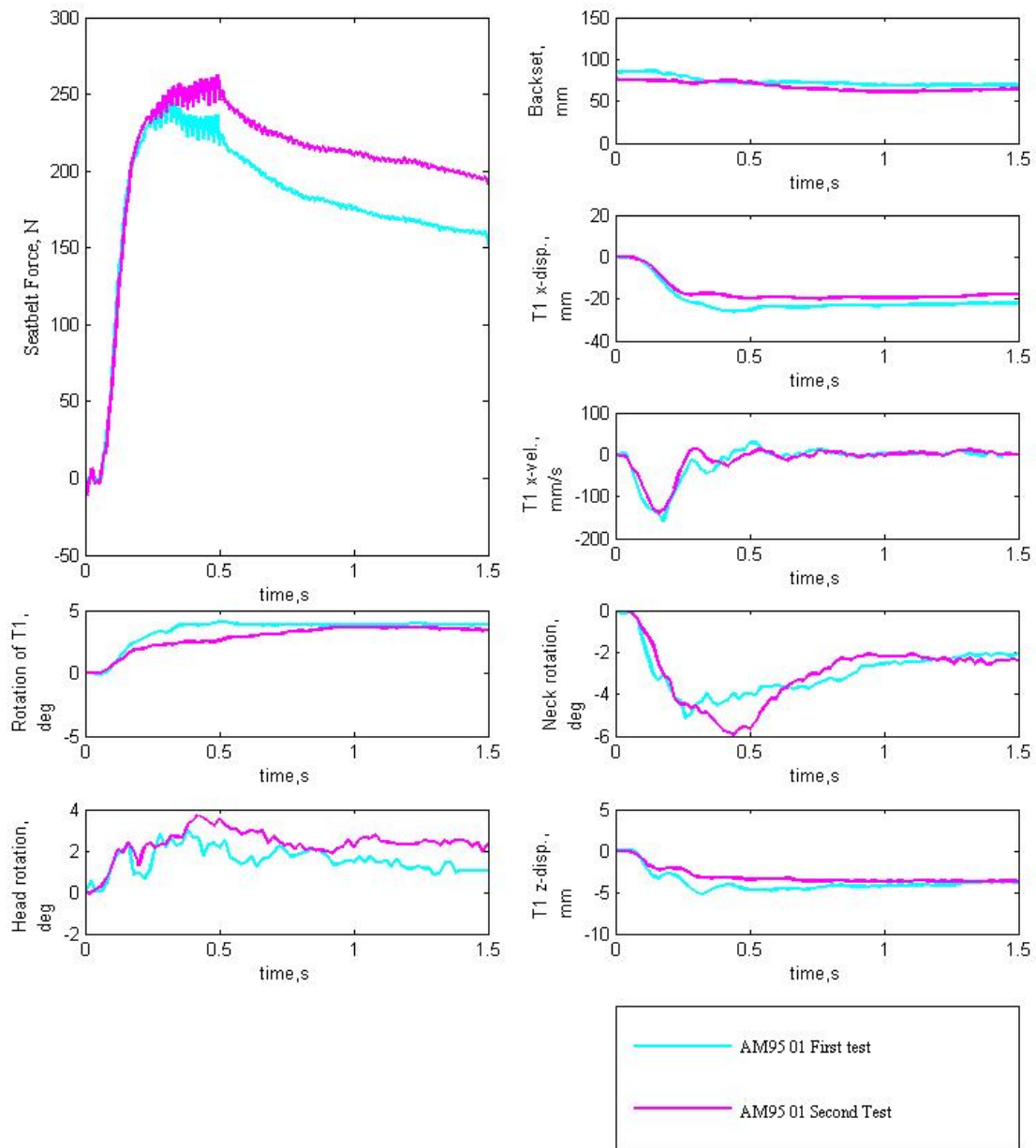


Figure 4.11: Differences in response between the 1<sup>st</sup> and 2<sup>nd</sup> tests for AM95 01

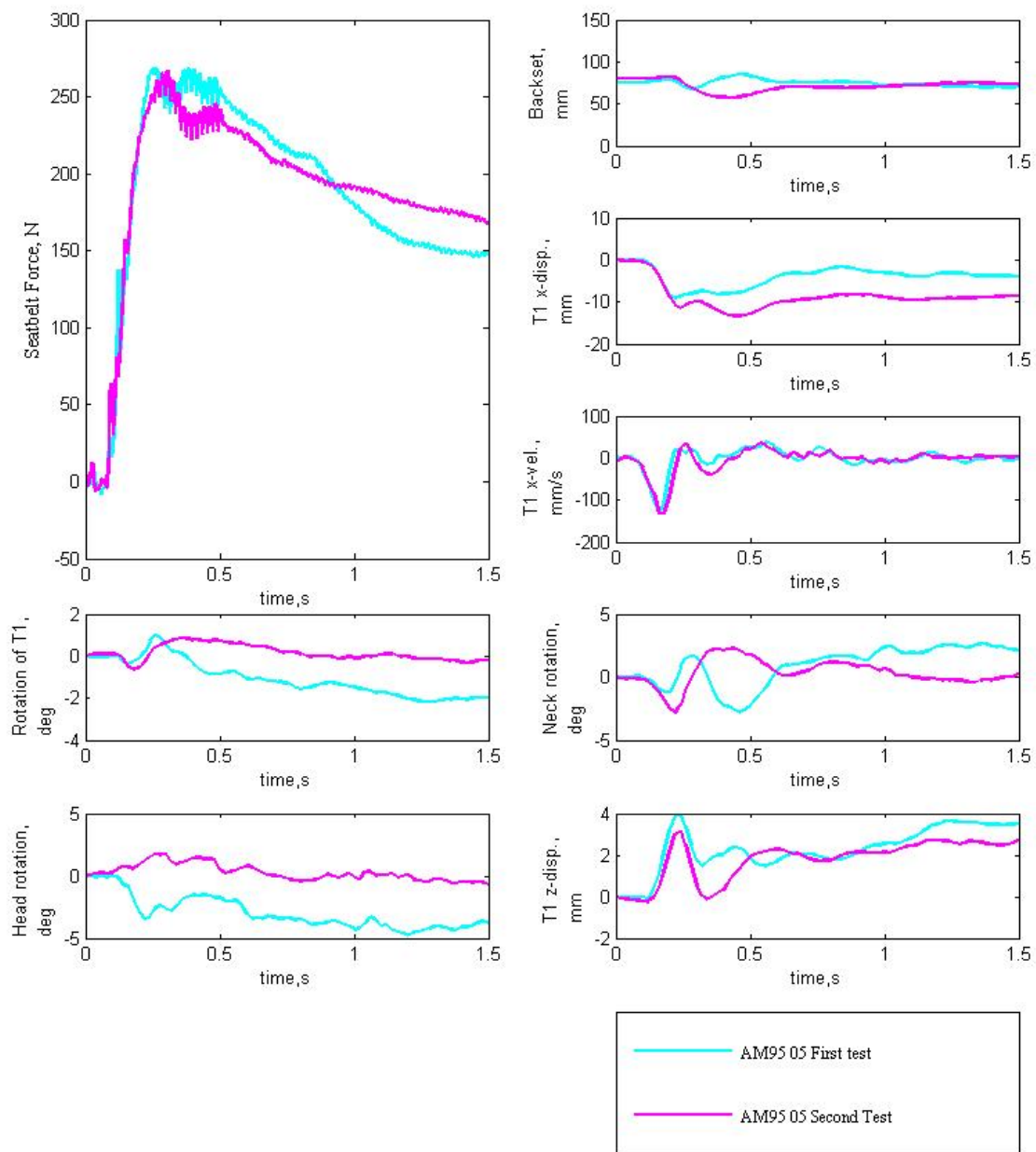


Figure 4.12: Differences in response between the 1<sup>st</sup> and 2<sup>nd</sup> tests for AM95 05

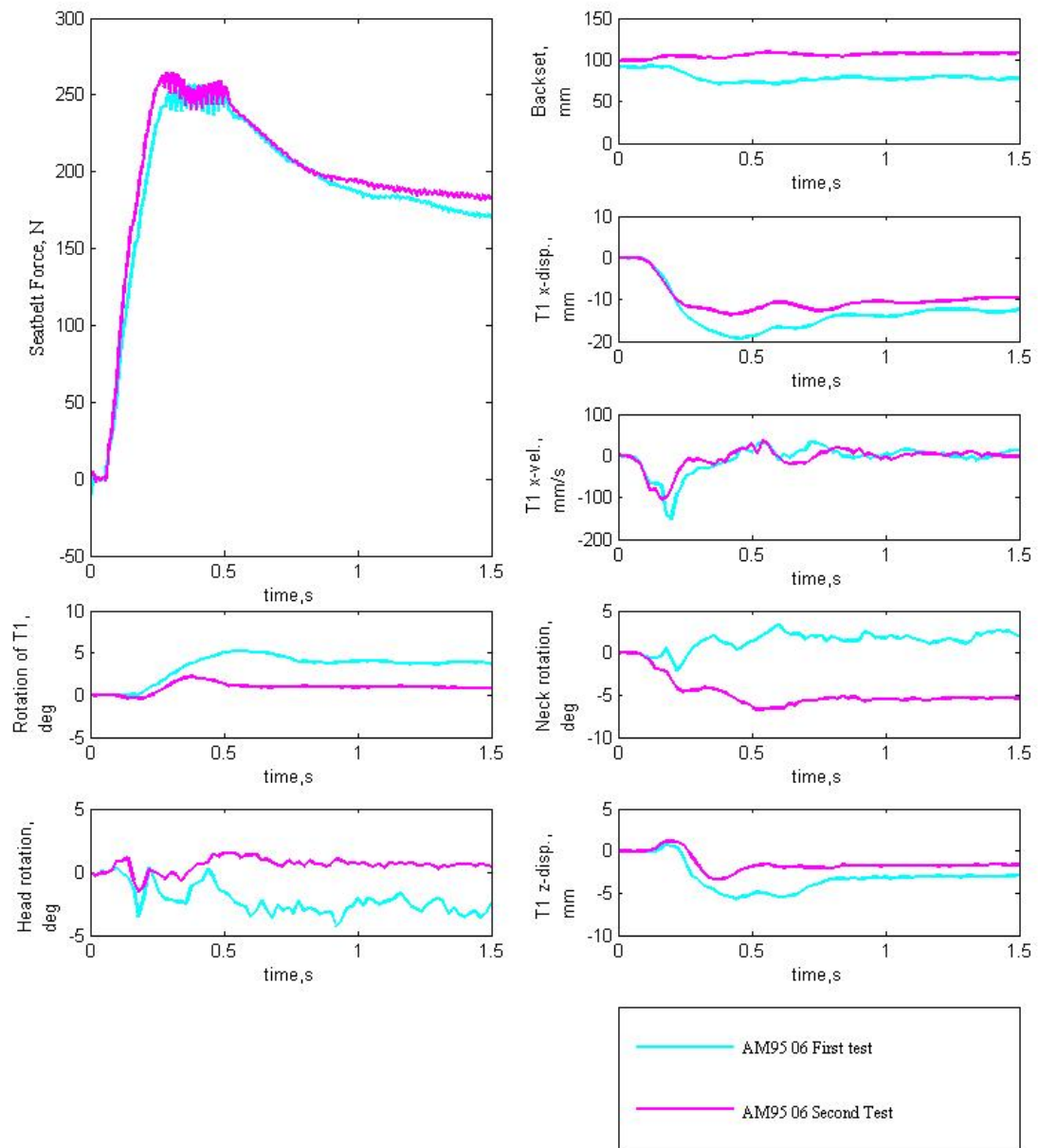


Figure 4.13: Differences in response between the 1<sup>st</sup> and 2<sup>nd</sup> tests for AM95 06



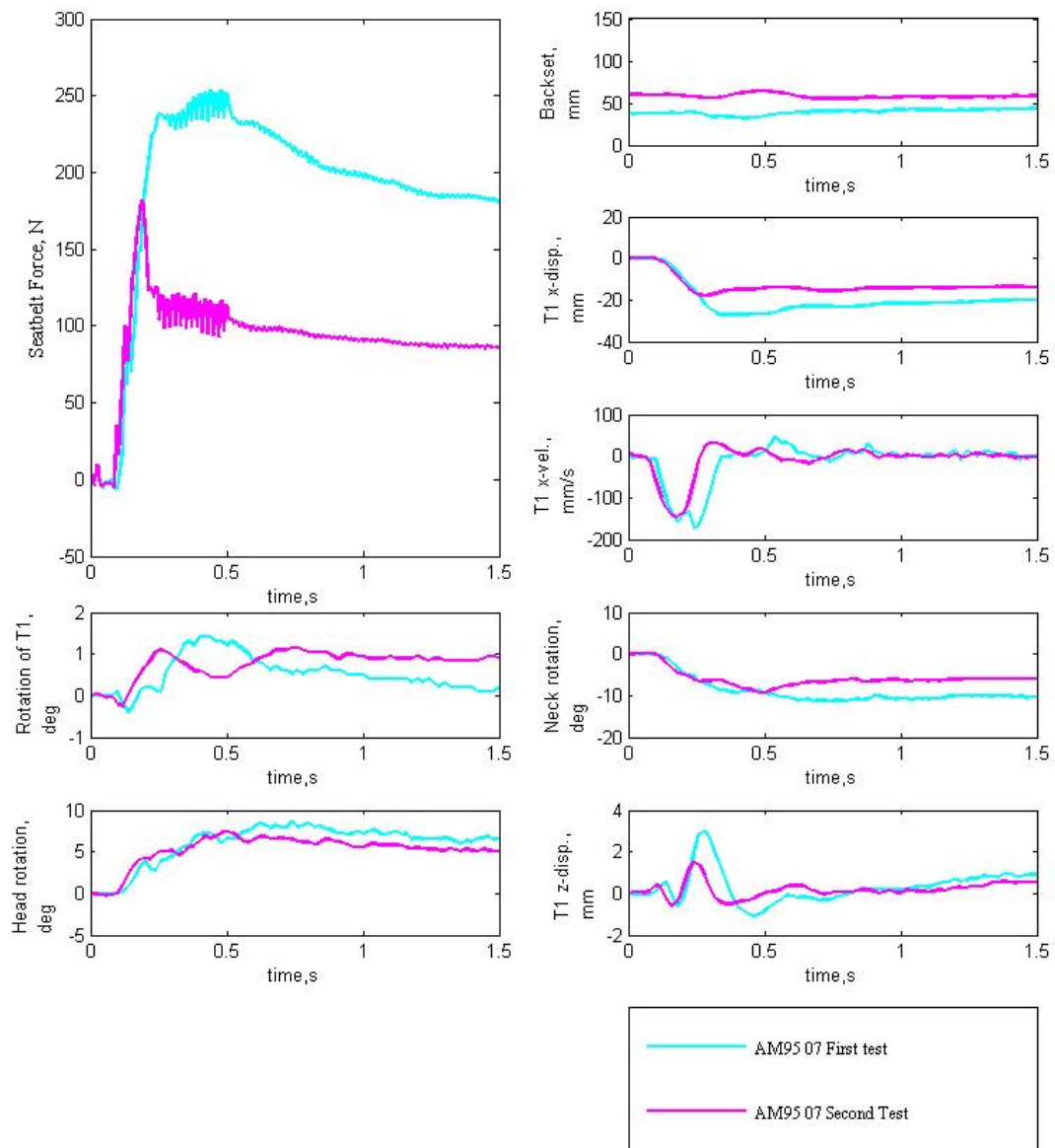


Figure 4.14: Differences in response between the 1<sup>st</sup> and 2<sup>nd</sup> tests for AM95 07



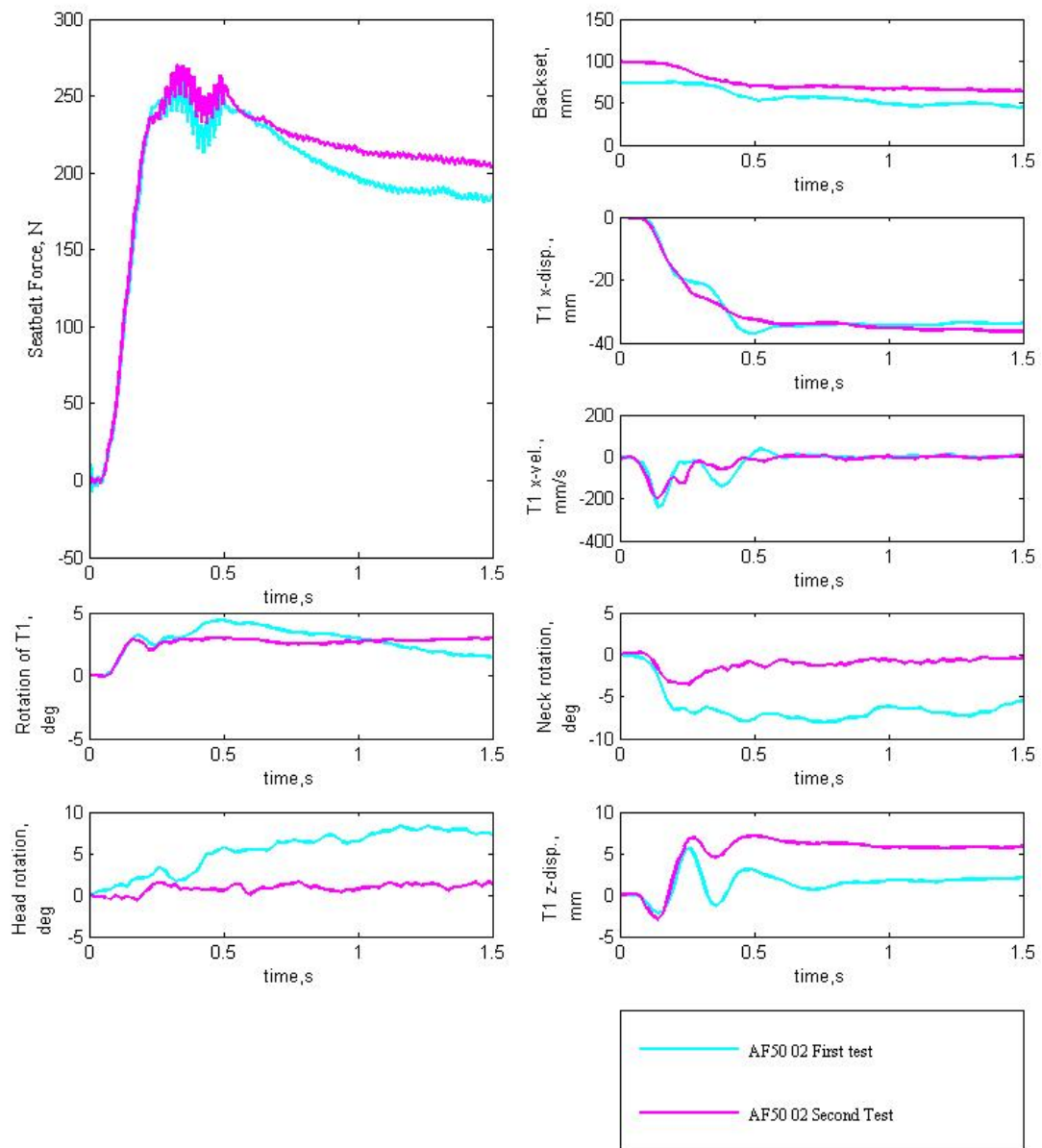


Figure 4.15: Differences in response between the 1<sup>st</sup> and 2<sup>nd</sup> tests for AF50 02

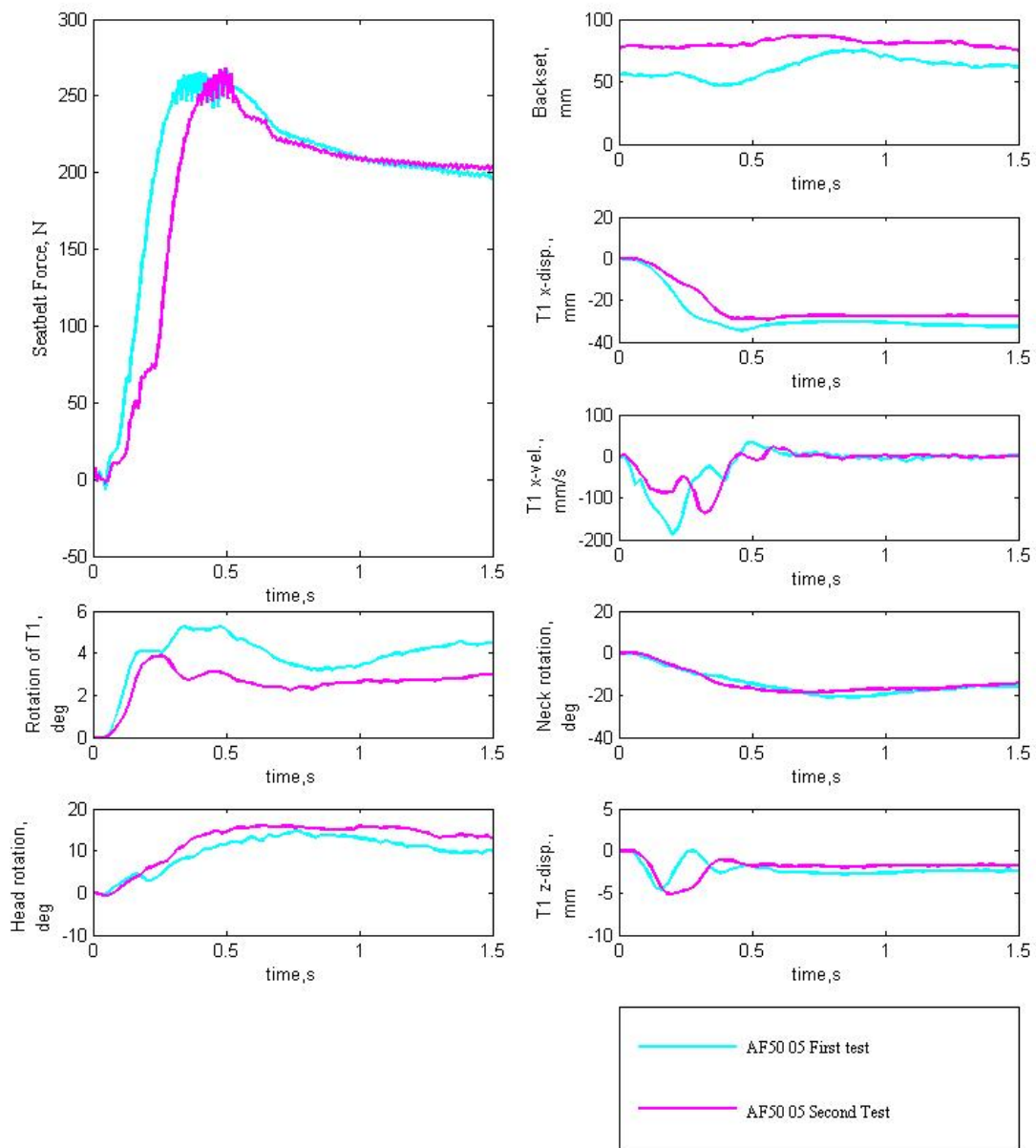


Figure 4.16: Differences in response between the 1<sup>st</sup> and 2<sup>nd</sup> tests for AF50 05

### 4.3 Differences in kinematics of AM95, AM50, AF50 and AF05

Various volunteer sizes were plotted in a graph in order to compare differences in kinematics. AM50, AF50, AM95 data were represented with volunteers' mean response and AF05 data was represented with two curves, one for each of the two volunteers (AF05 01 and AF05 03). The tests were performed with the same power supply, controller and PPT unit.

**Seat belt force characteristics:** In *position 1*, (Figure 4.17) force levels and peak occurrence were closer for all volunteer research subjects (1<sup>st</sup> peak: ~245N at ~0.3s and 2<sup>nd</sup> peak: ~245N at 0.5s) except for AF05 03 which shows lower values of seatbelt force. One possible explanation for the low force value might be that the volunteer was potentially helping during the test.

In *position 2*, (Figure 4.18) all volunteers follow the same trend in seatbelt force response, however AM50 has lower force values.

In *position 3*, (Figure 4.19) the force levels have differences and force values are lower (except for AM95 volunteers). It is observed that the force oscillates after the 2<sup>nd</sup> peak, which is due to a minor rebound.

In *position 4*, (Figure 4.20) all-volunteer sizes produce a similar seatbelt force response (force levels between 220N and 270N and 1<sup>st</sup> peak occurrence at ~0.28 s and 2<sup>nd</sup> peak occurrence at 0.5s).

**Backset:** In *position 1*, (Figure 4.17) there is a difference in the initial backsets between AM95 (~25mm), AF50 (~25mm), AF50 03 (~60mm), AF50 01 (23mm) and AM50 (~75mm). Backset reduction is greater for AM50 and AF50 01. A difference in asymptote values can be observed in all volunteers.

In *position 2*, (Figure 4.18) the 5<sup>th</sup> percentile females have lower initial backsets (~110 mm). All volunteers experience a backset reduction. The final asymptote values are in the range of ~50 mm - ~100 mm.

In *position 3*, (Figure 4.19) the backset reduction response is similar for all volunteer sizes except AM95. The backset reduction is not very evident in large males. The initial backset values (AM50, AF50, AF05) are within the range of ~400mm - ~500mm, the peak occurrence is at 0.6s and reaches an asymptote of ~100mm.

In *position 4*, (Figure 4.20) all the volunteers present a similar response as well. The initial backset values lie in the range 110mm - 170mm. The asymptote values are between ~70mm- ~100mm.

**T1 x-displacement and T1 x-velocity:** In *position 1*, (Figure 4.17) AM95 volunteers show lowest amplitude of T1 kinematics preceded by AF50 and AM50 while the AF05 01 volunteer experiences the highest T1 x-displacement and T1 x-velocity.

In *position 2*, (Figure 4.18) AM50 volunteers have a steeper slope than the rest of the volunteers. They reach greater T1 x-displacement (178mm) and T1 x-velocity (600 mm/s). AF05 volunteers experience the lowest amplitude of the T1 kinematics.

In *position 3*, (Figure 4.19) it is observed that AM95 has low T1 kinematics amplitudes (displacement 45mm and velocity 275 mm/s). The rest of the volunteers experience similar T1 kinematics.

In *position 4*, (Figure 4.20) all volunteers follow a similar trend and it can be seen that the small females exhibit larger T1 kinematics.

**Head and neck complex:** In *position 1*, (Figure 4.17) it is seen that smaller the size of the volunteer, larger is the head-neck motion. According to this, the AF05 03 experiences larger amplitude of head and neck movement (~18deg.) in comparison with the AM95 volunteers, which show the smallest head-neck movement (head rotation: ~1.7deg, neck rotation: ~4deg.). All the volunteers present an initial flexion motion followed by an extension.

In *position 2*, (Figure 4.18) the same trend as is position 1 is observed. AF05 volunteers show the largest amplitude of head and neck rotation (AF05 01: 11deg and 16 deg respectively; AF05 03: 25deg and 23deg respectively) and AM95 volunteers experience the lowest amplitude of head and neck rotation (6deg and 8deg respectively).

In *position 3*, (Figure 4.19) a flexion-extension motion is observed in all volunteer sizes, except for AF05 01 that shows only an extension motion. AM95 volunteers have the smallest amplitude of head-neck motion compared to the rest of the volunteers, who present similar amplitude values.

In *position 4*, (Figure 4.20) all volunteers show the same trend as previous positions. It is observed that AM95 volunteers experience the lowest flexion amplitudes whereas the neck extension amplitude is larger than in the other positions. AF05 volunteers show the highest head-neck motion amplitudes (AF05 01: 7deg and 14.5deg respectively; AF05 03: 7deg and 10deg respectively).

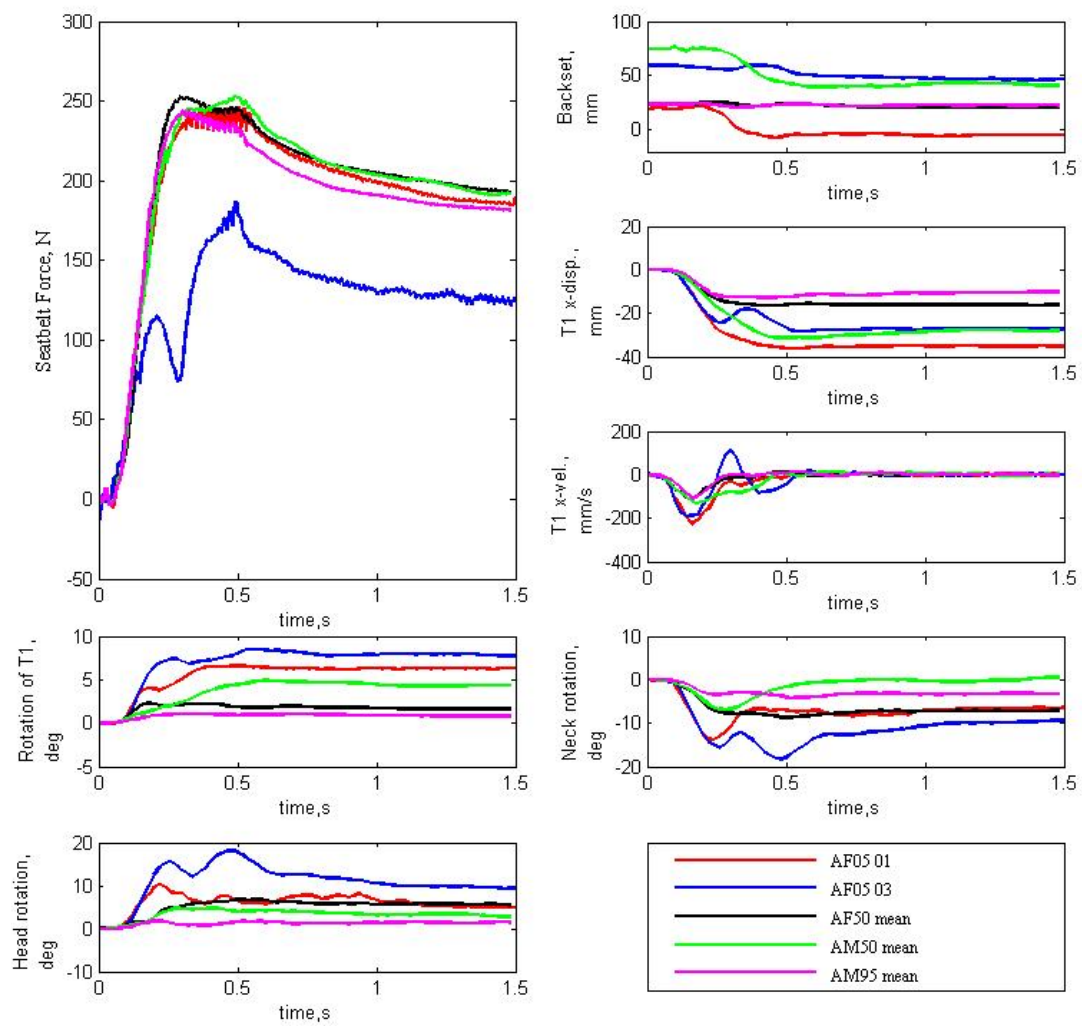


Figure 4.17: Differences in responses between all sizes of volunteers for position 1

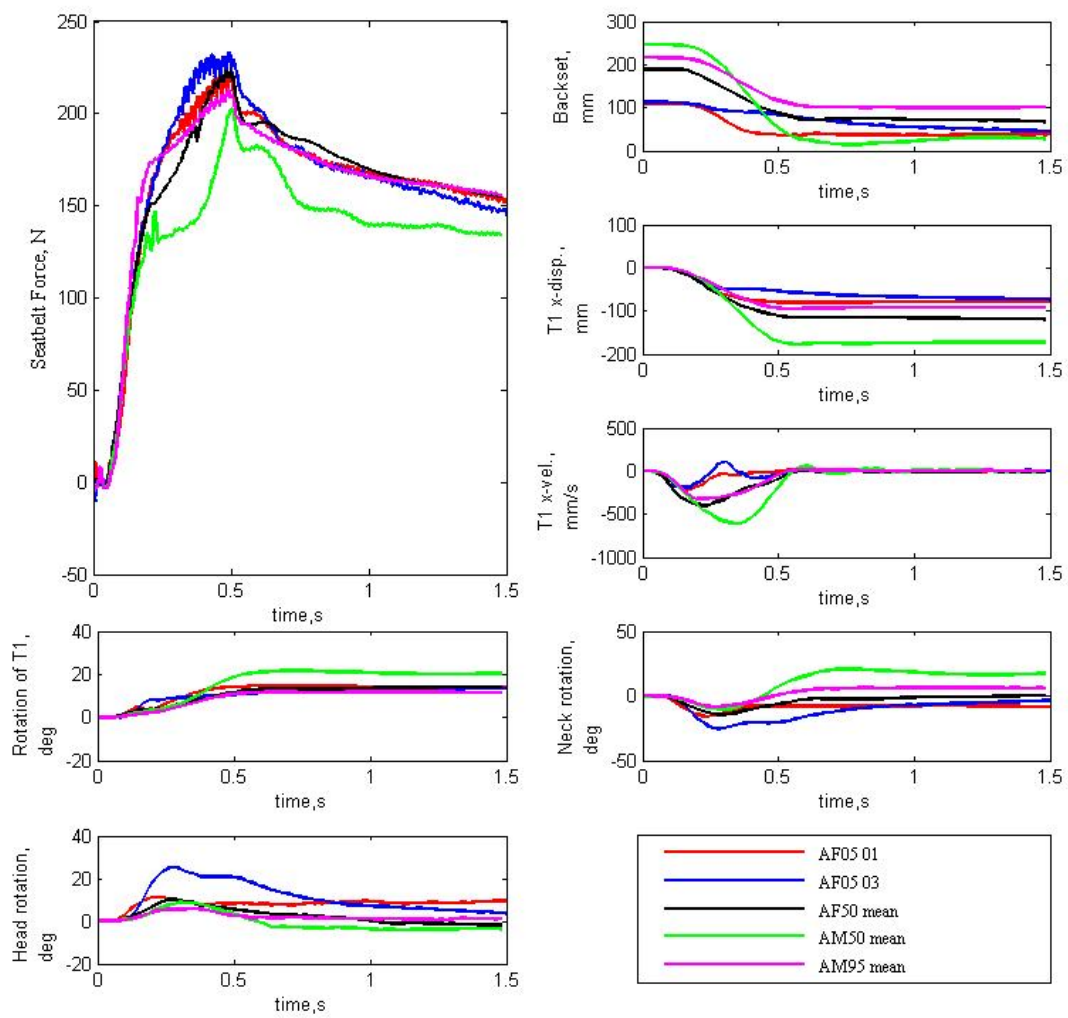


Figure 4.18: Differences in responses between all sizes of volunteers for position 2

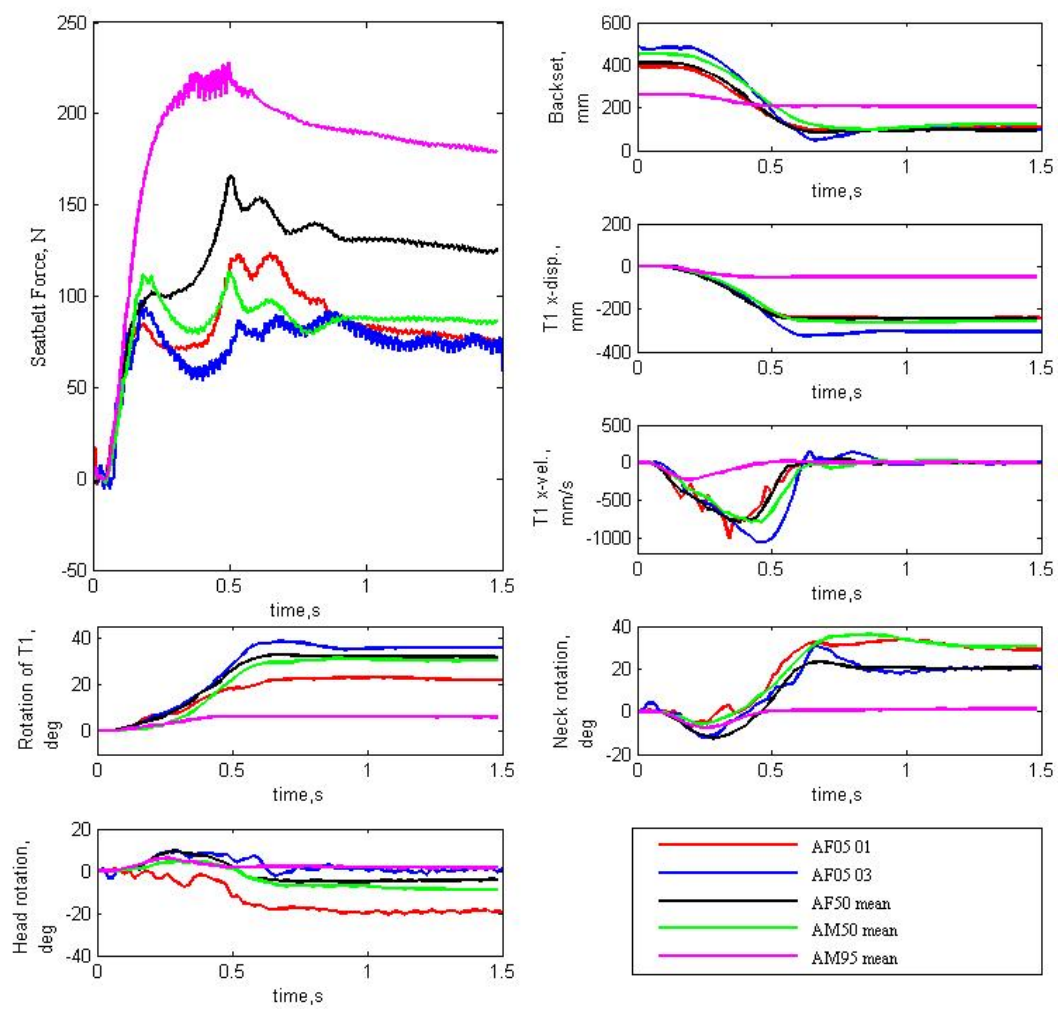


Figure 4.19: Differences in responses between all sizes of volunteers for position 3

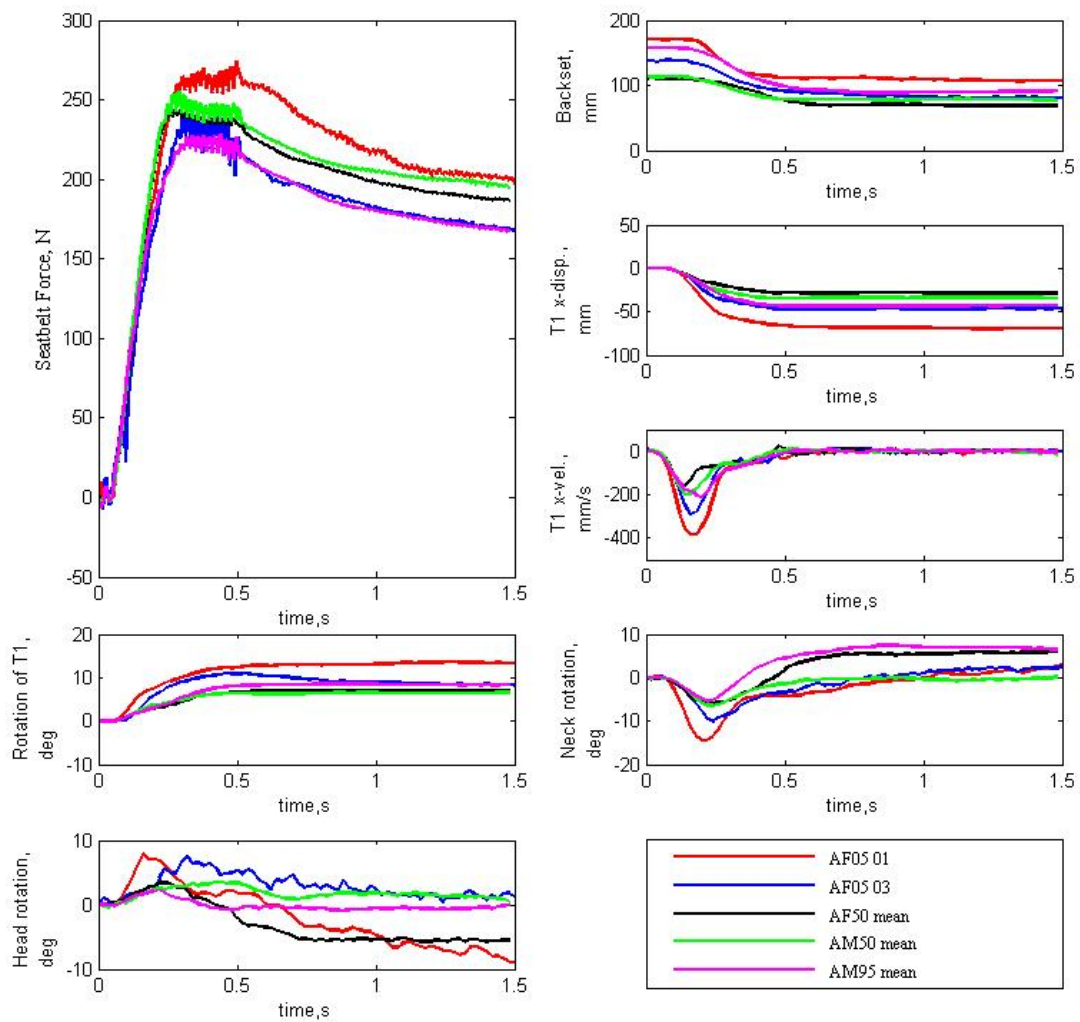


Figure 4.20: Differences in responses between all sizes of volunteers for position 4



## 5 Discussions

**Impact of individual behavior on responses:** Data was collected for a number of volunteers (*Table 3.4*), the plots however does not include all the tests since some of the volunteer data were not valid. For example, AM95 volunteers in position2 had nine out of ten cases that were valid whereas in position3 they had only five out of ten cases.

The biofidelity of the ATD was evaluated by comparing the response of the dummy with the volunteer mean response  $\pm 1$  standard deviation (corridor). Since the volunteers have different responses, the mean would be more representative if it was calculated considering a larger group of volunteers. Individual anatomical differences and mental state contributes to varied responses in different volunteer groups.

Two classes of behavior; tensed and relaxed, were noticed in the test subjects. Tensed volunteers exhibit limited range of head-neck motion and a faster response compared to relaxed volunteers [45]. AF05 01 was tensed during the testing [34]. This phenomenon can be observed in the plots of all four positions. The volunteer has high seatbelt force value, limited neck and head motion and faster response which can be explained due to the activation of neck muscles making it stiffer [46]. On the other hand, AF05 03 was relaxed during the testing [34]. In position1 and 2 AF05 03 shows higher neck and head motion, this is delayed in comparison with AF05 01. In position 1, 3 and 4 AF05 03 has low force levels, which might be because the volunteer was potentially helping.

Other size groups also exhibit behavioral differences. AF50 01 in position1 shows flexion-extension motion of the head while the other volunteers show only a flexion motion. Also, AF50 01 has low seatbelt force value. This phenomenon might be due to the fact that the volunteer was relaxed during the test. AF50 04 in position 4 and AM95 04 in position 3 exhibit high neck-head motions and have low force values indicating the volunteers might be relaxed. However, in the previous tests (position 2 and position 1 and 2 respectively) they seem to be tensed. The relaxed behavior in the later tests might be a result of accustomization.

**Habituation:** In the 1<sup>st</sup> test, AF50 02 shows higher head-neck motion than in the 2<sup>nd</sup> test. In addition, AF50 05 shows higher T1-kinematics in the 1<sup>st</sup> exposure. One possible explanation to this phenomenon is that AF50 volunteers might be more tensed after the 1<sup>st</sup> exposure to PPT loading resulting in lower range of motion. However, this trend cannot be generalized for all AF50 volunteers since two cases only were valid and plotted. A larger sample of valid results is essential to conclude a general behavior of the volunteers.

AM95 volunteers do not exhibit any general behavior. In the 2<sup>nd</sup> exposure, some of them seem to be more relaxed as they show slightly higher range of motion while others seems to be more tensed exhibiting lower range of motion. The absence of a general trend can be attributed to the fact that the individuals respond in a different way to the same system. There is no clear evidence to state whether muscle activation aggravates or mitigates whiplash injuries. If muscle activation mitigates whiplash, then warning in advance would help the volunteer in tensing the muscles before the

impact. If muscle activation aggravates whiplash injury, not warning the driver before would reduce peak muscle activation [47]. Tensed neck muscles reduce the flexion and extension motion however; they could induce stress in neck joints and other surfaces increasing the risk of injury [86]. Further investigation to study the role of muscle activation in whiplash injuries can aid in the development of future PPT systems.

**Differences due to front and rear seat:** Position 1 in the test corresponds to the driver seated in the front seat while position 4 corresponds to a passenger seated in the rear seat. In position 4, the head-neck complex of AM95 and AF50 shows both flexion and extension motion while in position 1, only flexion motion is observed. An explanation for this behavioral difference could be that the volunteers in the rear were more relaxed as they were accustomed to the system since the test for position 4 was performed after several tests in other positions. Another reason could be that geometric differences between rear and front seat might have influenced the head-neck kinematics of the volunteers. This head-neck motion is significant in assessing whiplash injuries. A study suggests that risk of suffering a whiplash injury is higher in the rear seat passengers compared to front seat passengers for females [48].

The angle that the seatbelt makes with the shoulder and the horizontal line (x-direction) is larger for the front seat compared to the rear (*Figure 5.1 a*). As a result, the component of the force acting perpendicular to the chest (x-direction) is larger for the rear passenger. (*Figure 5.1 b*)

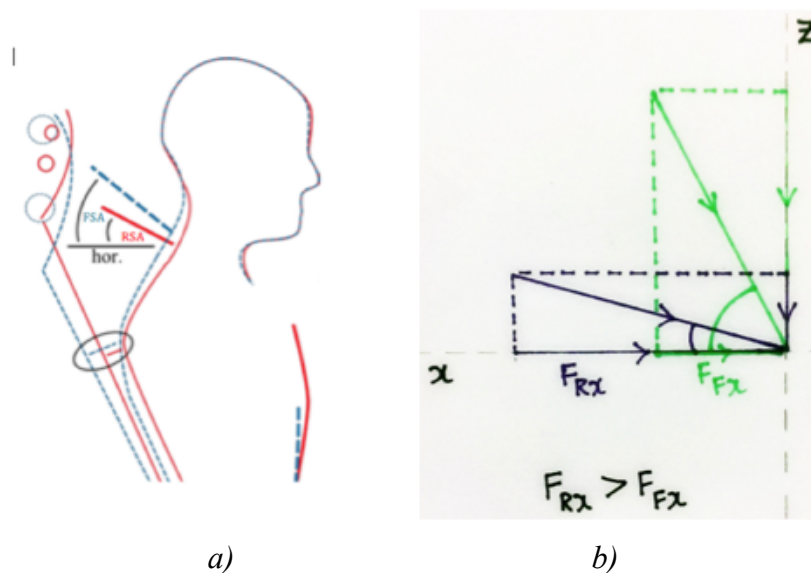


Figure 5.1: a) Contours of AM50.4 at the front (blue dashed line) and at the rear (red solid line) seat with the seatbelt. Adapted from Adrien. J [34].

\*FSA=Front seat angle, RSA=Rear seat angle

b) Representation of variation in force components with respect to seatbelt angle

**Comparison between different size groups:** Differences in initial backset for various sizes were noticed in all positions. Backset might be influenced by the head shape, position of the support rod and differences in seated height. Shape of the skull and the seated height differ for volunteers of different gender and size resulting in different distances between the back of the skull and the head restraint. In order to maintain various positions, a support rod was held still by allowing changes in head and neck angles also contributing to changes in initial backset. (Figure 5.2)

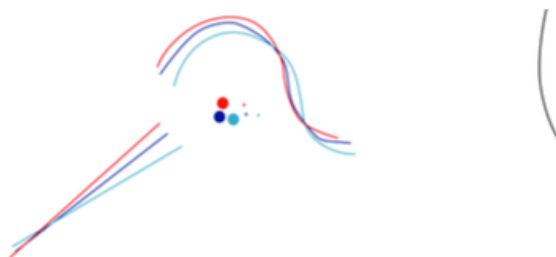


Figure 5.2: Different initial seated posture for three volunteers in position 3. Adopted from Adrien.J [34].

The same force level was applied to all volunteers during testing. As a result of this, in position 1 and 3 AM95 volunteers do not show a backset reduction and they have the lowest T1 kinematics. Also in position 2, they present the lowest backset reduction and low T1 kinematics compared to other volunteer groups. Higher forces might be necessary to reposition these volunteers. In position 2, 3 and 4 it can be observed that the volunteer group that has the highest initial backset also has the highest T1 x-displacement and T1 x-velocity. This could be due to availability of more distance in x-direction for the movement of the upper torso.

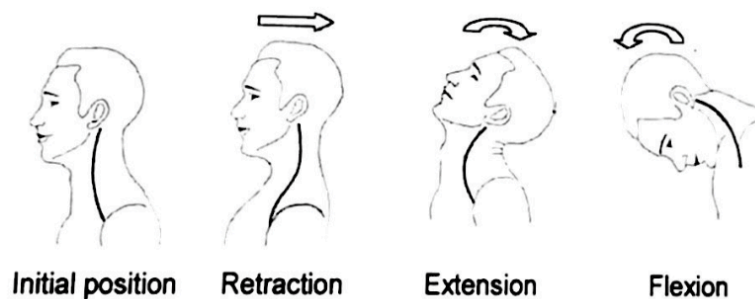
AF05 volunteers have a different seatback interaction compared to AM95 volunteers. Small female volunteers were found to interact more with the inner seat area while large male volunteers interact more with the external seat frame. This difference in seatback interaction might affect the kinematics.

Females have a higher range of head-neck motion approximately 1-12deg higher than the males, depending on their age. Age has a dominant effect on the degradation of the range of motion; females tend to lose mobility gradually while the males exhibit a more rapid degradation in their youth and middle age [49]. Research subjects in the present study were relatively young and healthy people. It can be observed that the least head-neck motion is in AM95 volunteers while AF05 volunteers show the highest motion in all four positions. Another possible explanation for this contrast is physiological differences (Chapter 1.5) between males and females. This behavior in female volunteers might help in understanding the risk of whiplash better.

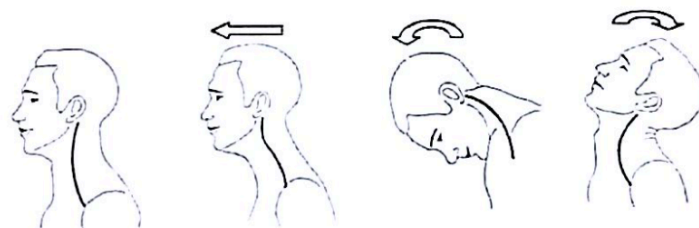
**Evaluation of biofidelity of ATDs under PPT loading:** HIII (5<sup>th</sup> and 95<sup>th</sup> percentile) does not reproduce the human-like motion of head-neck complex under PPT loading. The neck and torso of the HIII are stiff and most likely to not interact with the seatback like humans [50]. Studies indicate that humans show more complex head motion than the HIII [51].

In order to study light frontal loading conditions such as PPT loading, it is suggested to modify some components of the HIII to be more representative of the human head-neck complex. Changes to the stiffness and damping could be a possible solution. New dummies that show more biofidelic responses like the BioRID-II (low speed rear-end impact dummy) and THOR (frontal impact dummy) are being developed. THOR is being considered as a replacement for HIII 50th percentile male in future EuroNCAP frontal impact tests [52]. Subsequent ATD development should consider designing more biofidelic dummies to reproduce 5<sup>th</sup> and 95<sup>th</sup> percentile populations in order to efficiently test all loading conditions.

The neck experiences the same type of inertial loading but in the opposite direction in a frontal impact compared to a rear-end impact. As a result, the general neck kinematics varies according to the type of impact (*Figure 5.3 and Figure 5.4*).



*Figure 5.3: General neck kinematics in rear-end impact. Adopted from Linder A [53].*



*Figure 5.4: General neck kinematics in frontal impact. Adopted from Linder A [53].*

AF50 volunteers show a flexion-extension motion (PPT loading is similar to a light frontal impact) while BioRID50F shows an extension-flexion motion. The BioRID50F is designed for rear-end impacts which could be a plausible explanation for this reversal in trend. The BioRID50F used in this study was the 1<sup>st</sup> physical prototype and adjustments in the stiffness of the spine were some recommended changes by the manufacturer to further improve the ATD's dynamic response [16].

**Population at risk:** Some vehicle occupants are more prone to serious injuries than others in the event of a crash. Future automotive systems, including in-vehicle restraint systems such as PPT seatbelts, should consider the protection of all passengers with different injury tolerance levels.

**Obese occupants:** Obesity is a growing concern worldwide and automotive safety industry is considering the impact of this health problem in the performance of occupant protection systems [54]. Adults are defined as obese if they have a body mass index (BMI) of 30 kg/m<sup>2</sup> or higher. About 34% of United States adults were obese in 2010 [55]. Obesity increases the risk of some types of injuries in motor vehicle crashes [56]. Morbidly obese occupants have lower seatbelt use [57]. This can be explained due to insufficient webbing length for comfortable usage [58]. Seatbelt use is optimal when the belt is tight and loads the bony structures early in the impact. Seatbelt placement in obese occupants is not always over the bony structures of the shoulder and the pelvis [56]. According to a study, obesity introduces slack in the seatbelt system, which may increase the probability of contacts with the vehicle interior [56]. In addition, the likelihood of submarining in frontal crashes will increase due to the higher routing of the lap belt with respect to the pelvis [56].

**Elderly occupants:** The population over 65 years has increased by 10 times in the last century [59]. Elderly people have an increased risk of suffering injury in a crash. They have lower thoracic injury threshold hence older occupants sustain more hemo/pneumothorax as well as rib fractures than younger occupants [60]. In a vehicle crash, most of rib and sternum fractures in extreme elderly occupants (80 years or older) are caused by seatbelts. It is recommended to consider the fragility of older people in the design of safety belts by reducing the loading of the thorax in frontal impacts [61]

**Children:** Children present structural differences compare to adults such as the head mass in relation to the neck, body proportions, location of important organs, biomechanical properties of tissues as well as the location of the center of gravity [87]. Adequate children restraint systems should consider these critical anatomical differences to ensure children protection. According to a study performed in a H-III6C seated on different booster cushions, adding a pretensioner and a load limiter to a standard retractor decreased loading of the neck, head and chest for all booster cushions [88].

**PPTs and drivers' acceptance:** An active safety system produces a warning after compiling information from the vehicle, driver and surroundings. False alarms are inevitable considering the rarity of accidents. Repeated false alarms may influence the drivers' acceptance to the system. These alarms can be annoying; moreover, they can reduce the trust in system reliability. Effect of false alarms, influence of PPT loading on drivers' performance and familiarization of the driver to the system are some areas of interest for future research. Active seatbelts are comparatively new in the market hence there is a need to collect more data from realistic driving situations to comprehend their performance.

## 5.1 Future work

Some ideas and recommendations for further research are suggested:

- Evaluation of PPT loading considering population at risk (obese occupants, elderly occupants, children and pregnant women).
- Larger groups of volunteers, particularly AF05 volunteers to obtain more representative results.
- Investigating 4-point seatbelts with PPT for distributed chest loading in elderly occupants.
- Adaptive PPT loading for different occupants (anthropometry and gender).
- Examining driver acceptance to the system in real life scenarios.
- Evaluation of biofidelity of new prototype of BioRID50F.
- New technologies in PPT activation.
- Explore the options of using higher loads in PPTs to reposition the occupants.

## 6 Conclusion

The Hybrid III family (5<sup>th</sup> and 95<sup>th</sup> percentile) does not reproduce the human-like motion of the head-neck complex under PPT loading due to the stiffness of the neck and torso. Changes in stiffness and damping may lead to improvements in biofidelity of these dummies under low load conditions (PPT loading). Another suggestion is to develop more biofidelic ATDs taking into account 5<sup>th</sup> and 95<sup>th</sup> percentile populations. BioRID50F shows a reversed trend compared to the flexion-extension motion of the volunteers under PPT loading. Further adjustments in stiffness of the spine are recommended to improve the biofidelity of this 1st BioRID50F prototype. In general, small females are observed to have larger head-neck rotation amplitudes. This may contribute to higher whiplash risk in females. Large males show lower backset reduction and low T1 kinematics compared to other sizes of volunteers. This may be because the force level of PPT was not sufficient enough to reposition them. It was observed that individual anatomical differences and mental state contributes to varied responses. Tense volunteers exhibit limited range of head-neck motion. Further investigations in neck muscle activation are suggested to understand its influence on whiplash injuries. Differences in head-neck motion between the front and rear seat passengers were observed. Geometric differences in the seats might have influenced the kinematics of the volunteers. Moreover, tests in the rear seat were performed after several tests suggesting that familiarization effect could have affected the kinematics. The results of this study might be significant in the development and adoption of pre-tensioners in future vehicles worldwide.

# PART – II



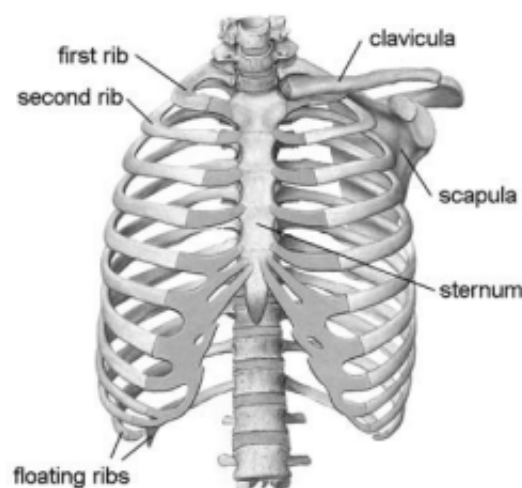
## 7 Introduction

### 7.1 Background

Seatbelts are effective safety systems. Nevertheless, there are constant attempts in the automotive sector to improve and develop new seatbelt technologies to reduce the risk of injuries. Pre-pretensioners seatbelts (PPT) combine active and passive safety systems. They enhance occupant position and remove seatbelt slack. This reversible system is adaptive to the situation and reduces the out of position risks. These seatbelts assist in positioning the occupants better and provides a warning before a potential crash. It is able to protect occupants in different crash scenarios such as frontal, rear-end and side impacts [62]. Rollover crash scenarios are not been studied but a positive effect is assumed for these types of impacts. Current studies about PPT seatbelts suggest that there is a scope to develop more powerful systems that may use higher forces to reposition the occupant before an impact. As mentioned in the first part of the study, the upper limit of seatbelt tension should be adjusted to occupant's tolerance limit. Two main system design parameters for active seatbelts are the amount of tension or the retraction to be activated and the timing at which the device activated the motor retractor. Occupant size has an important effect in the retraction time to reposition the torso since larger occupants require more time because of a slower retraction velocity [63]. Low-level motorized shoulder belt tensioning is well tolerated by occupants but optimized performance by occupant size is undiscovered [63]. Information and studies about occupant response to PPT seatbelt tension are limited.

### 7.2 Thorax

The thorax is composed of the ribcage and the subjacent soft tissue organs. The diaphragm determines the lower limit of the thorax. Twelve pairs of ribs form the rib cage. All ribs are connected posteriorly to their corresponding vertebrae through the costovertebral joints. The rib cage is a quite stiff deformable cover that protects and supports the internal organs and facilitates respiration [64].



*Figure 7.1: Anatomy of the ribcage*

**Thoracic Injuries:** Blunt injuries are produced when an object impacts the thorax without penetrating it. The injury mechanisms related to these kinds of injuries are: compression, viscous loading and inertial loading as well as a combination of these mentioned mechanisms. Some examples of injuries produced by these mechanisms are - fractures in the ribcage, lung contusions and aorta lacerations respectively [65]. The Abbreviated Injury Scale (AIS) of the Association for the Advancement of Automotive Medicine (AAAM) is a standard method to classify the level of injury to a body region. Common skeletal and soft tissue injuries to the thorax ranked by AIS (2005) are presented. (Figure 7.2)[64]

AIS Skeletal Injury	AIS Soft tissue injury
1 one rib fracture	1 contusion of bronchus
2 2-3 rib fractures; sternum fracture	2 partial thickness bronchus tear
3 4 or more rib fractures on one side; 2-3 rib fractures with hemothorax or pneumothorax	3 lung contusion; minor heart contusion
4 flail chest; 4 or more rib fractures on each of two sides; 4 or more rib fractures with hemo- or pneumothorax	4 bilateral lung laceration; minor aortic laceration; major heart contusion
5 bilateral flail chest	5 major aortic laceration; lung laceration with tension pneumothorax
	6 aortic laceration with hemorrhage not confined to mediastinum

Figure 7.2: AIS rating for skeletal and soft tissues thoracic injuries [AAAM 2005]

The influence of seatbelt loading has been under investigation since the late 1970s. Seatbelt injuries affect the chest more than the abdomen region since current automotive restraints generate a complex loading environment on the chest. The shoulder seatbelt generates concentrated forces on fewer anatomical structures such as the clavicle, sternum and ribs. Under this concentrated loading, the thorax is more vulnerable to suffer an injury.

**Thoracic injury criteria in frontal impacts:** Injury criteria establish a relationship between a certain loading of the thorax and a corresponding injury risk. The most commonly used thoracic injury criterion is the Compression Criterion. Maximum thorax compression correlates well with AIS (Eq.1). Compression (C) is defined as the chest deformation divided by the thickness of the thorax.

$$AIS = -3.78 + 19.56C \quad \dots [Eq. 1]$$

For example, 92 mm of thorax deflection for the 230 mm chest of the 50th percentile male THOR dummy results in a compression of 40 % and predicts AIS4 [64].

Thoracic injury risk is well predicted by maximum compression but it is strongly age-dependent for frontal impact loading. Chest deflection is measured as the posterior displacement of the anterior chest relative to the posterior chest under frontal loading and it is a predictor of thoracic injury risk.

According to cadaver studies, with increase in chest deflection the risk of injury increases [66]. Moreover, chest deflection tolerance is reduced with increasing age [67]. Anatomical changes related to ageing produce this decline. After the age of 30, the mineral density, fracture toughness and failure strain of the bone decreases [68]. There is also a decrease in the cortical bone thickness, which increases the injury susceptibility [69]. Reduction in chest deflection tolerance may be also due to progressive calcification of the costal cartilage by decreasing the failure strain of the cartilage. After the mid-thirties, 0.3% to 0.5 % bone loss per year is observed [70]. With increasing age, slope of ribs in the sagittal plane may decrease which may result in increased strain in the rib for a level of chest deflection [71]. The tolerance to concentrated force is lower in elderly occupants. Restraint development and design should consider this decrease in chest deflection tolerance to protect all occupants.



Figure 7.3: Cortical bone thickness [69]

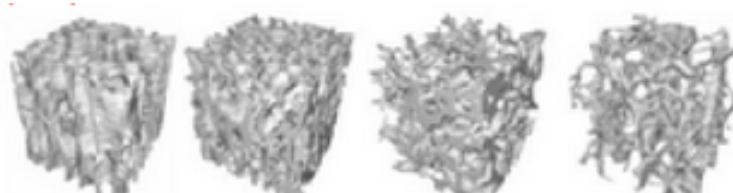


Figure 7.4: Bone loss with increase in age [70]

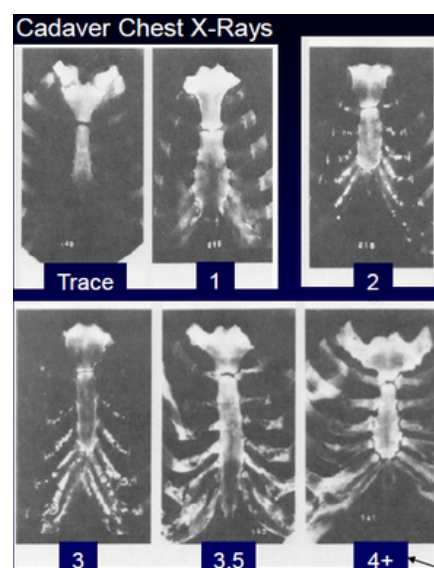


Figure 7.5: Calcification in costal cartilages [72]

A new age-dependent thoracic injury criterion was established for frontal impact loading. Data from a cadaver test (age range 17-86 years) was used to develop thoracic injury risks [73]. A 30-year-old has a 50 % risk of sustaining one rib fracture at 35 % of chest deflection while a 70-years-old has a 50 % risk of sustaining one rib fracture at 13 % of deflection [73].

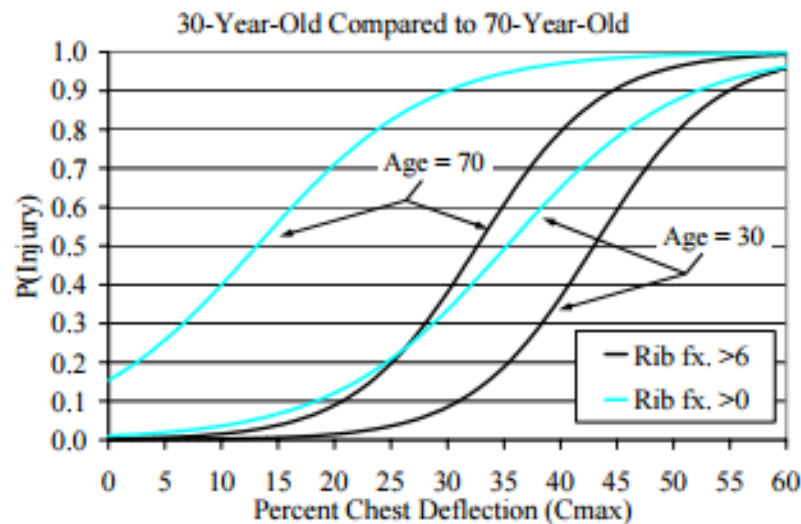


Figure 7.6: Injury onset risk and severe injury risk for two ages [73]

Maximum chest deflection ( $C_{max}$ ), as measured on the cadaver, can be considered to be an objective injury criterion for different restraint conditions since the deflection injury tolerance is not sensitive to the loading case. However, this insensitivity cannot necessarily be applied to chest deflection as measured by a dummy since HII and THOR dummy biofidelity is sensitive to the type of restraint used. HII chest deflection injury risk function is dependent on the restraint type [74]. This introduces a new problem about how to evaluate new restraints since the injury risk function is restraint dependent for dummies. Additional research is needed to test changes in dummies' chest deflection injury tolerance levels for different types of restraints.

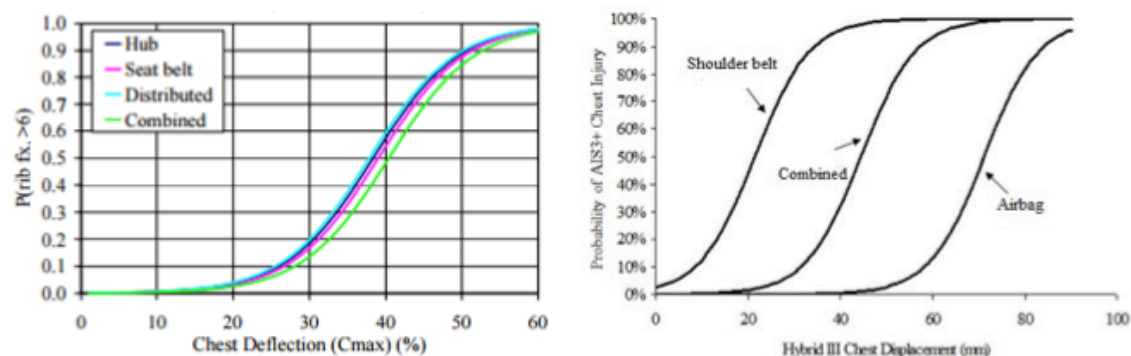


Figure 7.7: Load condition insensitivity of  $C_{max}$  injury threshold for 60-year-old male cadavers (left). Hybrid III chest deflection injury risk function for different restraint systems (right)

### 7.3 Neck

The spine as a whole consists of 7 cervical, 12 thoracic, 5 sacral and 4 coccygeal vertebrae. Each of these vertebrae is composed of cylindrical vertebral body connected to a series of bony elements collectively referred to as the posterior elements. The spine provides mechanical protection for the spinal cord and contributes to the stability and kinematics of the vertebral column. The cervical spine consists of 7 vertebrae the forms eight-motion segments between the base of the skull and the 1<sup>st</sup> thoracic vertebra, T1 [75].

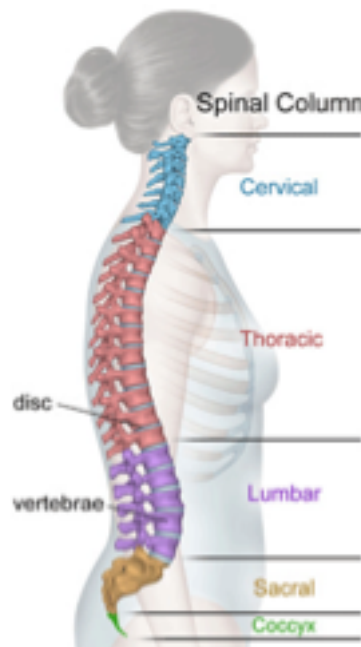


Figure 7.8: Anatomy of the human spine [76]

**Neck injuries:** The injury mechanisms observed in cervical spine injuries are: compression (vertical compression), compression-flexion, compression-extension, tension, tension-extension, tension-flexion, torsion, horizontal shear and lateral bending. Some of the injuries caused by these mechanisms are whiplash, hyperflexion sprain and burst fracture [75]. In case of automotive crashes the main loading to the neck is either due to the head contact forces or combined axial or shear load with bending. Injuries are a result of indirect loading caused due to the inertial loads that is transferred from the torso to the head or head to torso after an impact or acceleration differences. Neck is highly sensitive and comprises of a vertebrae joined by cartilages and muscles, which together assist in producing varied range of complex motions.

**Neck injury criteria:** Two commonly used neck injury criteria to estimate the injury risk are - NIC and  $N_{IJ}$ .

**Neck Injury Criterion (NIC):** AIS 1 neck injuries sustained in rear-end impacts can be evaluated by using the NIC. It was proposed by Boström (1996) based on the relative motion between the head and lower neck, acknowledging the damage found in the cervical spinal ganglia that is produced by the transient pressure changes in the spinal canal. NIC is calculated considering the accelerations between the center of gravity of the head and T1. It is representative of the neck movement in retraction phase [77].

$$NIC = a_{rel} * 0.2 + V_{rel}^2 \quad [m^2/s^2]$$

$$a_{rel} = a_{T1} - a_{Head} \quad [m/s^2]$$

$$v_{rel} = \int a_{rel} dt \quad [m/s]$$

NIC is sensitive to the acceleration of the crash pulse, the value of the peak, shape of the pulse, the shape and position of the head restraint and the properties of the seat [78].

*Neck Injury Criterion in protraction (NIC<sub>protraction</sub>):* Boström proposed another neck injury criteria, NIC<sub>protraction</sub>, to estimate AIS1 neck injuries in frontal collisions. It was formulated by considering that the injury occurs in the starting phase, when the neck exhibits a protraction motion [79]. The NIC does not consider the sign of the relative velocity in its calculation. A generic formula for extreme NIC value was developed, which is expressed as:

$$NIC_{generic} = a_{rel} * 0.2 + V_{rel} * |V_{rel}| \quad [m^2/s^2]$$

Based on the NIC<sub>generic</sub>, the NIC<sub>protraction</sub> was formulated for frontal collisions [77].

$$NIC_{protraction} = |minimum NIC_{generic}| \quad [m^2/s^2]$$

*Normalized Neck Injury criterion (N<sub>IJ</sub>):* It considers the extension and flexion motion in both tension and compression. The criterion is determined by considering the axial compression force, axial tensile force and the shearing forces at a transition from the head to neck.

$$N_{IJ} = \frac{F_z}{F_{int}} + \frac{M_y}{M_{int}}$$

F<sub>Z</sub> - axial load, F<sub>int</sub> - critical intercept value of load used for normalization, M<sub>y</sub> - flexion/extension bending moment, M<sub>int</sub> - critical intercept value for moment used for normalization [80].

## 8 Purpose

Current PPT seatbelts pull the occupants with a force level less than 300N. In a pre-crash scenario, occupants are probably out of position increasing the risk of injuries. Higher forces might help to reposition them better under these situations.

A literature review aided in identifying two crash pulses; one safe for children and adults and another safe for adults. These crash pulses are used to perform a dynamic test in order to establish a threshold for injury criteria. In previous studies, tests have been conducted for the 50th percentile male. However, these studies do not include females and children.

Females are more prone to whiplash injuries than males [16]. Children have a lower risk of injuries leading to permanent medical impairment compared to adults. Nevertheless, injuries that lead to permanent medical impairment in children are mainly in the head and cervical spine [81]. Consequently, it is important to consider females and children in the development of new seatbelt systems.

The first objective of the study is to identify thresholds for neck injury criteria in females and children by performing dynamic tests on ATDs representative of 50th percentile female and a 6 year-old child.

Thereafter, static tests are conducted with these ATDs under the loading of PPT seatbelts for varying forces. The second objective is to obtain neck injury data and compare them with the thresholds from the dynamic testing in order to identify optimal force values to be used in future PPT seatbelts.

## 9 Methodology

### 9.1 Research subjects

*H-III6C* (Hybrid III six-year-old child) is a scaled down version of the HIII 50th percentile male ATD. It was designed to evaluate the risk of out-of-position child in an airbag environment. The *H-III6C* is equipped with 3 accelerometers in the head and 6 axis load cells in upper and lower neck. The dummy is tested dynamically under latest frontal crash environments.

*BioRID50F* the 50<sup>th</sup> percentile female is described in Part I under Section 3.2.1. (Page 9)

### 9.2 Dynamic tests

A series of sled tests were performed with two ATDs: a *BioRID50F* and a *H-III6C*. The dummies were positioned in a Volvo V60 [Y352] driver seat and fastened with a 3-point standard Volvo V60 seatbelt with no pyrotechnic pretensioning. The seat was at the mid low position with a seat back angle of 20 degrees. The child dummy was seated on a Volvo child booster (*Appendix 14.7*). The seat belt geometry and position were kept the same for repeated tests. Two compact high-speed cameras, MotionXtra N4-S2 with a resolution of 1016x1016pixels, were used to record the side and front views during the test. Coordinate systems were selected in agreement with SAE J211. *H-III6C* was equipped with an additional accelerometer at the T1 in order to collect data for injury criteria calculation. For safety reasons, the *BioRID50F* was strapped at the elbow joint ensuring that the motion was not compromised.

From an amusement park bumper car impact, a non-injurious crash pulse in children was identified [82]. A similar crash pulse was recreated with a maximum deceleration of 4g at 56ms and a delta V of 9km/h for the *H-III6C* test. A crash pulse with a mean acceleration of 6g and a delta V of 28km/h is non-injurious for AIS1 neck injuries in adults according to Kullgren et al [83]. *BioRID50F* was subjected to a similar pulse during the testing (*Appendix 14.7*).

### 9.3 Static tests

Static tests were performed on a test rig equipped with a Volvo 850 seat and a Volvo S60 pre-pretensioner seatbelt. *H-III6C*, *BioRID50F*, HIII50M and THOR were tested under PPT loading. The seat back was inclined at 20 degrees. A Casio EX-F1 high-speed camera of 1920x1080pixels was used to record the test. The sign convention compiled with the SAE J211 standard. The *H-III6C* was instrumented with an additional T1 accelerometer and was seated in a Volvo booster seat. A combination of batteries modulated the voltage to obtain different seatbelt forces (*Appendix 14.8*).



## 9.4 Data Analysis

The neck injury criteria used in this study to define injury assessment reference values were the  $N_{IJ}$  and the  $NIC_{protraction}$ . These are neck injury criteria that have been identified as relevant in this actual load case [79].

The seatbelt and ATDs were instrumented with sensors hence data was acquired directly from the data acquisition system. The filtering of the signals was carried out using DIAdem software. The  $N_{IJ}$  values were calculated with this program. However, the  $NIC_{protraction}$  values were calculated externally. The head x-acceleration signal was filtered with a CFC 1000 according to the FMVSS-208 regulation and the T1 x-acceleration was filtered with a CFC 60. Later, data was exported to MATLAB where the  $NIC_{protraction}$  values were obtained.

## 10 Results

### 10.1 Injury assessment reference values

Two different injury criteria were selected to define the risk of suffering AIS1 neck injuries:  $NIC_{\text{protraction}}$  and  $N_{IJ}$ . Data from mechanical sled tests and mathematical models are available and presented in the following paragraphs.

*Data from mechanical sled tests with physical dummies:* Injury criteria for the HIII 50<sup>th</sup> percentile male were taken from a research [79]. However, the values for BioRID50F and H-III6C were obtained from the dynamic tests performed during this study.

Table 10.1: Injury assessment reference values from mechanical sled tests

ATD	Acceleration [g]	Delta Velocity [km/h]	$N_{IJ}$	$NIC_{\text{protraction}}$ [m <sup>2</sup> /s <sup>2</sup> ]	Acquired from
HIII 50 <sup>th</sup> percentile male	6 (mean value)	28	0.26	25	Literature review [77]
BioRID50F	6 (mean value)	28	0.25 $N_{TF}$	20	Dynamic testing
H-III6C	4 (max. value)	9	0.1 $N_{TF}$	4	Dynamic testing

\* $N_{TF}=N_{IJ}$  in tension-flexion,  $N_{TE}=N_{IJ}$  in tension-extension,  $N_{CF}=N_{IJ}$  in compression-flexion,  $N_{CE}=N_{IJ}$  in compression-extension

*Data from MADYMO models of the HIII 50<sup>th</sup> percentile male:* In another study, injury assessment reference values for HIII 50<sup>th</sup> percentile male were obtained from MADYMO simulations. Real-world data from Folksam database involving 172 belted occupants in 144 real frontal crashes with known crash pulses were simulated and analyzed. The average delta velocity of the car was 22km/h and the average acceleration was 5g. The injury outcomes were defined as long term (injury after 6-months), short term and no neck injury. The assessment reference values were calculated based on the rounded median values of the neck injury criteria for the different injury outcomes [79].

Table 10.2: Injury assessment reference values from MADYMO simulations of HIII 50<sup>th</sup> percentile male [79]

Injury Outcome	$N_{IJ}$ (Median)	$NIC_{\text{protraction}}$ (Median) [m <sup>2</sup> /s <sup>2</sup> ]
Non injured	0.1	11
Injured (short term + long term)	0.16	15
Long term	0.21	25

Development of new restraint systems demands that the dummy loading in terms of NIC and  $N_{IJ}$  are lower than the injury assessment reference values. It can be observed that these reference values are more conservative in the mathematical simulations than in the mechanical models. Since PPT seatbelts are active restraints, they should be designed to ensure that there is no injury to the occupants. Therefore, the more conservative  $NIC_{protraction}$  and  $N_{IJ}$  values are selected as the injury assessment reference values.

### 10.3: Injury assessment reference values for static testing

Occupants	$N_{IJ}$	$NIC_{protraction}$ [m <sup>2</sup> /s <sup>2</sup> ]	Acquired from
Adults	0.1	11	Literature review [79]
Children	0.1	4	Dynamic testing

## 10.2 Neck loading for different seatbelt forces

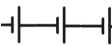
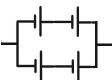
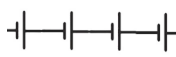
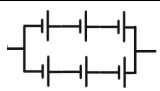
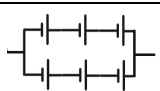
$N_{IJ}$  obtained for the H-III6C and BioRID50F at different seatbelt forces in a static test set-up are tabulated below.  $NIC_{protraction}$  values for H-III6C and BioRID50F were calculated but some inconsistencies were observed in T1 x-acceleration and head x-acceleration signals and hence the results were discarded.

Table 10.4: Injury criteria for different seatbelt forces in H-III6C

Voltage [V]	Seatbelt force [N]	$N_{IJ}$
22	200	0.05 $N_{TE}$ , 0.05 $N_{CE}$
22	370	0.03 $N_{TE}$ , 0.03 $N_{CE}$
37	544	0.04 $N_{TE}$ , 0.04 $N_{CE}$
37*	566	0.18 $N_{TE}$

\*The H-III6C was seated leaning forward

Table 10.5: Injury criteria for different seatbelt forces in BioRID50F

Voltage [V]	Battery configuration	Seatbelt force [N]	$N_{IJ}$
37		601	0.02 $N_{TE}$
24		599	0.01 $N_{TE}$ , 0.01 $N_{CE}$
50		603	0.01 $N_{TE}$ , 0.01 $N_{CE}$ , 0.01 $N_{CF}$
38		684	0.02 $N_{TE}$
38*		614	0.01 $N_{TE}$ , 0.01 $N_{CF}$ , 0.01 $N_{TF}$

\*The BioRID50F was seated leaning forward (Out of position) with the help of easy tear tape

A voltage value of more than 50V resulted in motor damage and as a consequence higher forces were not tested.

## 11 Discussions

In this study, neck injury assessment reference values were established for children and females. The thresholds in children are -  $NIC_{protraction}=4m^2/s^2$  and  $N_{IJ}=0.1$ . Similarly, thresholds in females are  $NIC_{protraction}=11m^2/s^2$  and  $N_{IJ}=0.1$ . These reference values could be used as a threshold for active seatbelt development in the future. Furthermore, these values were used as IARV (Injury assessment reference values) in the conducted static tests.

In static tests, it was observed that similar seatbelt forces produced higher T1 and head accelerations in the H-III6C than in BioRID50F. This observation is in congruence with Newton's second law; for the same force level, lower the mass, higher the acceleration. These results suggest that higher forces in active seatbelts may result in higher loadings to children than to adults.

The calculated  $N_{IJ}$  value ( $N_{IJ}=0.18$ ) for the H-III6C in a slightly forward leaning position exceeds the threshold ( $N_{IJ}=0.1$ ) when the seatbelt force is close to 600 N. In real life scenarios, children in a booster tend to sit in this position. According to a study, more than half of the driving time children were seated with the head in front of the front edge of the head side supports in a booster [84]. Another study indicates that children sitting postures are influenced by different factors, for example the activities performed, type of protection or discomfort. Some activities such as playing with electronic devices prolonged over a period of time. Playing resulted in a forward flexed sitting posture with the head leaning forward [85]. The results of the current study suggest that forces around 600N in a slightly leaning forward position might be harmful hence further investigation is required in order to implement active seatbelts with higher forces in children.

As a part of the study,  $NIC_{protraction}$  values for H-III6C and BioRID50F were calculated but some inconsistencies as discussed below were observed in T1 x-acceleration and head x-acceleration signals.

During the webbing retraction, the seatbelt contacts the torso first while the head moves later due to its inertia. As a result, the head x-acceleration signal lags behind the T1 x-acceleration as noticed in the dynamic tests results. However, this phenomenon was not observed in some static test results. Moreover, in static tests, the H-III6C acceleration signals indicate that the head and the T1 move in the opposite direction, which is not in harmony with the video observations. Due to these discrepancies, the  $NIC_{protraction}$  values were not enlisted as they might not be credible.

One possible explanation for these discrepancies is that the accelerometers used during the testing had a large range of measurement i.e poor resolution. Hence, they might not accurately measure very low acceleration values. In comparison with standard crash tests the static tests in this study were performed under relatively low loads. Accordingly, the head and T1 x-accelerations values were also very low and the sensor might not have registered them accurately. Another possibility is that the H-III6C was designed to evaluate the risk of out-of-position child in an airbag environment and might not produce precise results under low load conditions. Also,

the BioRID50F was a first prototype and the remaining tension in the neck spring after each test might have affected the results (*Appendix 14.9*).

There is a need to conduct further research for the development of active seatbelts. Aspects such as the risk of thoracic injuries, volunteers' kinematics or sensors' resolution should be taken into consideration.

## **11.1 Future work**

Recommendations for further research are suggested:

- It is recommended to consider PPT testing as a low load scenario and alter the data acquisition system and the sensors accordingly (higher resolution).
- Further investigation with high seatbelt forces should be done in adults and forces close to 600N in forward leaning position should be done in children.
- For better understanding of the results, it is suggested to record T1 x-acceleration and head x-acceleration signals by instrumenting volunteers with sensor during testing.
- It is needed to evaluate the risk of thoracic injuries in the development of active seatbelts particularly considering the elderly population. Due to time constraints, this was not included in the scope of the study.

## 12 Conclusion

Dynamic tests and literature review resulted in obtaining injury assessment reference values for neck injury evaluation under active seatbelt loading. The thresholds in children are-  $NIC_{\text{protraction}}=4\text{m}^2/\text{s}^2$  and  $N_{IJ}=0.1$ . Similarly, thresholds in females are  $NIC_{\text{protraction}}=11\text{m}^2/\text{s}^2$  and  $N_{IJ}=0.1$ . Static test results suggest that seatbelt forces close to 600N might be harmful in children when seated slightly leaning forward, which is one of the common positions.  $NIC_{\text{protraction}}$  values obtained from the static tests were discarded due to technical limitations. The static test was a low load scenario; hence the high-range accelerometers were not able to accurately measure the low acceleration values. For future testing, it is recommended to use sensors and data acquisition systems according to the loading scenarios. The results of this study could be a baseline to future restraint development in the automotive safety industry.

## 13 References

1. World Health Organization (2013): *Global status report on road safety -Supporting a decade of action*.
2. Peden M, Scurfield R, Sleet D, Mohan D, Hyder A.A, Jarawan E, Mathers C (2004): *World Report on Road Traffic Injury Prevention*, World Health Organization.
3. Fumihito K, Teruhiko K, Toshihito M, Takuhiro S: *Crash sled test based evaluation of a pre-crash seatbelt and an airbag to enhance protection of small drivers in vehicles equipped with autonomous emergency braking systems*, Japan, Paper Number 13-0241.
4. RCAR–IIWPG: *Seat/Head Restraint Evaluation Protocol (2008)*, Insurance Institute for Highway Safety, Arlington.
5. Keun J, Wook L.K: *Study on effectiveness of pre-crash active seatbelt using real time controlled simulation*, Lee Hyundai Mobis, Korea, Paper number 13-0097.
6. Hideo T, Hideo T, Chinmoy P, Shunichi F: *Development of pre-crash active seatbelt system for real-world safety*, Nissan Motor Co., Ltd. Japan Paper No. 189.
7. Good C.A, Viano D.C, Ronsky J.L (2008): *Biomechanics of Volunteers Subject to Loading by a Motorized Shoulder Belt Tensioner*.
8. Luders M (2003): *Out of Position Real Life Data, Representative Investigation in Germany*. Linz, Austria: European Vehicle Passive Safety Network II (EVPSN2) Workshop; June 30–July 2003.
9. Viano D.C, Gargan M.F (1995): *Headrest position during normal driving: Implications to neck injury risks in rear crashes*. The 39<sup>th</sup> Annual Proceedings of the AAAM, Association for the Advancement of Automotive Medicine, Des Plaines, OH, pp. 215–229
10. States J.D, Balcerak J.C (1973): *The effectiveness of head restraints in rear end impacts* (DOT-HS-800 877). National Highway Traffic Safety Administration, US Department of Transportation, Washington
11. Siegmund G.P, Heinrichs B.E, Wheeler J.B: *The influence of head restraint and occupant factors on peak head: neck kinematics in low-speed rear-end collisions*
12. Galasko C.S.B, Murray P.M, Pitcher M, Chambers H, Mansfield S, Madden M, Jordon C, Kinsella A, Hodson M (1993): *Neck Sprain after Road Traffic Accidents: A Modern Epidemic*, Injury, Vol. 24, No. 3, pp. 155–157
12. Krafft M (1998): *A Comparison of Short- and Long-Term Consequences of AISI Neck Injuries, in Rear Impacts*, Proc. IRCOBi Conf., Göteborg (Sweden), pp. 235–248

12. Hell W, Langwieder K, Walz F (1998): *Reported Soft Tissue Neck Injuries After Rear-End Car Collision*, Proc. IRCOBI Conf., Göteborg (Sweden), pp 261–274
13. Pobereskin L.H (2005): *Whiplash following rear end collisions: a prospective cohort study*. J Neurol Neurosurg Psychiatry, 2005. 76(8): p. 1146-1151.
14. Hohl M (1974): *Soft tissue injuries of the neck in automobile accidents: Factors influencing prognosis*. J Bone Joint Surg., 1974. 56A: p. 1675-1682.
15. Cassidy J.D (2000): *Effect of eliminating compensation for pain and suffering on the outcome of insurance claims for whiplash injury*. N Engl J Med, 2000. 342(16): p. 1179-1186.
16. Carlsson A (2012): *Addressing Female Whiplash Injury Protection A Step Towards 50<sup>th</sup> Percentile Female Rear Impact Occupant Models*. Department of Applied Mechanics Chalmers University of Technology SE-412 96 Gothenburg, Sweden
17. Kullgren A, Stigson H, Krafft M (2013): *Development of Whiplash Associated Disorders for Male and Female Car Occupants in Cars Launched Since the 80s in Different Impact Directions*, IRCOBI Conference 2013
18. Richter M, Otte D, Pohlemann T, Krettek C, Blauth M (2000): *Whiplash-Type Neck Distortion in Restrained Car Drivers: Frequency, Causes and Long-Term Results*, Eur. Spine J., Vol.9, No. 2, pp. 109–117
19. Kullgren A, Krafft M, Lie A, Tingvall C (2007): *The Effect of Whiplash Protection Systems in Real-Life Crashes and Their Correlation to Consumer Crash Test Programmes*, Proc. 20<sup>th</sup> ESV Conf. (07-0468), Lyon (France), pp. 1–7
20. Galasko CSB, Murray PM, Pitcher M, Chambers H, Mansfield S, Madden M, Jordon C, Kinsella A, Hodson M (1993): *Neck Sprain after Road Traffic Accidents: A Modern Epidemic*, Injury, Vol. 24, No. 3, pp. 155–157
21. Delannoy P, Diboine A (2001): *Structural Front Unit Global Approach*, Proc. 17th ESV Conf., Amsterdam (The Netherlands), pp. 1–11
22. Viano D (2008): *Seat Design Principles to Reduce Neck Injuries in Rear Impacts*, Traffic Inj.Prev., Vol. 9, No. 6, pp. 552–560
23. Otremski I, Marsh JL, Wilde BR, McLardy Smith PD, Newman RJ (1989): *Soft tissue cervical injuries in motor vehicle accidents*, Injury, Vol. 20, No. 6, pp. 349–351
24. Morris, A. and P. Thomas (1996): *Neck injuries in the UK cooperative crash injury study*. 40th Stapp Car Crash Conf, 1996, Albuquerque, NM: Society of Automotive Engineers, Inc.
25. Youdas J.W (1992): *Normal range of motion of the cervical spine: An initial goniometric study*. Phys Ther, 1992. 72(11): p. 770-780.



26. Van den Kroonenberg A (1998): *Human head-neck response during low-speed rear end impacts*, 42nd Stapp Car Crash Conf. 1998. Tempe, AZ
27. Stemper B.D, Yoganandan N, Pintar F.A (2004): *Gender- and region-dependent local facet joint kinematics in rear impact: implications in whiplash injury*. *Spine*, 2004. 29(16): p. 1764-1771.
27. Stemper B.D, Yoganandan N, Pintar F.A(2003): *Gender dependent cervical spine segmental kinematics during whiplash*, *J Biomech*, 2003. 36(9): p. 1281-1289.
28. Yoganandan N (2003): *Anatomic study of the mophology of human cervical facet joint*, *Spine*, 2003. 28(20): p. 2317-2323.
29. Chandrashekar N (2006): *Sex-based differences in the tensile properties of the human anterior cruciate ligament*, *J Biomech*, 2006. 39: p. 2943-2950.
30. Vasavada A.N, Li S, Delp S.L (2001): *Three-dimensional isometric strength of neck muscles in humans*, *Spine*, Vol. 26, No. 17, pp. 1904–1909.
30. Vasavada A.N, Danaraj J, Siegmund G.P (2008): *Head and Neck Anthropometry, Vertebral Geometry and Neck Strength in Height-Matched Men and Women*, *J Biomech*. Vol. 41, No.1, pp. 114–121.
31. Foust D.R, Chaffin D.B, Snyder R.G, Baum J.K (1973): *Cervical Range of Motion and Dynamic Response and Strength of Cervical Muscles*, Proc. 17th Stapp Car Crash Conf, Society of Automotive Engineers (730975), Warrendale, PA (USA), pp. 285–308.
32. States J.D, Balcerak J.C, Williams J.S, Morris A.T, Babcock W, Polvino R, Riger P, Dawley R.E (1972): *Injury Frequency and Head Restraint Effectiveness in Rear-End Impact Accidents*, Proc. 16th Stapp Car Crash Conf, SAE 720967, pp. 228–257.
33. Desantis K.K (2004): *Cervical spine geometry in the automotive seated posture: variations with age, stature, and gender*. *Stapp Car Crash J*, 2004. 48: p. 301-30.
34. Develet J.A (2013): *Evaluation of Anthropomorphic Test Devices under Seatbelt Pre-Pretensioner Loading. Collecting volunteer subjects data for crash test dummies Characterization towards further development of active restraints*, Master's Thesis in the Programme of Automotive Engineering 2013 Chalmers University of Technology, Sweden.
35. Beeman S, Kemper A, Madigan M, Franck C, Loftus S (2012): *Occupant kinematics in low-speed frontal sled tests: Human volunteers, Hybrid III ATD and PMHS*. *Journal of Accident Analysis and Prevention* (47), 128-139.
36. Törnqvall F.V, Holmqvist K, Davidsson J, Svensson M.Y, Håland Y and Öhrn H A (2007): *New THOR Shoulder Design: A Comparison with Volunteer s, the Hybrid III and THOR NT*. *Traffic Injury Prevention*, 8(2): 205–215, 2007.

37. Svensson M, *Lecture slides from Vehicle and Traffic Safety course* (2013): Chalmers University of Technology, Sweden.
38. Scott M.W, McConnell W.E, Guzman H.M, Howard R.P, Bomar J.B, Smith H.L, Benedict J.V, Raddin J.H and Hatsell C.P (1993): *Comparison of human and ATD head kinematics during low-speed rearend impacts*, SAE No. 930094.
39. Linder A, Thomson R, Svensson M, Carlsson A, Lemmen P, Schmitt K.U, Tomasch E (2013): *Occupant diversity in modeling and evaluation related to soft tissue neck injuries in low severity impact*, 16th Road Safety on Four Continents Conference, Beijing, China 15 - 17 May 2013.
40. Schneider L.W, Robbins D.H, Pflug M.S, Snyder R.G(1983): *Development of anthropometrically based design specifications for an advanced adult anthropometric dummy family*, Volume 1. University of Michigan Transportation Research Institute, Report No. UMTRI-83-53-1.
41. Doherty T.J, Vandervoort A.A, Brown W.F (1993): *Effects of ageing on the motor unit: a brief review*, Can J Appl Physiol 1993.
42. Pritz HB, Ulman MS (1989): *KMVSS 208 Belt Evaluation—Possible Modification to Accommodate Larger People*. SAE 890883, Society of Automotive Engineers, Warrendale, PA.
43. Jonsson B, Svensson M, Linder A, Björnstig U: *BioRID II manikin and human seating position in relation to car head restraint*, Department of Surgical and Perioperative Sciences, Division of Surgery.
44. Pheasant S (2006): *Bodyspace*, 2nd ed., CRC Press, London, UK, 2006.
45. Horst V.D, Thunnissen M, Happee J, Haaster V.R (1997): *The Influence of Muscle Activity on Head-Neck Response During Impact*, SAE Technical Paper 973346, 1997, doi: 10.4271/973346.
46. Ono K, Ejima S, Suzuki Y, Kaneoka K, Fukushima M, Ujihashi S (2006): *Prediction of Neck Injury Risk Based on the Analysis of Localized Cervical Vertebral Motion of Human Volunteers During Low-Speed Rear Impacts*. Proc. IRCOBI Conf., Madrid (Spain), pp.103–113.
47. Richmond B.C, Siegmund G.P: *What occupant kinematics and neuromuscular responses tell us about whiplash injury*.
48. Krafft M, Kullgren A, Lie A, Tingvall C (2003): *The Risk of Whiplash Injury in the Rear Seat Compared to the Front Seat in Rear Impacts*, Traffic Inj. Prev., Vol. 4, No. 2, pp. 136–140.
49. Foust D, Chaffin D, Snyder R, Baum J (1973): *Cervical Range of Motion and Dynamic Response and Strength of Cervical Muscles*, SAE Technical Paper 730975, 1973, doi: 10.4271/730975.

50. Davidsson J, Svensson M.Y, Flogård A, Håland Y, Jakobsson L, Linder A, Lövsund P, Wiklund K (1998): *BioRID - A New Biofidelic Rear Impact Dummy*, Proc. 1998 Int. IRCOBI Conference on the Biomechanics of Impact, Göteborg, Sweden, pp. 377-390.
51. Scott M.W, McConnell W.E, Guzman H.M, Howard R.P, Bomar J.B, Smith H.L, Benedict J.V, Raddin J.H, Hatsell C.P (1993): *Comparison of Human and ATD Head Kinematics During Low-Speed Rear-end Impact*. SAE paper 930094, SAE/SP-93/945, Society of Automotive Engineers, Warrendale, Philadelphia, ISBN 1-56091-330-4, pp. 1-8.
52. Humanetics. (n.d.). *Humanetics ATD*. Retrieved 03 23, 2015, from THOR: <http://www.humaneticsatd.com/crash-test-dummies/frontal-impact/thor-m>
53. Linder A (2001): *Neck injuries in Rear Impacts*, PhD Thesis, Department of Machine and Vehicle Systems, Crash Safety Division, Chalmers University of Technology, Göteborg, Sweden. ISBN 91-7291-106-9
54. David C, Viano, Chantal S, Parenteau L, Mark L, Edward: *Crash Injury Risks for Obese Occupants Using a Matched-Pair Analysis*, USA.
55. Flegal K M, Carroll M D, Ogden C L, Curtin L R (1999-2008): *Prevalence and trends in obesity among US adults, 1999–2008*. JAMA. 2010, 303:235–241.
56. Matthew P, Reed, Sheila M. Hamilton E, Jonathan D.R: *Effects of Obesity on Seat Belt Fit*, University of Michigan, USA.
57. Viano D.C, Parenteau C.S (2008): *Crash Injury Risks for Obese Occupants*, SAE 2008-01-0528, Society of Automotive Engineers, Warrendale, PA.
58. Pritz H.B, Ulman M.S (1989): *KMVSS 208 Belt Evaluation—Possible Modification to Accommodate Larger People*. SAE 890883, Society of Automotive Engineers, Warrendale, PA.
59. Lutz W, Sanderson W, Scherbov S (2008): *The coming acceleration of global population aging*. Nature 451, 716–719.
60. Kent R, Lee S.H, Darvish K, Wang S, Poster C.S, Lange A.W, Brede C, Lange D, Matsuoka F (2005): *Structural and material changes in the aging thorax and their role in crash protection for older occupants*, Stapp Car Crash J.49, 231–249.
61. Bansal V, Conroy C, Chang D, Tominaga G.T, Coimbra R (2010): *Rib and sternum fractures in the elderly and extreme elderly following motor vehicle crashes*.
62. Mages M, Seyffert M, Class U: *Analysis of the pre -crash benefit of reversible belt pre -pretensioning in different accident scenarios*, TRW Automotive GmbH Germany.
63. Craig A, Viano, David C, Ronsky, Janet L: *Biomechanics of Volunteers Subject to Loading by a Motorized Shoulder Belt Tensioner*.

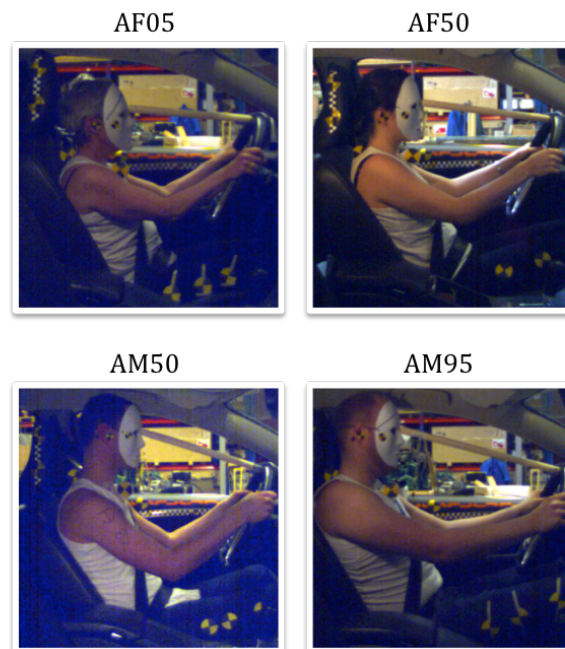
64. Schmitt K U (2010): *Trauma biomechanics: accidental injury in traffic and sports*, 2010, 3rd ed.
65. Mendoza Vazquez M (2014): *Thoracic injuries in frontal car crashes: risk assessment using a finite element human body model*, Chalmers University of Technology, 2014 Göteborg, ISBN: 978-91-7597-097-4.- 60 s.
66. Morgan R, Eppinger R, Haffner M (1994): *Thoracic trauma assessment formulations for restrained drivers in simulated frontal impacts*, Society of Automotive Engineers, Paper 942206, 1994.
67. Zhou, Rouhana S, Melvin J (1996): *Age effects on thoracic injury tolerance*, 40th Stapp Car Crash Conference, 1996, pp. 137–148.
68. Yamada H, Gaynor F, Williams E, Wilkins (1970): *Strength of biological materials*, University of Michigan, USA.
69. Stein I.D, Granik G (1976): *Rib structure and bending strength: an autopsy study*, *Calcified tissue research*, Vol. 20, pp.61-73.
70. Wheelless C.R: *Wheelless' Textbook of Orthopaedics*, Data Trace Publishing Company, Duke University Medical Center's Division of Orthopaedic Surgery, USA.
71. Kent R, Patrie J (2004): *Chest deflection tolerance to blunt anterior loading is sensitive to age but not load distribution*, Center for Applied Biomechanics, University of Virginia, USA.
72. McCormick W.F(1980): *Mineralization of the costal cartilages as an indicator of age: preliminary observations*, *J Forensic Sci* 25:736-741.
73. Kent R, Patrie J, Poteau F, Matsuoka F, Mullen C: *Development of an age-dependent thoracic injury Criterion for frontal impact restant loading*, University of Virginia USA, Toyota Motor Corporation Japan Paper No. 72.
74. Kent R, Patrie J, Benson N: *The hybrid III dummy as a discriminator of injurious and non-injurious restraint loading*, Department of Mechanical and Aerospace Engineering University of Virginia Charlottesville, VA Collision Safety Engineering, LC Orem, UT.
75. Nahum A.M, Melvin J.W(1993): *Accidental injury. Biomechanics and Prevention*, Springer-Verlag.
76. DePuy Synthes Spine. (n.d.), Retrieved April 24, 2015, Allaboutbackandneckpain.com <http://www.allaboutbackandneckpain.com/understand/anatomy.asp#>
77. Bohman K, Boström O, Håland Y, Kullgren A (2000): *A Study of AISI Neck Injury Parameters in 168 Frontal Collisions Using a Restrained Hybrid III Dummy*, Autoliv Research, Folksam Research, 44th Stapp Car Crash Conference, The Stapp Association.

78. Eichberger A, Steffan H (1999): *The neck injury criterion (NIC) in dummy tests: a mathematical simulation study*, International IR- COBI Conference on the Biomechanics of Impact, Sitges, Spain, pp. 535–537.
79. Boström O, Bohman K, Håland Y, Kullgren A, Krafft M (2000): *New AISI long term neck injury criteria candidates based on real frontal crash analysis*, IRCOBI conference proceedings, Montpeiller, France, 2000.
80. Eppinger R, Sun E, Bandak F, Haffner M, Khaewpong N, Maltese M, Kuppa S, Nguyen T, Takhounts E, Tannous R, Zhang A: *Development of Improved Injury Criteria for the Assessment of Advanced Automotive Restraint Systems - II*, National Highway Traffic Safety Administration, National Transportation Biomechanics Research Center (NTBRC), Conrad Technologies, Inc.
81. Bohman K, Stigson H, Krafft M (2014): *Long-Term Medical Consequences for Child Occupants 0 to 12 Years Injured in Car Crashes*, Autoliv Research; Department of Clinical Neuroscience, Karolinska Institutet; Folksam Research; Department of Surgical and Perioperative Sciences, Umeå University; Sweden.
82. Arbogast K.B, Balasubramanian S, Seacrist T, Maltese M.R, García-España J.F, Constans E, Lopez-Valdes F.J, Kent R.W, Tanji H (2009): *Comparison of Kinematic Responses of the Head and Spine for Children and Adults in Low-Speed Frontal Sled Tests*, Stapp car crash journal.
83. Kullgren A (1998): *Validity and reliability of vehicle collisions data*, Doctoral Thesis, Karolinska institute, 1998. ISBN 91-628-3280-8.
84. Anderson M, Bohman K, Osvalder A.L (2007): *Effect of Booster Seat Design on Children's Choice of Seating Positions During Naturalistic Riding*; Sweden.
85. Osvalder A.L, Hansson I, Stockman I, Carlsson A, Bohman K, Jakobsson L (2013): *Older Children's Sitting Postures, Behaviour and Comfort Experience during Ride – A Comparison between an Integrated Booster Cushion and a High-Back Booster*; IRCOBI Conference 2013.
86. Ono K, Kaneoka K, Wittek A, Kajzer J (1997): *Cervical Injury Mechanism Based on the Analysis of Human Cervical Vertebral Motion and Head-Neck-Torso Kinematics During Low Speed Rear Impacts*; SAE Technical Paper 973340, 1997, doi: 10.4271/973340.
87. Burdi A R, Huelke D F, Snyder R G, Lowrey G H: *Infants and children in the adult world of automobile safety design: Pediatric and anatomical considerations for design of child restraints*.
88. Bohman K, Boström O, Olsson J, Håland Y (2006): *The effect of a Pretensioner and a Load Limiter on a HIII 6Y, Seated on Four Different Types of Booster Cushions in Frontal Impacts*; Proc. IRCOBI 2006; 34: 377

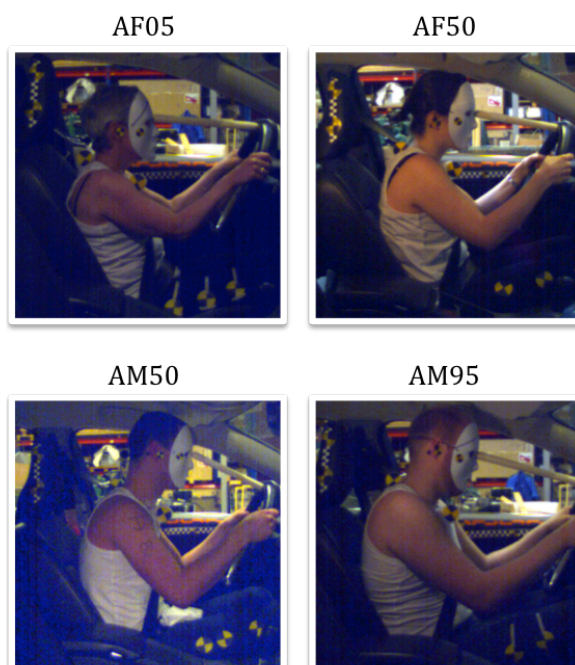
## 14 Appendix

### 14.1 Initial test positions for all volunteer sizes

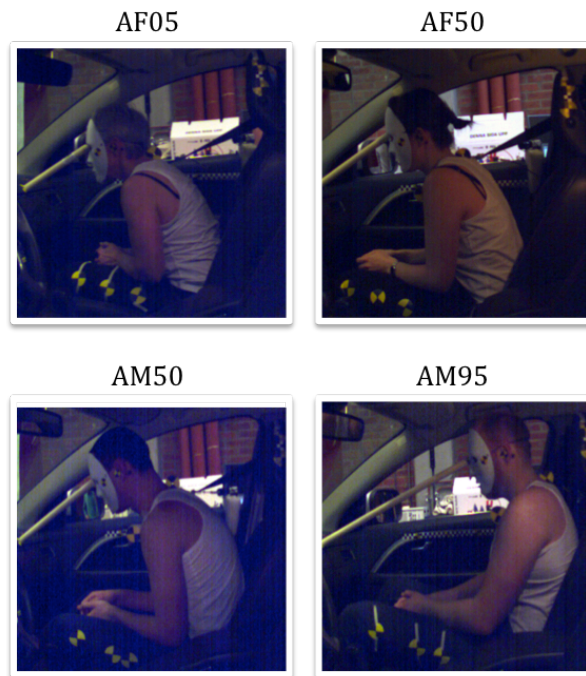
Volunteers of different sizes seated in the same position were captured as screenshots from TEMA3.5-012. The captures illustrate the differences and similarities amongst the varying size groups.



*Figure 14.1: Position 1, Real life normal driving*



*Figure 14.2: Position 2, Attempting to increase visibility at intersections*



*Figure 14.3: Position 3, Searching the glove box*



*Figure 14.4: Position 4, Talking to forward occupants*

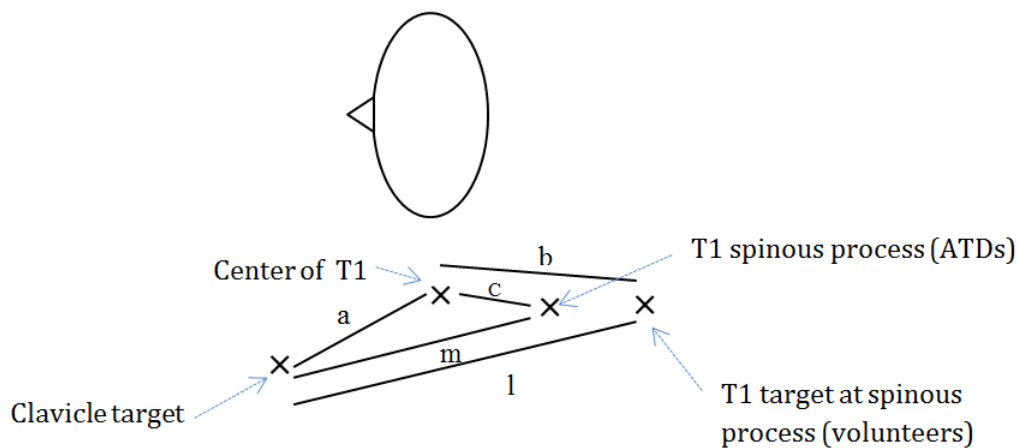


## 14.2 Locating the centre of T1

Three-dimensional medical imaging techniques such as computed tomography (CT) are utilized to capture anatomic information. The International Center for Automotive Medicine (ICAM) morphomics database was created after the analysis of CT scans to construct more detailed and anatomically correct human body models. Consistency was maintained with the previous master thesis [34] by following the same procedure to locate the center of T1. A set of N=150 subjects from the ICAM morphomics database was available. These subjects were grouped based on the anthropometric criteria used for the volunteer subjects recruitment resulting in N=3 AF05 subjects, N=9 AF50 subjects and N=12 AM95 subjects. Different notations were used for volunteer subjects (“T1 target at spinous process”) and for ATDs (“T1 spinous process”).

*Table 14.1: Location of the centre of T1 based on anthropometric landmarks.  
Procedure adopted from J.Adrien [34]*

Distances [mm]		AF05		AF50		AM95	
		Average	SD	Average	SD	Average	SD
l	Clavicle target to T1 skin target at spinous process	182	20	196	8	233	19
a	Clavicle target to the center of T1	102	7	100	7	119	10
b	T1 skin target at spinous process to the center of T1	82	13	97	10	115	12
c	Spinous process of T1 to the center of T1	47	2	49	2	57	2
m	Spinous process of T1 to clavicle target	148	9	148	6	175	11



*Figure 14.5: Graphical representation of the distances for Table 13.1. Adapted from J.Adrien 2013 [34].*

This method was validated against skeleton projections for AM95 and AF05 from the University of Michigan Research Institute (UMTRI). Film targets were placed on scaled drawings and hand measurements were performed to validate the method.



Table 14.2: Validation of the method for AM95 (N=12)

	Distances [mm]	Morphomics Average	SD	UMTRI	Relative difference	Percentage difference
l	Clavicle target to T1 skin target at spinous process	233	19	230	3	1.3 %
a	Clavicle target to the center of T1	119	10	116	3	2.6 %
b	T1 skin target at spinous process to the center of T1	115	12	123	8	6.5 %

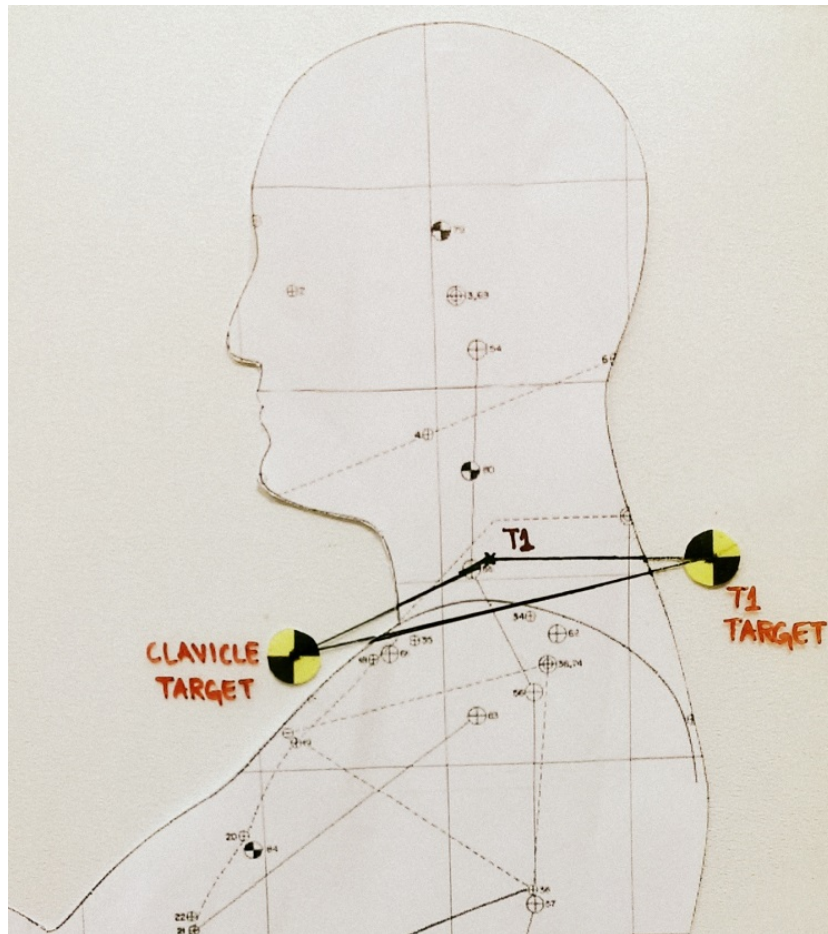
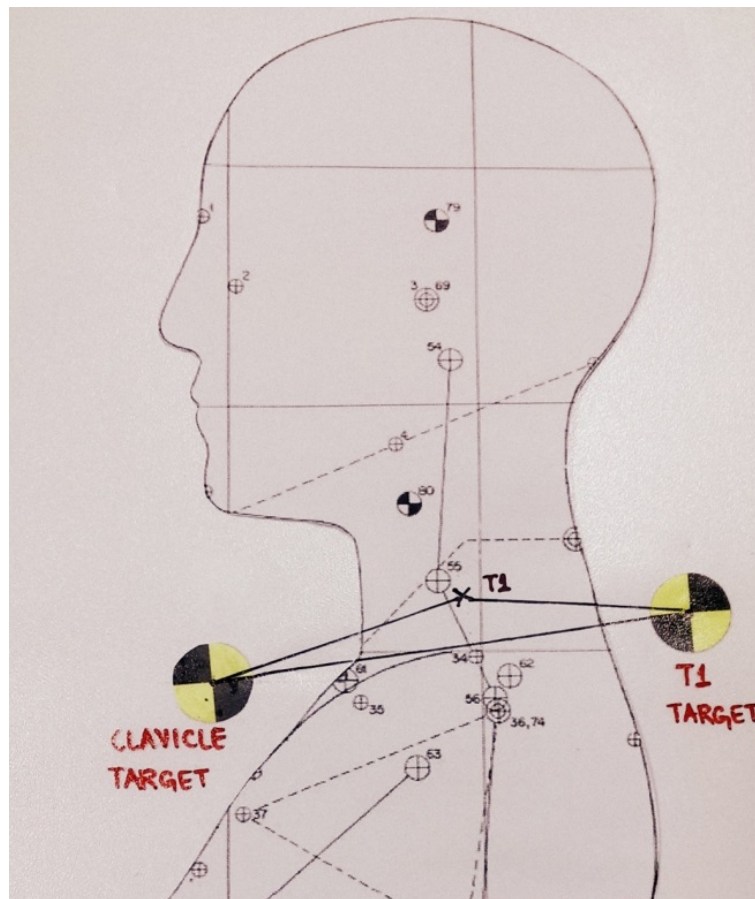
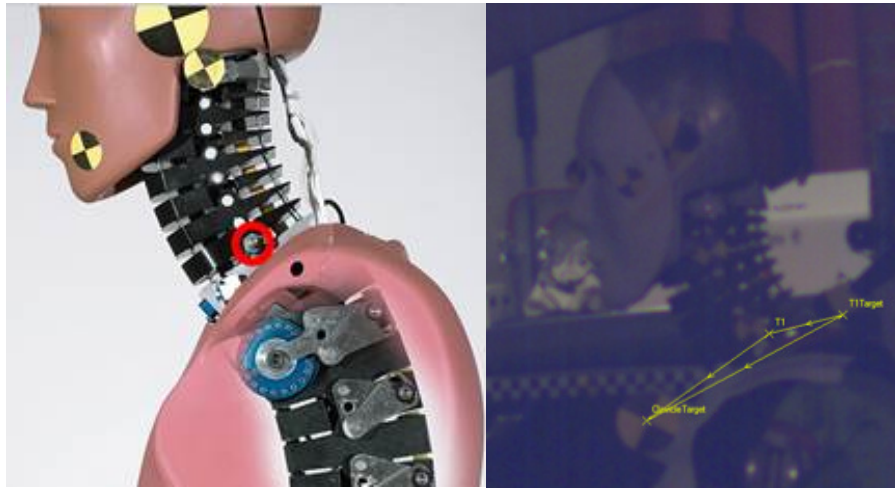


Figure 14.6: Validation of the method with UMTRI data (AM95)

Distances [mm]		Morphomics Average SD		UMTRI	Relative difference	Percentage difference
l	Clavicle target to T1 skin target at spinous process	182	20	193	11	5.7 %
a	Clavicle target to the center of T1	102	7	105	3	2.9 %
b	T1 skin target at spinous process to the center of T1	82	13	91	9	9.9%



There is no UMTRI data available for the evaluation of AF50 subjects. However, it was possible to verify if the method was matching the position of the T1 in the BioRID50F dummy. According to the manufacturer, the location of the center of T1 corresponds to the screw encircled in red (*Figure 13.8*). The previously discussed method was followed to locate the center of T1 on the BioRID50F video in TEMA3.5-012. It was verified that the center of T1 matches the position of the encircled screw as suggested by the manufacturer.



*Figure 14.8: Centre of T1 in BioRID50F (50<sup>th</sup> percentile female ATD)*

## 14.3 Volunteers' corridor plots

### 14.3.1 95<sup>th</sup> percentile male (AM95)

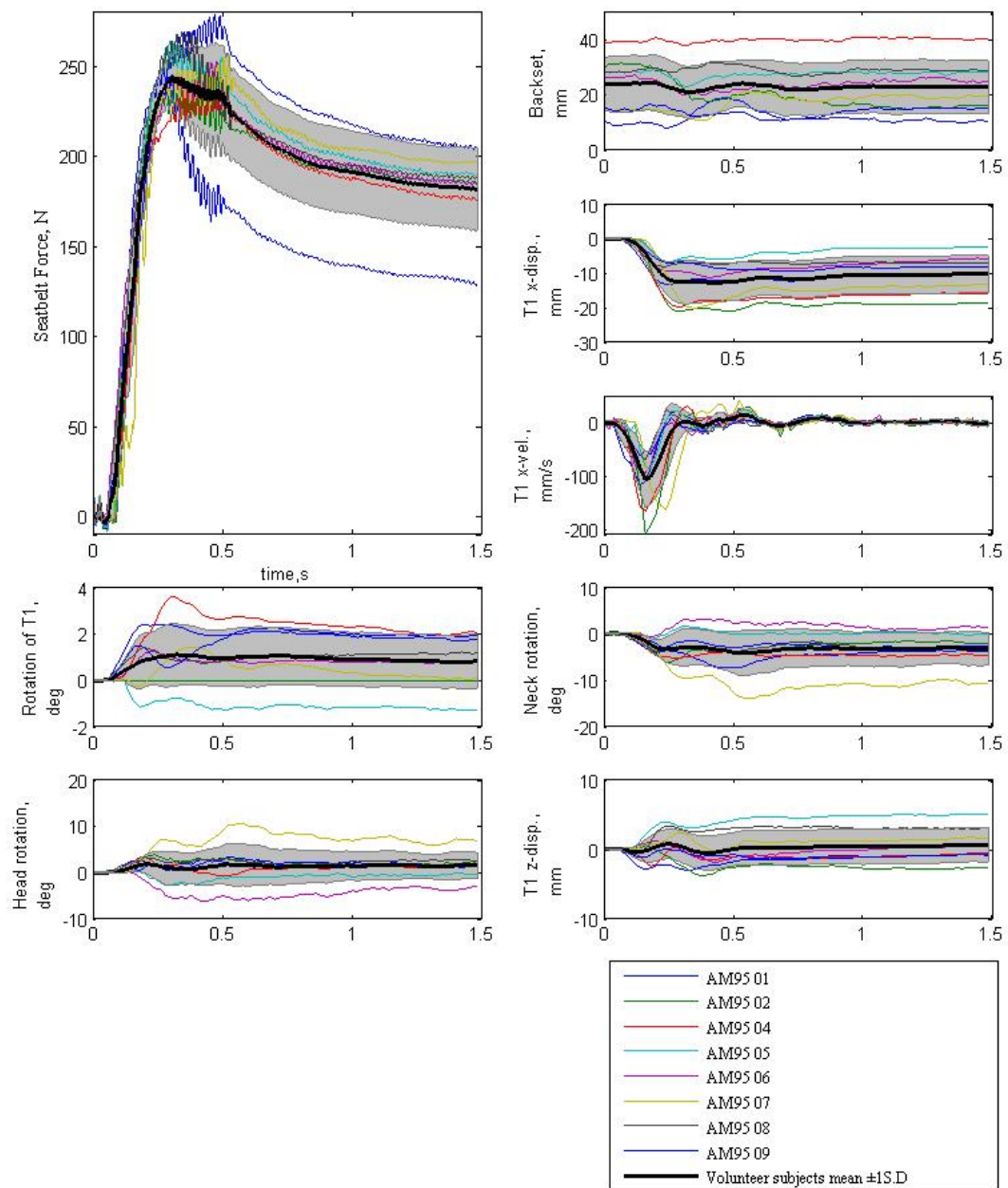


Figure 14.9: AM95 volunteers in position 1

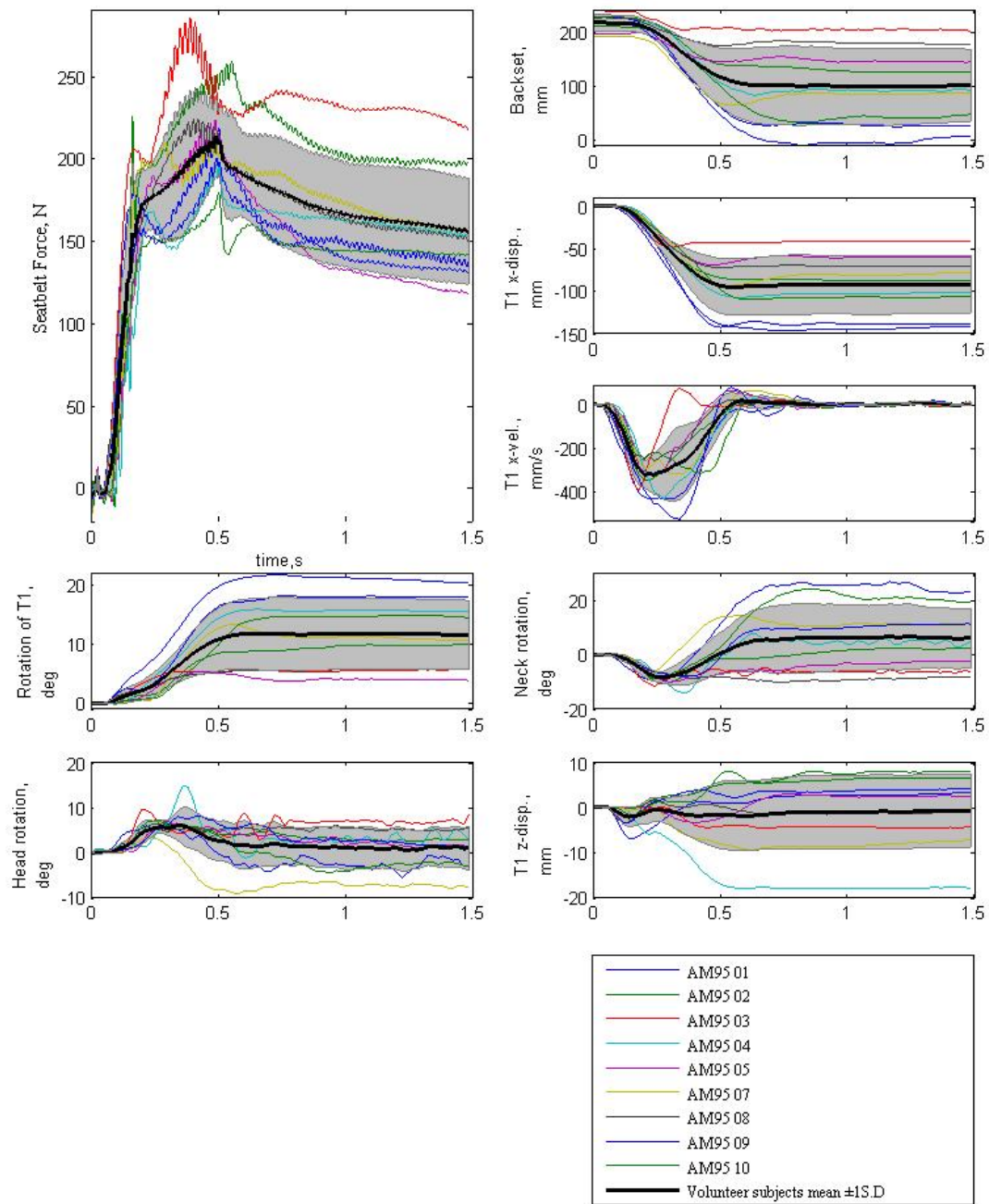


Figure 14.10: AM95 volunteers in position 2



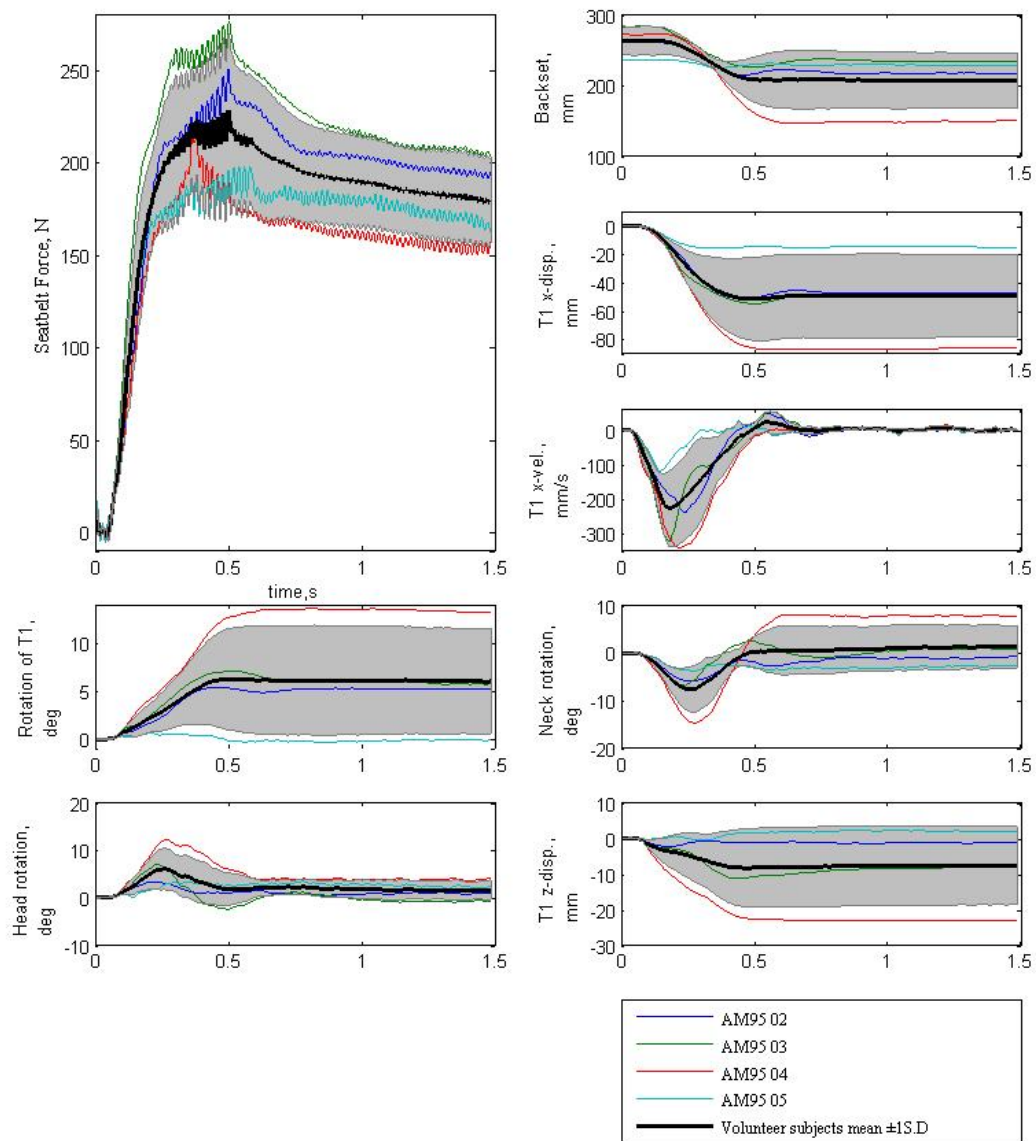


Figure 14.11: AM95 volunteers in position 3

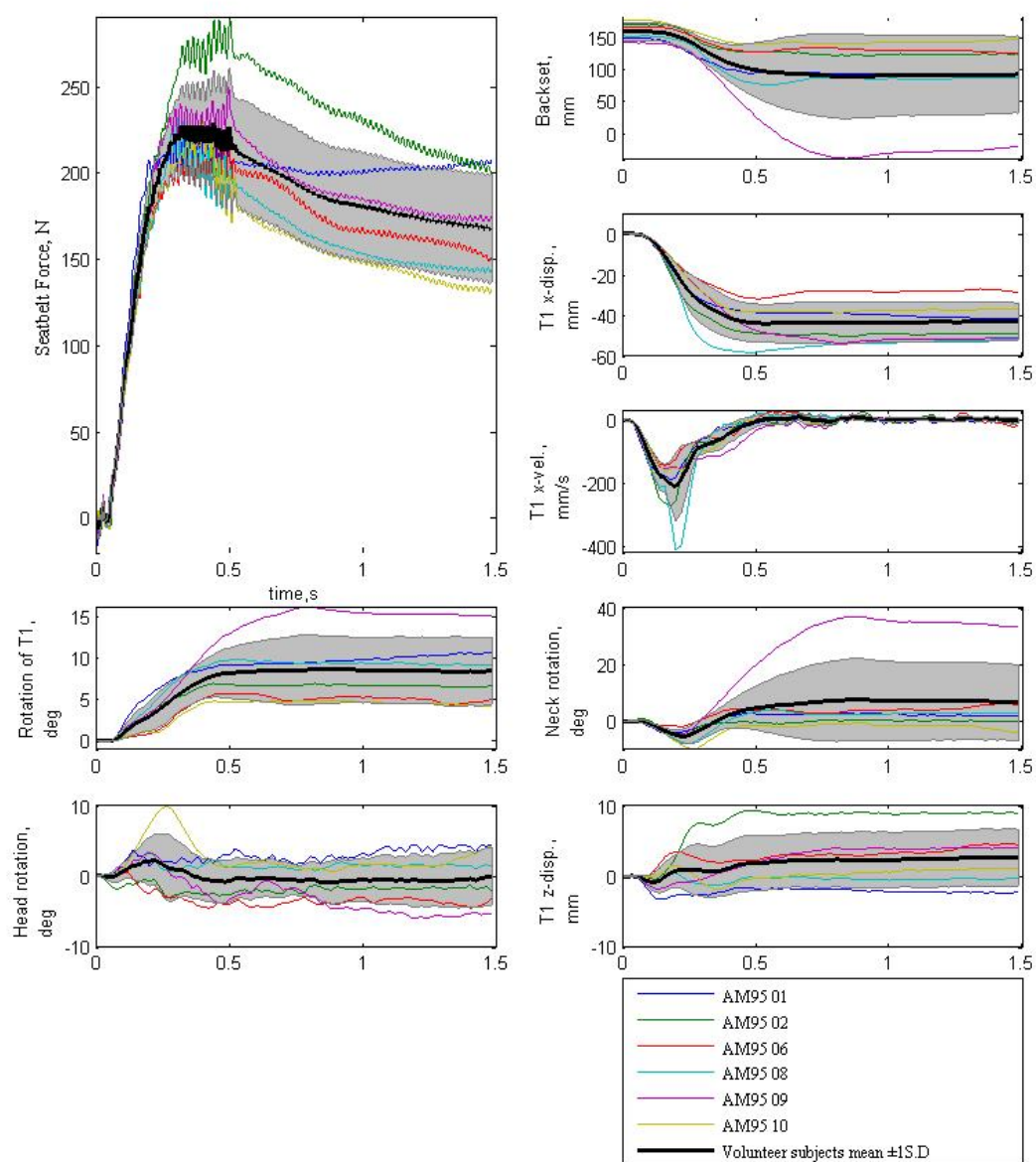


Figure 14.12: AM95 volunteers in position 4

### 14.3.2 50<sup>th</sup> percentile female (AF50)

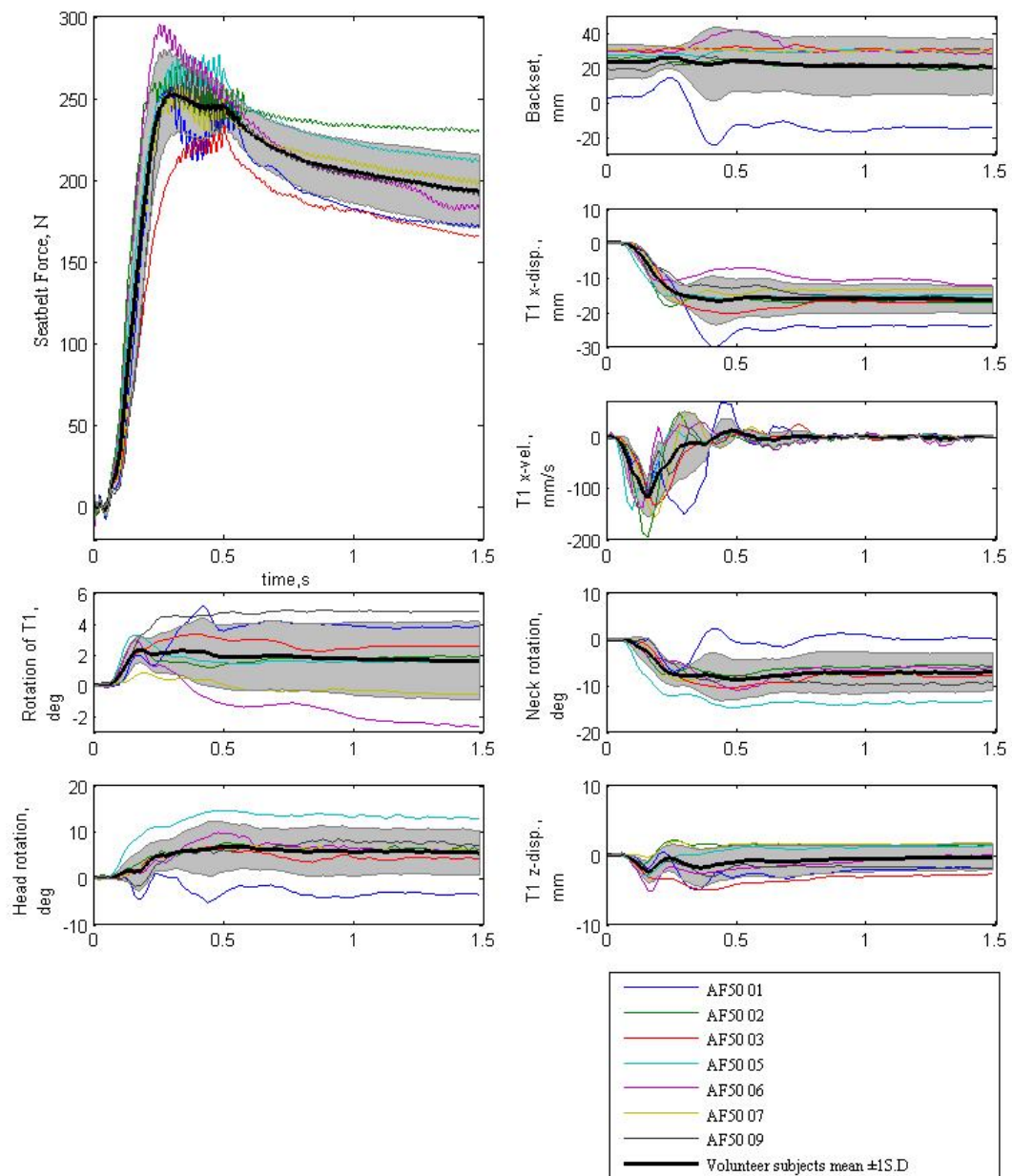


Figure 14.13: AF50 volunteers in position 1



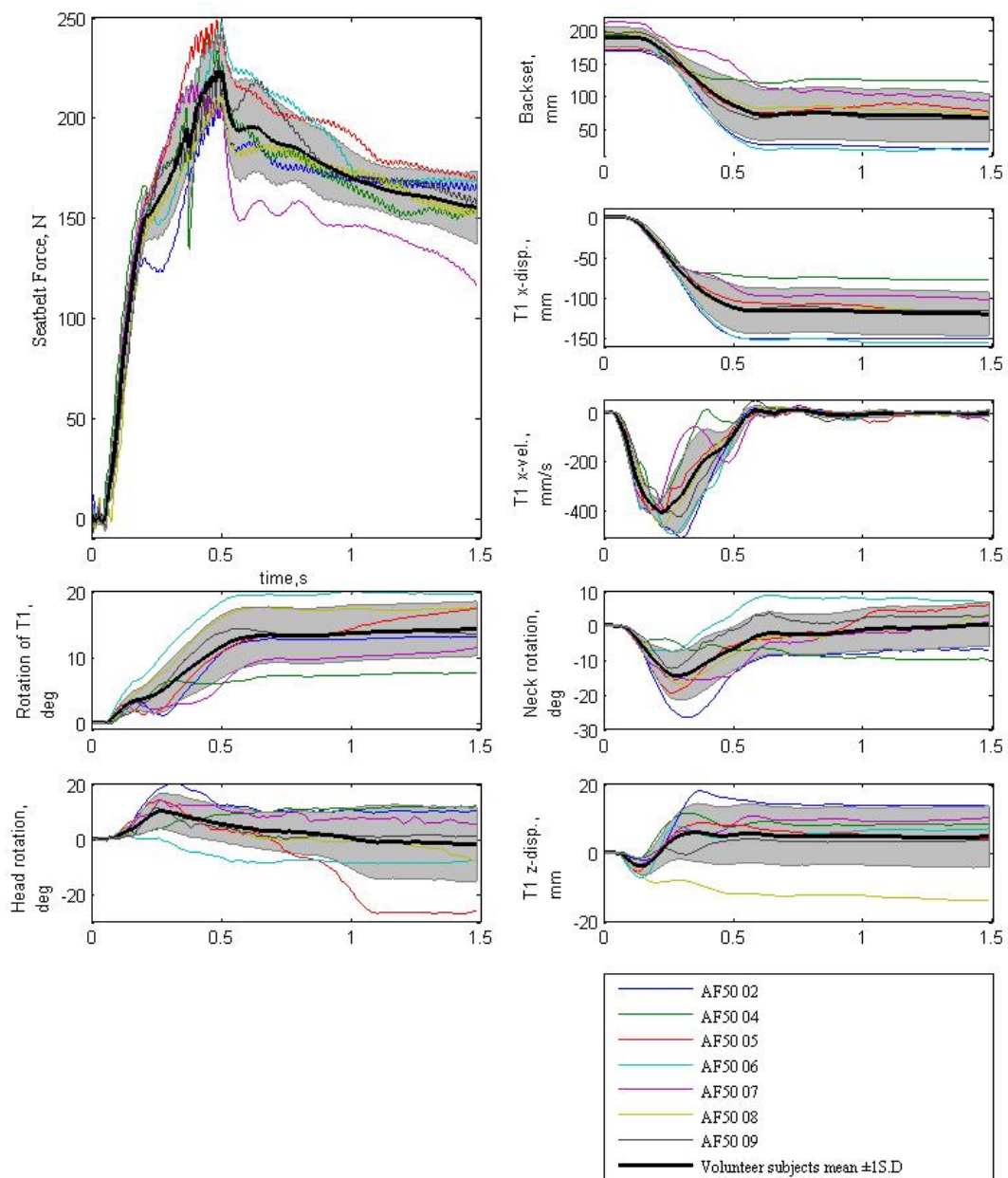


Figure 14.14: AF50 volunteers in position 2

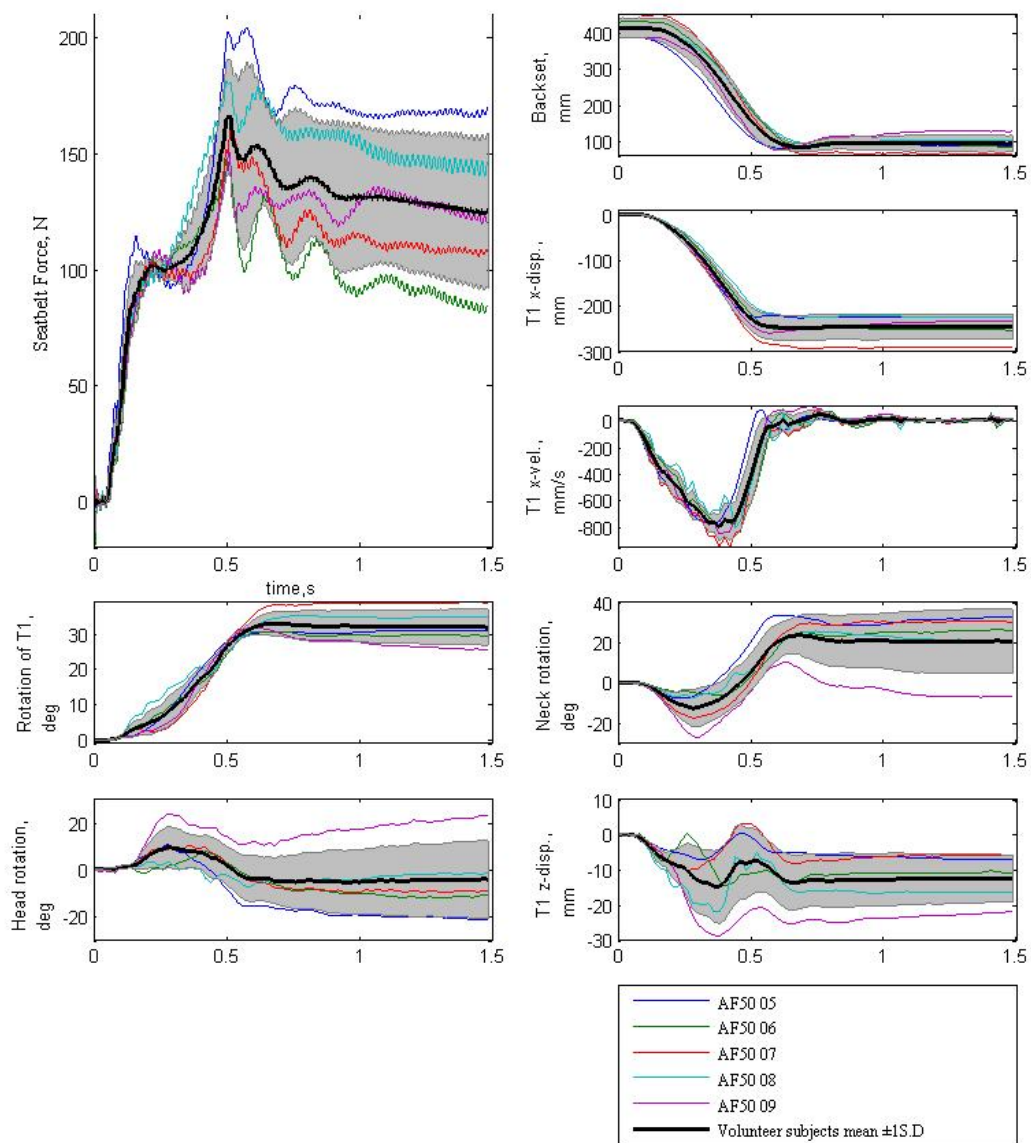


Figure 14.15: AF50 volunteers in position 3

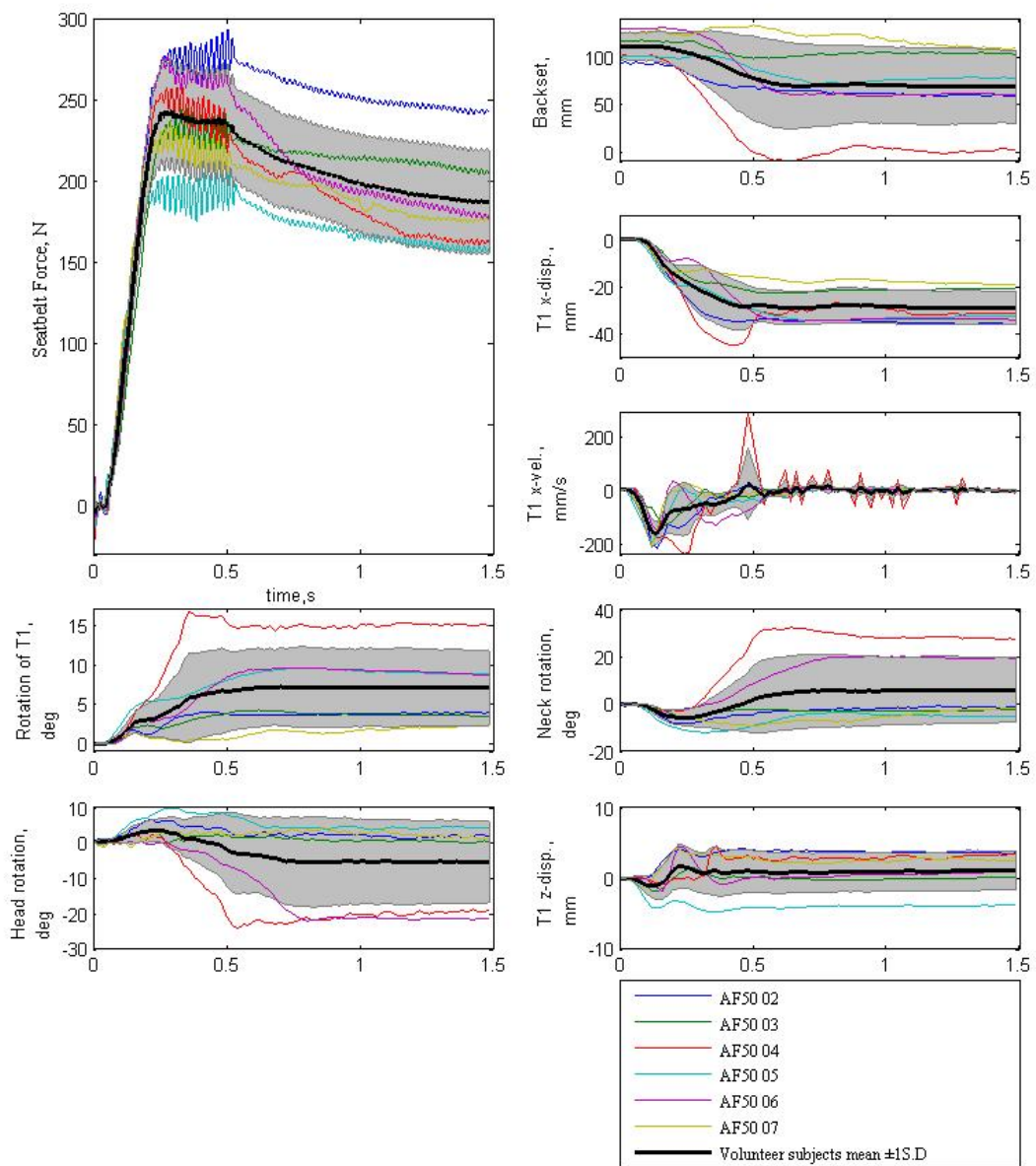


Figure 14.16: AF50 volunteers in position 4

### 14.3.3 5<sup>th</sup> percentile female (AF05)

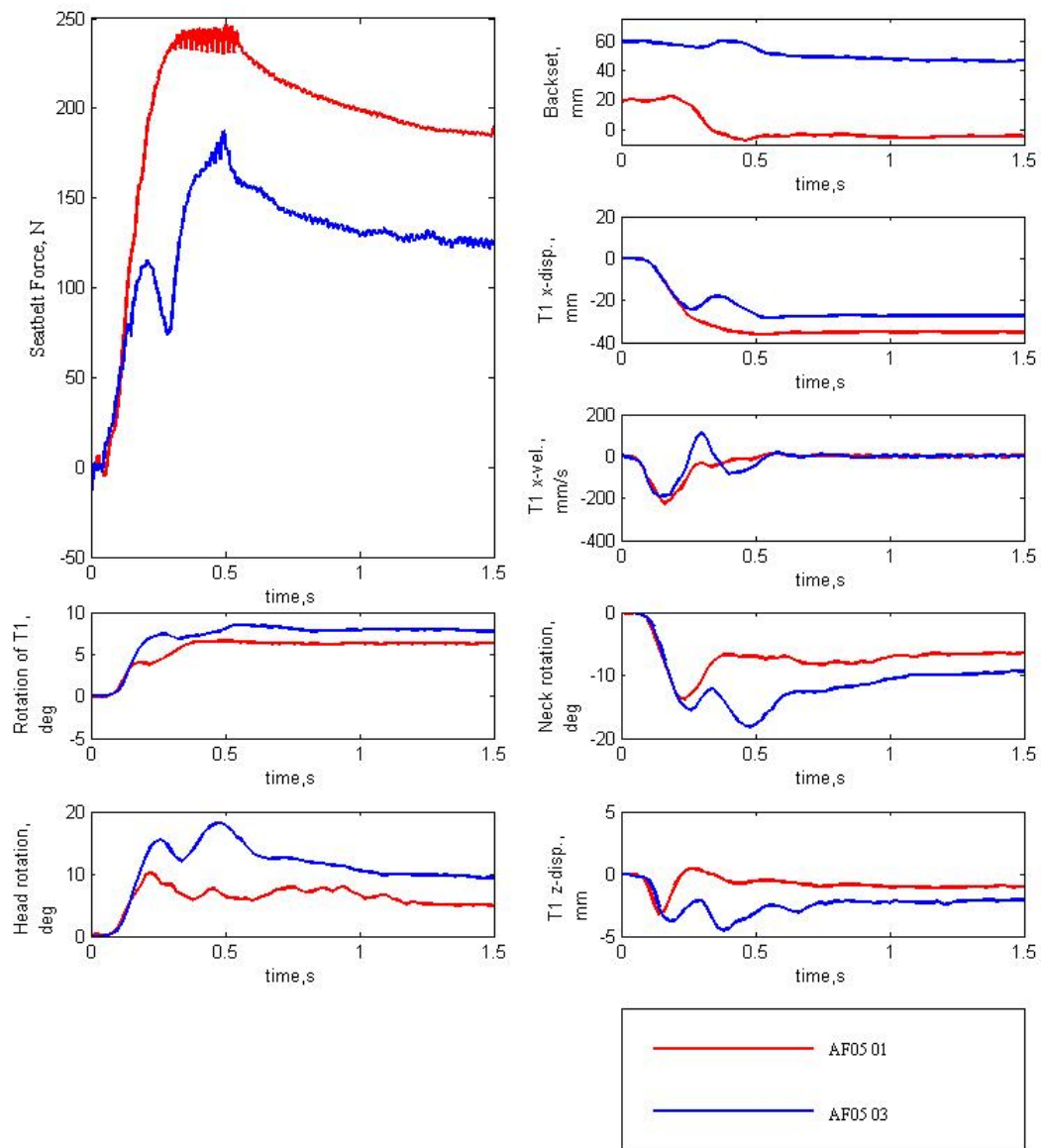


Figure 14.17: AF05 volunteers in position 1

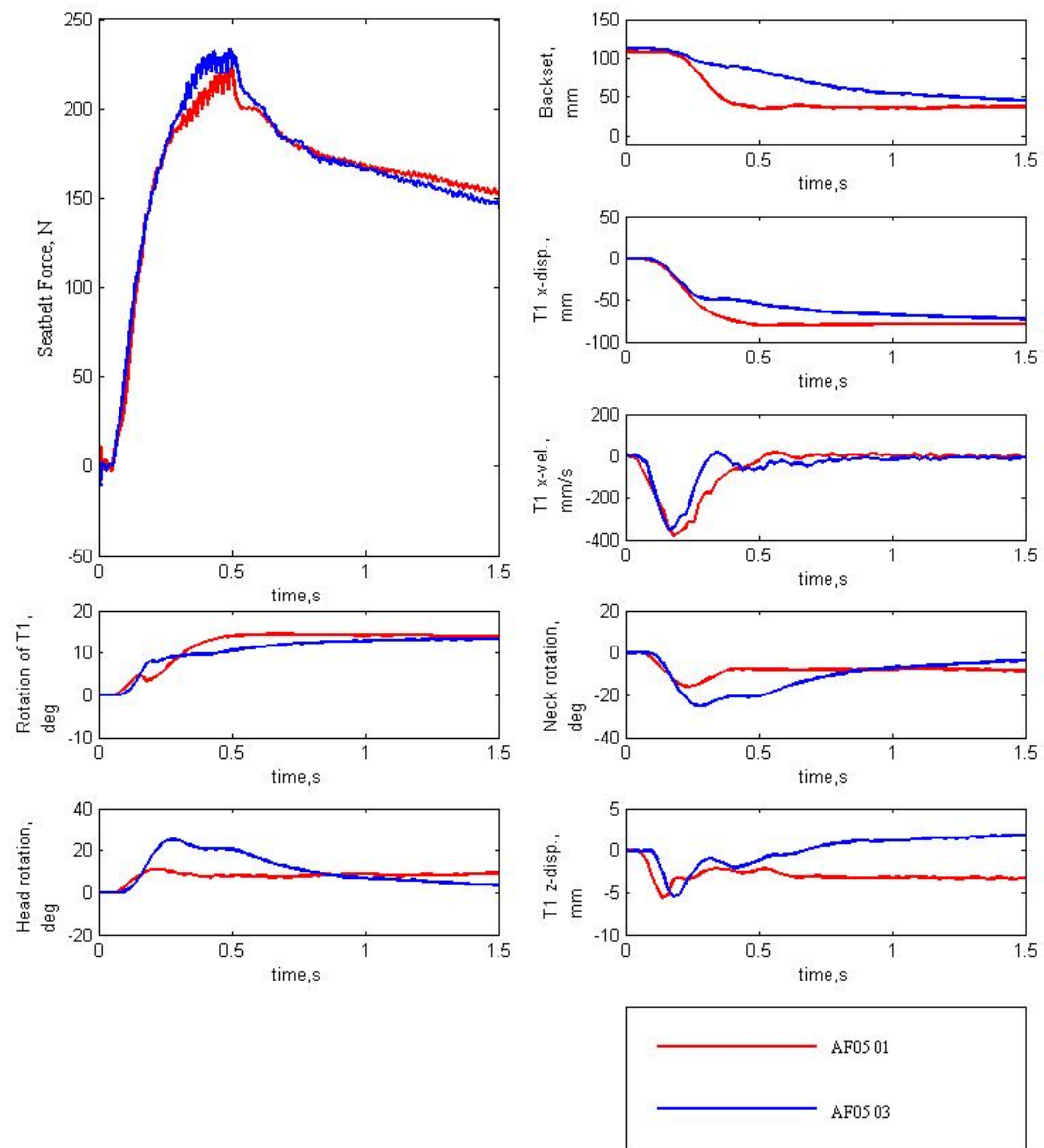


Figure 14.18: AF05 volunteers in position 2

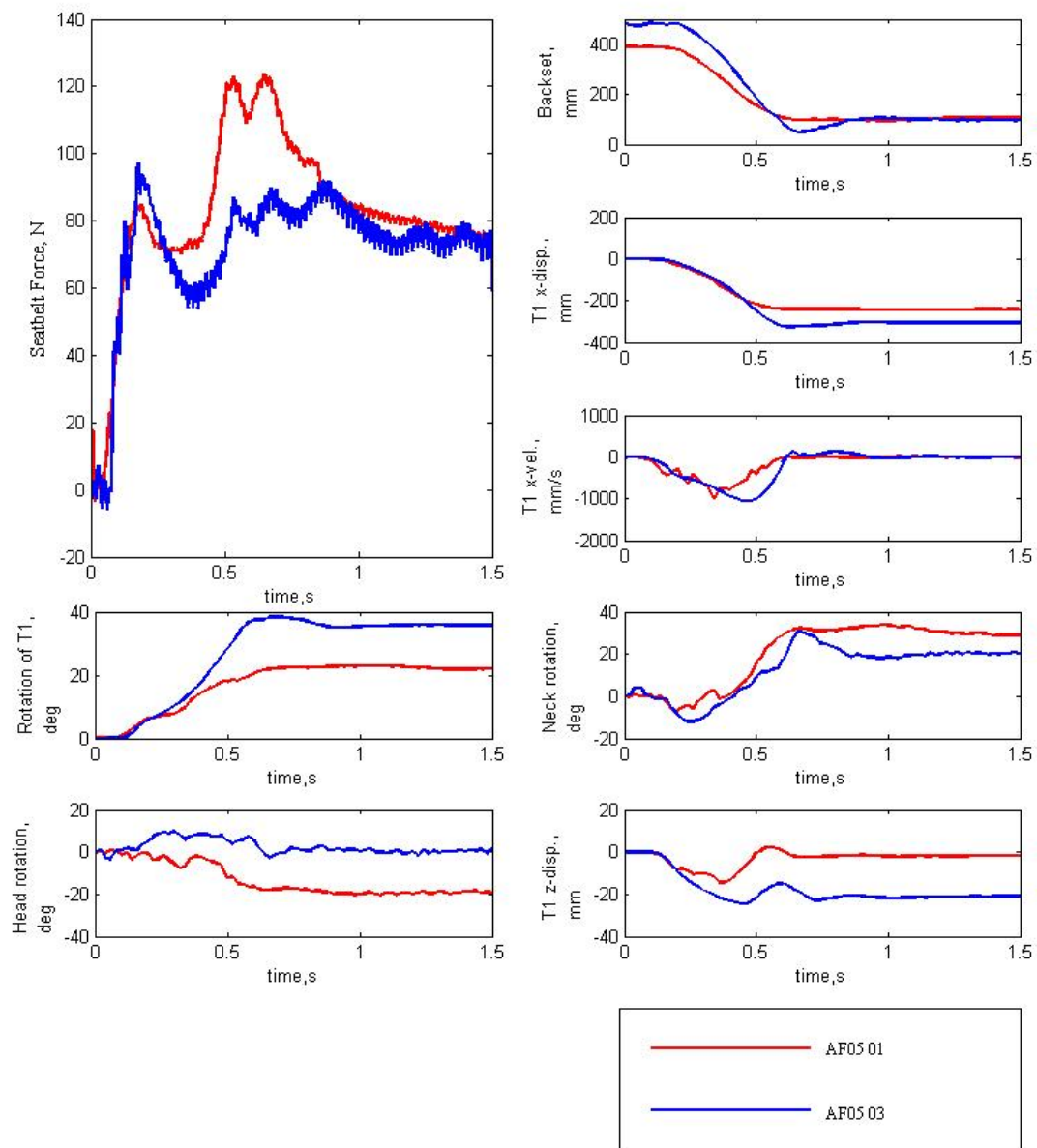


Figure 14.19: AF05 volunteers in position 3

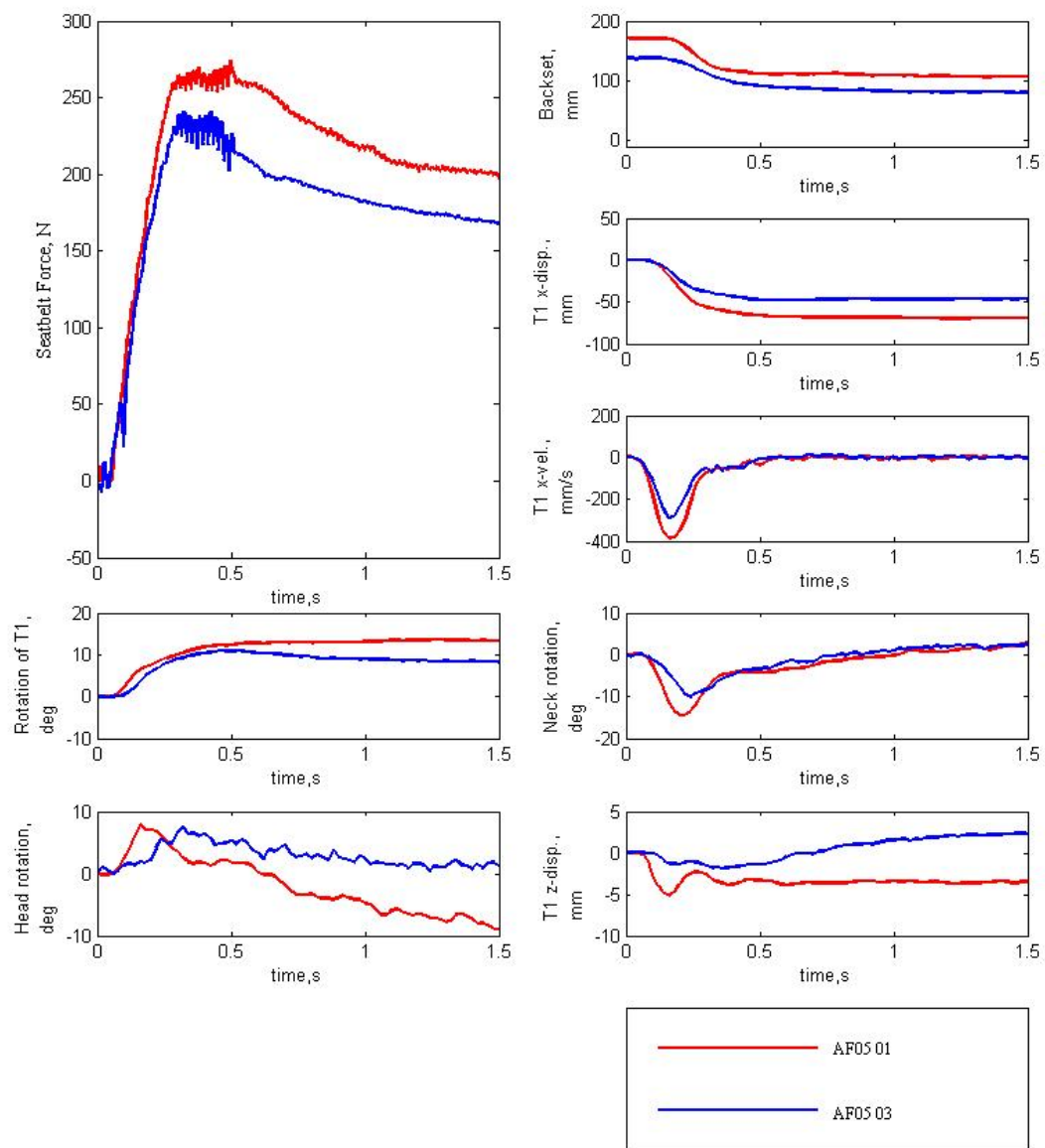


Figure 14.20: AF05 volunteers in position 4



## 14.4 Tables corresponding to habituation effect

### 14.4.1 95<sup>th</sup> percentile male (AM95)

*Table 14.4: Peak occurrence and seatbelt force for 1<sup>st</sup> and 2<sup>nd</sup> peak for driver seat, hands on the lap*

Subject	1 <sup>st</sup> Peak occurrence (s)	1 <sup>st</sup> Peak Force level (N)	2 <sup>nd</sup> Peak occurrence (s)	2 <sup>nd</sup> Peak Force level (N)
AM95 01 First Test	0.35	241	0.48	231
AM95 01 Second Test	0.35	248	0.48	252
AM95 05 First Test	0.25	266	0.4	263
AM95 05 Second Test	0.28	265	0.49	236
AM95 06 First Test	0.29	260	0.5	255
AM95 06 Second Test	0.29	250	0.51	250
AM95 07 First Test	0.25	240	0.48	252
AM95 07 Second Test	0.18	178	0.5	112

*Table 14.5: Amplitude, peak occurrence and asymptote of backset for driver seat, hands on the lap*

Subject	Amplitude (mm)	Peak occurrence (s)	Asymptote (mm)
AM95 01 First Test	15	/	70
AM95 01 Second Test	10	/	65
AM95 05 First Test	15	0.28	73
AM95 05 Second Test	22	0.4	73
AM95 06 First Test	20	0.38	78
AM95 06 Second Test	/	/	108
AM95 07 First Test	/	/	42
AM95 07 Second Test	/	/	57

*Table 14.6: Amplitude, peak occurrence and asymptote of T1 x-displacement for driver seat, hands on the lap*

Subject	Amplitude (mm)	Peak occurrence (s)	Asymptote (mm)
AM95 01 First Test	25	0.4	22
AM95 01 Second Test	17	0.3	17
AM95 05 First Test	9	0.22	1.5
AM95 05 Second Test	12	0.4	8.5
AM95 06 First Test	20	0.44	13
AM95 06 Second Test	14	0.42	9.5
AM95 07 First Test	32	0.26	20
AM95 07 Second Test	18	0.28	14



*Table 14.7: Amplitude, peak occurrence and asymptote of T1 x-velocity for driver seat, hands on the lap*

Subject	Amplitude (mm/s)	Peak occurrence (s)	Asymptote (mm/s)
AM95 01 First Test	157	0.18	1.5
AM95 01 Second Test	140	0.16	1.5
AM95 05 First Test	131	0.18	1.5
AM95 05 Second Test	131	0.18	1.5
AM95 06 First Test	182	0.2	1.5
AM95 06 Second Test	125	0.18	1.5
AM95 07 First Test	166	0.26	1.5
AM95 07 Second Test	177	0.2	1.5

*Table 14.8: Amplitude of head and neck rotations*

Subject	Head rotation (deg)	Neck rotation (deg)
AM95 01 First Test	2.5	5
AM95 01 Second Test	3.5	6
AM95 05 First Test	3	3
AM95 05 Second Test	2	3
AM95 06 First Test	3.5	3
AM95 06 Second Test	1.5	6
AM95 07 First Test	8	9
AM95 07 Second Test	7.5	11

*Table 14.9: Amplitude of T1 z-displacement for driver seat, hands on the lap*

Subject	T1- z displacement (mm)
AM95 01 First Test	5
AM95 01 Second Test	3
AM95 05 First Test	4
AM95 05 Second Test	3
AM95 06 First Test	5
AM95 06 Second Test	4
AM95 07 First Test	3
AM95 07 Second Test	1.5

### 14.4.2 50<sup>th</sup> percentile female (AF50)

*Table 14.10: Peak occurrence and seatbelt force for 1<sup>st</sup> and 2<sup>nd</sup> peak for driver seat, hands on the lap*

Subject	1 <sup>st</sup> Peak occurrence(s)	1 <sup>st</sup> Peak Force level (N)	2 <sup>nd</sup> Peak occurrence(s)	2 <sup>nd</sup> Peak Force level (N)
AF50 02 First Test	0.35	260	0.5	255
AF50 02 Second Test	0.35	267	0.5	255
AF50 05 First Test	0.39	260	/	/
AF50 05 Second Test	0.5	262	/	/

*Table 14.11: Amplitude, peak occurrence and asymptote of backset for driver seat, hands on the lap*

Subject	Amplitude (mm)	Peak occurrence (s)	Asymptote (mm)
AF50 02 First Test	30	0.52	45
AF50 02 Second Test	35	0.46	65
AF50 05 First Test	20	0.42	61
AF50 05 Second Test	3	/	75

*Table 14.12: Amplitude, peak occurrence and asymptote of T1 x-displacement for driver seat, hands on the lap*

Subject	Amplitude (mm)	Peak occurrence (s)	Asymptote (mm)
AF50 02 First Test	37	0.5	34
AF50 02 Second Test	36	0.56	36
AF50 05 First Test	34	0.44	32
AF50 05 Second Test	29	0.44	28

*Table 14.13: Amplitude, peak occurrence and asymptote of T1 x-velocity for driver seat, hands on the lap*

Subject	Amplitude (mm/s)	Peak occurrence (s)	Asymptote (mm/s)
AF50 02 First Test	228	0.16	1.5
AF50 02 Second Test	200	0.14	1.5
AF50 05 First Test	188	0.2	1.5
AF50 05 Second Test	131	0.34	1.5

Table 14.14: Amplitude of head and neck rotations

Subject	Head rotation (deg)	Neck rotation (deg)
AF50 02 First Test	8	8
AF50 02 Second Test	1.5	3
AF50 05 First Test	14	19
AF50 05 Second Test	15	18

Table 14.15: Amplitude of T1-z displacement for driver seat, hands on the lap

Subject	T1- z displacement (mm)
AF50 02 First Test	6
AF50 02 Second Test	9
AF50 05 First Test	5
AF50 05 Second Test	5

## 14.5 Tables corresponding to differences in kinematics of AM95, AM50, AF50 and AF05

Table 14.16: Peak occurrence and seatbelt force for 1<sup>st</sup> peak in positions 1,2,3,4 in all sizes

Subject	Position 1		Position 2		Position 3		Position 4	
	PO (s)	Force (N)	PO (s)	Force (N)	PO (s)	Force (N)	PO (s)	Force (N)
AM95	0.29	245	0.2	174	0.28	195	0.32	220
AF50	0.27	250	0.22	150	0.21	102	0.22	244
AM50	0.30	245	0.22	145	0.2	110	0.28	250
AF05 01	0.30	245	0.22	167	0.18	84	0.28	257
AF05 03	0.22	110	0.26	181	0.17	96	0.27	225

\*PO= Peak occurrence [s] As= Asymptote[mm] Ap= Amplitude[mm]

Table 14.17: Peak occurrence and seatbelt force for 2<sup>nd</sup> peak in positions 1,2,3,4 in all sizes

Subject	Position 1		Position 2		Position 3		Position 4	
	PO	Force (N)	PO	Force (N)	PO	Force (N)	PO	Force (N)
AM95	0.52	229	0.49	213	0.5	226	0.5	220
AF50	0.47	246	0.51	222	0.51	166	0.47	240
AM50	0.5	250	0.5	200	0.5	110	0.5	247
AF05 01	0.54	240	0.5	222	0.53	86	0.5	271
AF05 03	0.5	185	0.5	230	0.53	85	0.5	220

Table 14.18: Amplitude, peak occurrence and asymptote of backset for positions 1,2,3,4 in all sizes

Subject	Position 1			Position 2			Position 3			Position 4		
	Ap	PO	As	Ap	PO	As	Ap	PO	As	Ap	PO	As
AM95	/	/	23	120	0.45	100	48	0.45	208	60	0.5	90
AF50	24	/	24	120	0.58	74	325	0.6	95	40	0.6	68
AM50	28	0.6	41	220	0.6	28	350	0.66	123	30	0.52	76
AF05 01	23	0.18	4.2	73	0.52	37	295	0.6	108	60	0.34	106
AF05 03	14	0.38	46	66	0.66	46	437	0.66	96	50	0.42	85

Table 14.19: Amplitude, peak occurrence and asymptote of T1 x-displacement for positions 1,2,3,4 in all sizes

Subject	Position 1			Position 2			Position 3			Position 4		
	Ap	PO	As	Ap	PO	As	Ap	PO	As	Ap	PO	As
AM95	13	0.25	10.35	90	0.48	93	45	0.4	49	45	0.45	45
AF50	16	0.38	17	110	0.5	120	240	0.56	245	30	0.45	30
AM50	31	0.45	28	178	0.56	172	250	0.58	258	34	0.44	34
AF05 01	35	0.26	35	80	0.48	79	243	0.56	241	32	0.3	32
AF05 03	27	0.24	27	49	0.28	72	324	0.6	305	45	0.35	45

Table 14.20: Amplitude, peak occurrence and asymptote of T1 x-velocity for positions 1,2,3,4 in all sizes

Subject	Position 1			Position 2			Position 3			Position 4		
	Ap	PO	As	Ap	PO	As	Ap	PO	As	Ap	PO	As
AM95	115	0.16	2	320	0.2	2	245	0.7	1	210	0.2	2
AF50	130	0.16	3	402	0.22	5	840	0.38	5	180	0.12	4
AM50	170	0.2	2	600	0.34	2	790	0.46	2	185	0.16	2
AF05 01	226	0.16	4	400	0.18	7	1000	0.34	1.4	356	0.14	4
AF05 03	300	0.16	4	367	0.16	12	1059	0.46	8	300	0.2	2

\*Ap=Amplitude [mm/s], As=Asymptote [mm/s]

Table 14.21: Amplitude of head and neck rotations

Subject	Position 1		Position 2		Position 3		Position 4	
	HR	NR	HR	NR	HR	NR	HR	NR
AM95	1.7	4	6	8	6	8	3	5
AF50	6	8	10	15	9	13	6	6
AM50	5	7	9	20	5	35	3	5
AF05 01	10	13	11	16	20	32	7	14.5
AF05 03	18	18	25	23	10	30	7	10

\*HR=Head rotation [deg], NR=Neck rotation [deg]

## 14.6 Differences in kinematics of Hybrid III 5<sup>th</sup> percentile, BioRID50F, BioRID-II, THOR NT and Hybrid III 95<sup>th</sup> percentile

All ATDs' kinematics were plotted together for each position in order to compare their responses. In all positions, it is observed that the BioRID-II (50<sup>th</sup> percentile male) and the BioRID50F (50<sup>th</sup> percentile female) show greater head-neck motion compared to HIII 05 (5<sup>th</sup> percentile female) and HIII 95 (95<sup>th</sup> percentile male) that show the lowest head-neck movement. These results were expected since the HIII dummy is unable to reproduce the bending of the thoracic spine as seen in volunteers and PMHS and contributes to a poor head-neck motion of the HIII [app1]. Moreover, BioRID50F, BioRID-II and THOR NT present higher amplitude of T1 kinematics and higher backset reduction in comparison with HIII 05 and HIII 95. This difference may be due to stiffness and rigidity of the thoracic spine of the HIII crash dummy.

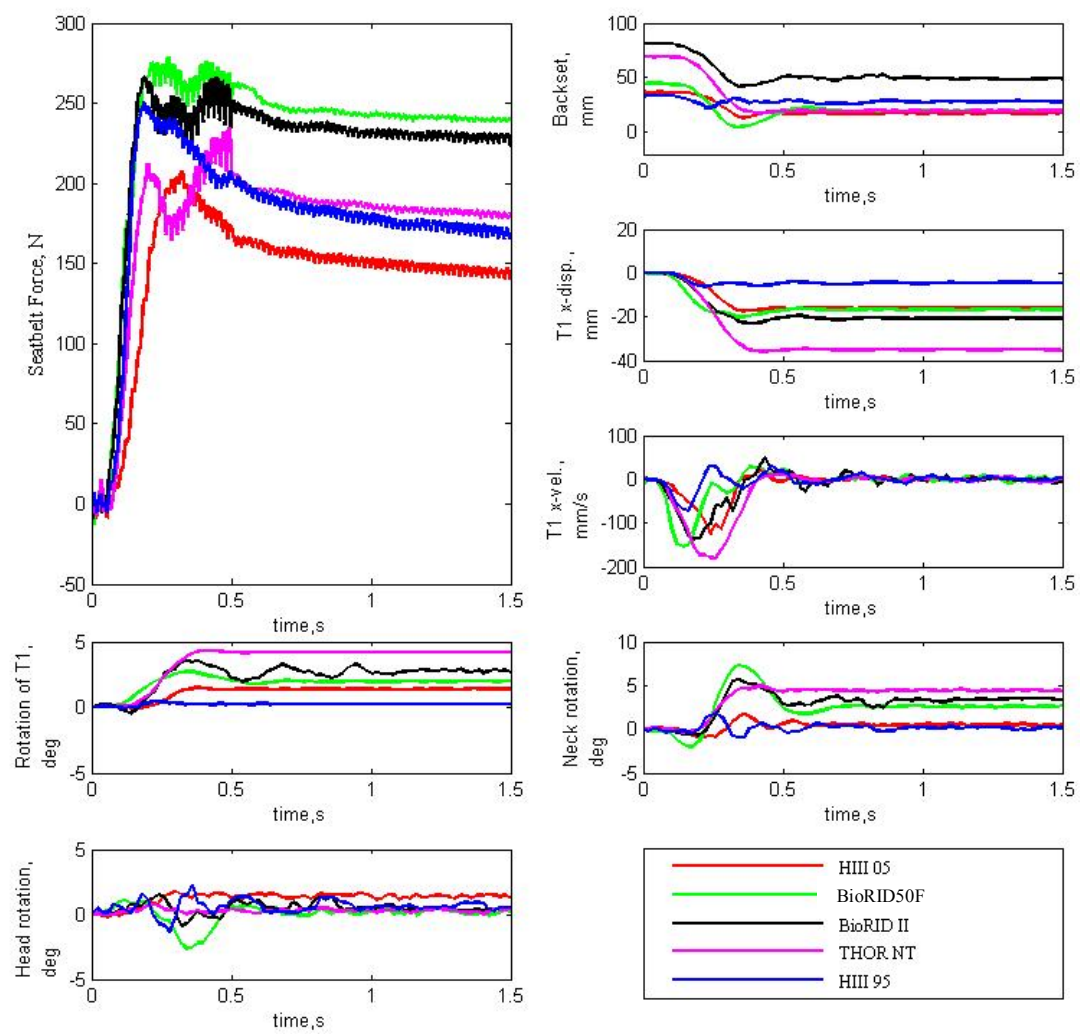


Figure 14.21: Differences in responses between all sizes of ATDs for position 1

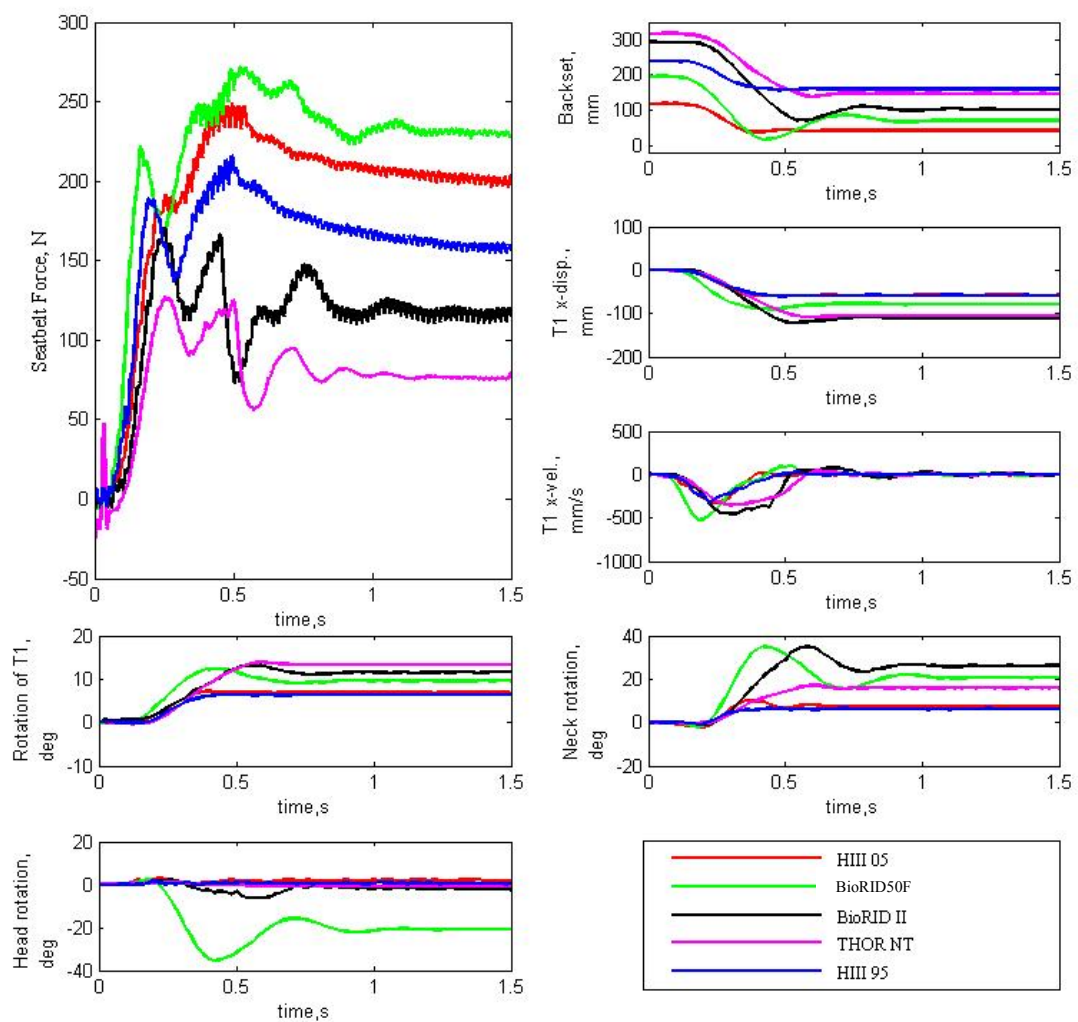


Figure 14.22: Differences in responses between all sizes of ATDs for position 2

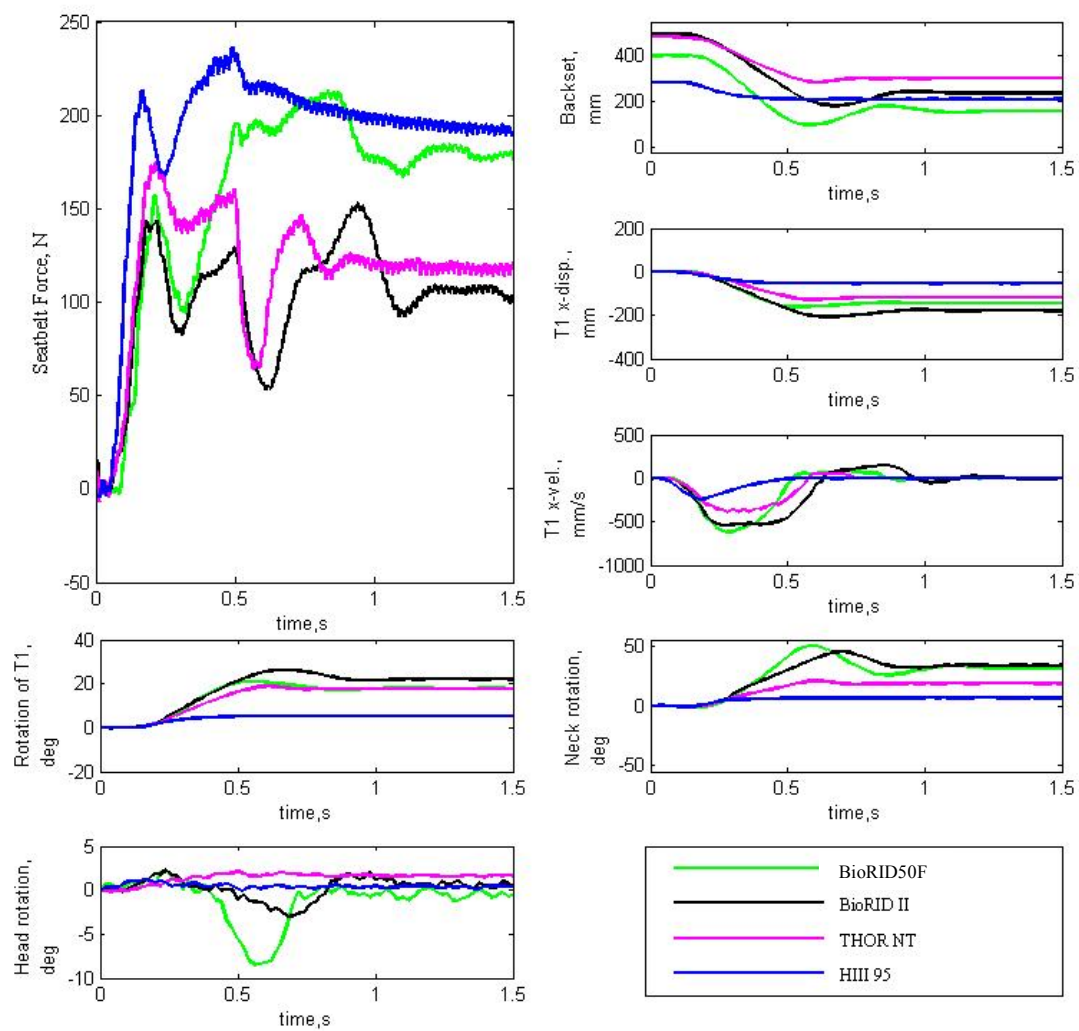


Figure 14.23: Differences in responses between all sizes of ATDs for position 3



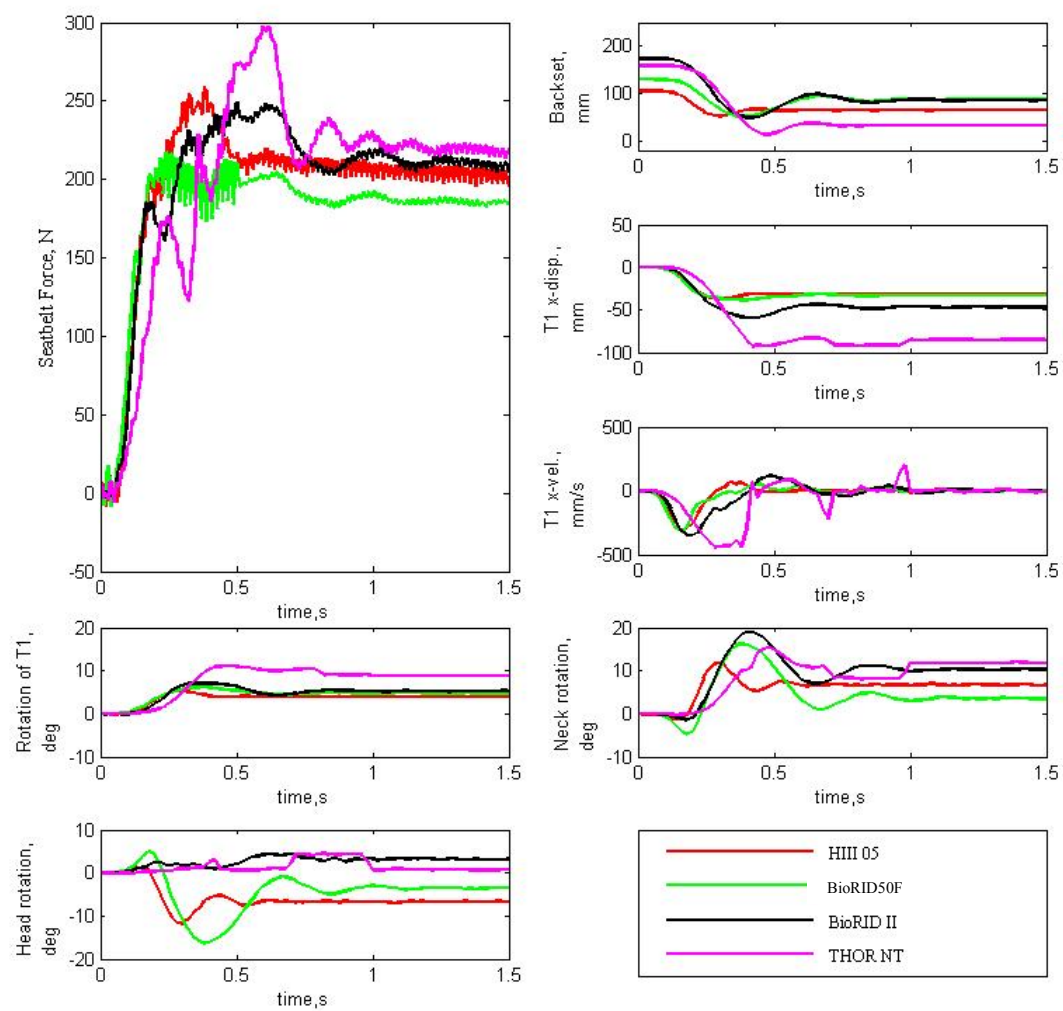
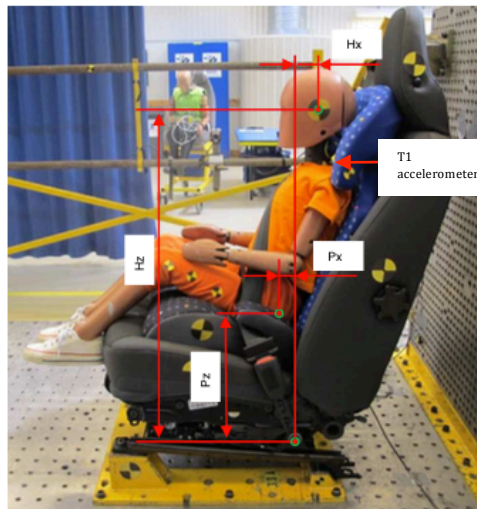


Figure 14.24: Differences in responses between all sizes of ATDs for position 4

## 14.7 Dynamic test setup



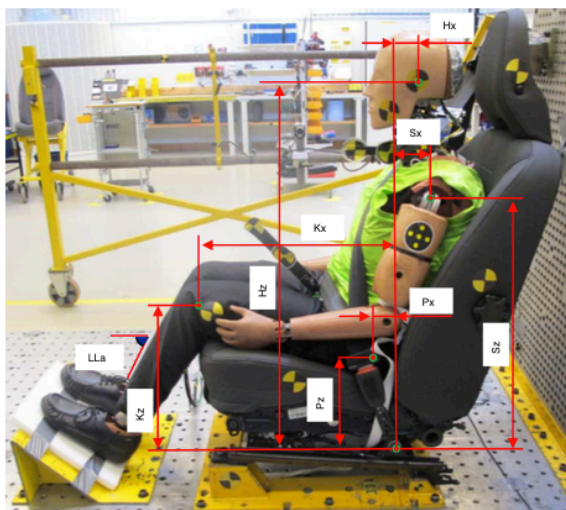
Head – buckle anchor point:  
 $Hx = 50 \text{ mm}$   
 $H_z = 710 \text{ mm}$

Pelvis – buckle anchor point:  
 $Px = 18 \text{ mm}$   
 $Pz = 450 \text{ mm}$

Knee distance:  
 $Ky = 120 \text{ mm}$

Chin – belt ( upper edge)  
 $Bz = 100 \text{ mm}$

*Figure 14.25: H-III6C installation in the sled test*



Head – buckle anchor point:  
 $Hx = 48 \text{ mm}$   
 $H_z = 780 \text{ mm}$

Shoulder – buckle anchor point:  
 $Sx = 65 \text{ mm}$   
 $Sz = 550 \text{ mm}$

Pelvis – buckle anchor point:  
 $Px = 70 \text{ mm}$   
 $Pz = 200 \text{ mm}$

Knee – buckle anchor point:  
 $Kx = 450 \text{ mm}$   
 $Kz = 295 \text{ mm}$

Lower leg angle:  
 $LLa = 59^\circ$

Knee distance:  
 $Ky = 145 \text{ mm}$

Chin – belt ( upper edge)  
 $Bz = 130 \text{ mm}$

*Figure 14.26: BioRID50F installation in the sled test*

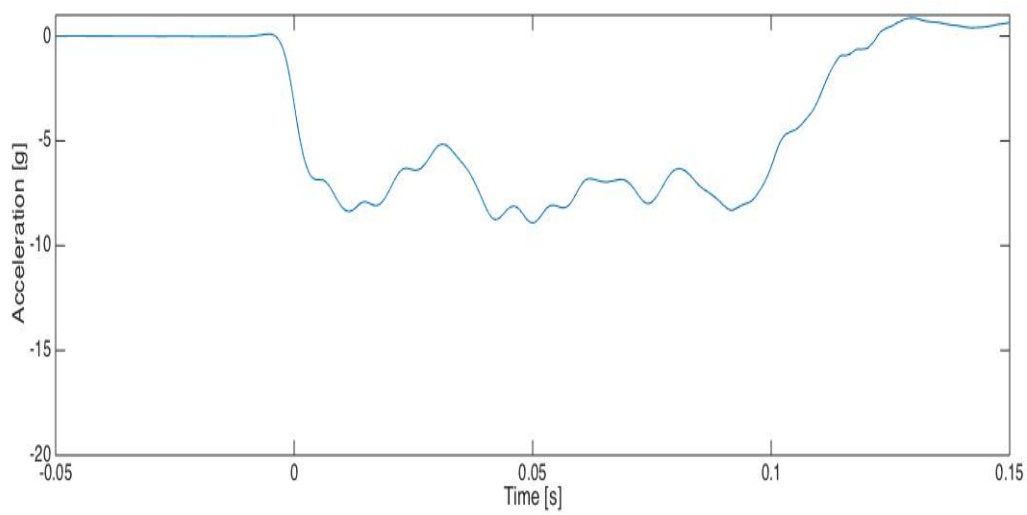


Figure 14.27: Crash pulse with a mean acceleration of 6g and a  $\Delta V$  of 28km/h

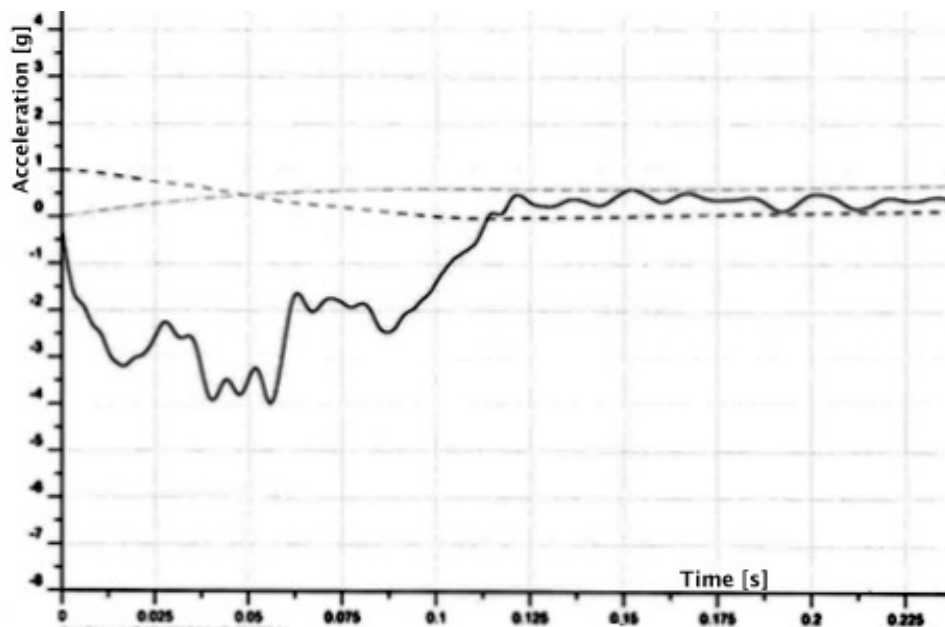


Figure 14.28: Crash pulse with a maximum deceleration of 4g at 56ms and a  $\Delta V$  of 9km/h

## 14.8 Static test setup

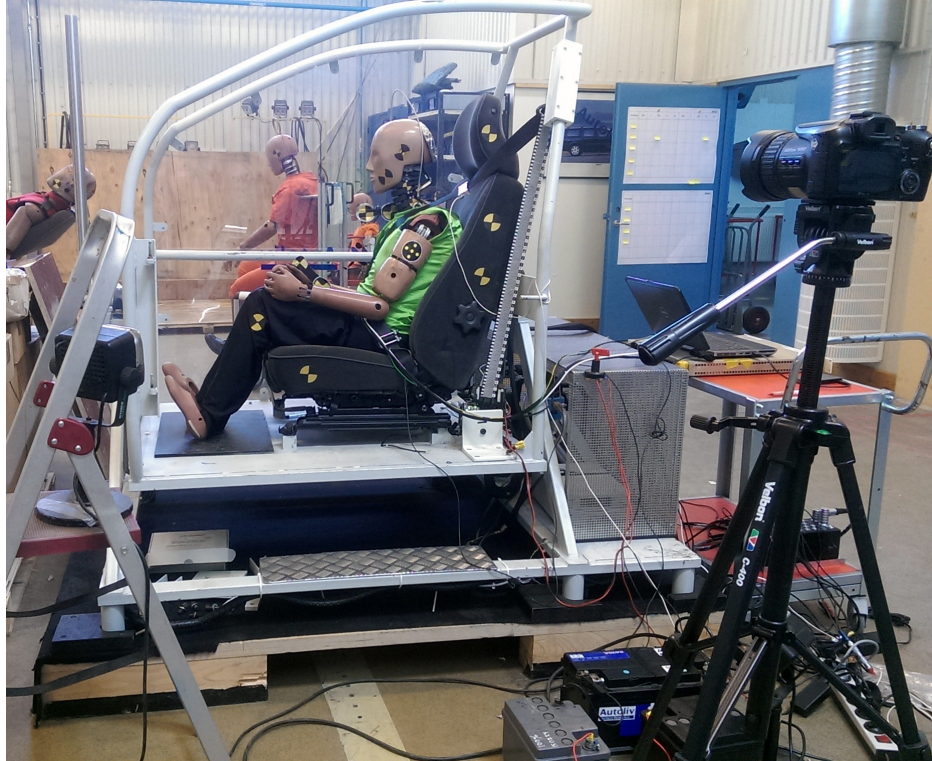


Figure 14.29: BioRID50F installation in the static test rig

## 14.9 T1 x-acceleration and Head x-acceleration plots

### 14.9.1 Dynamic tests

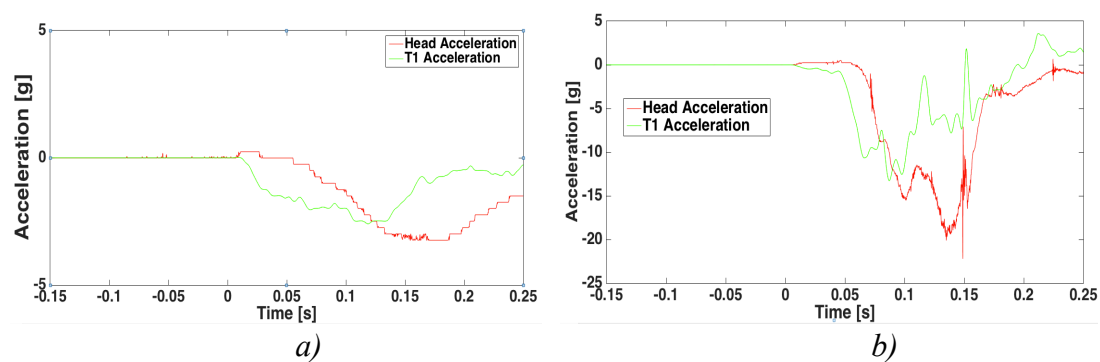


Figure 14.29: a) H-III6C acceleration signals

b) BioRID50F acceleration signals

## 14.9.2 Static tests

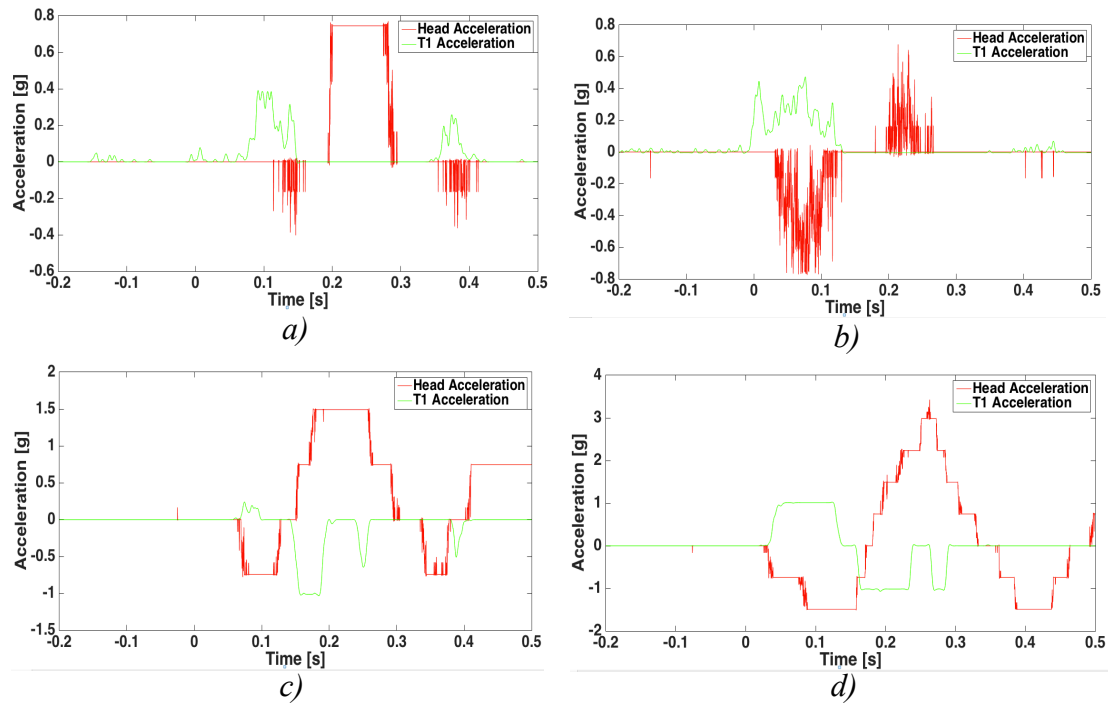
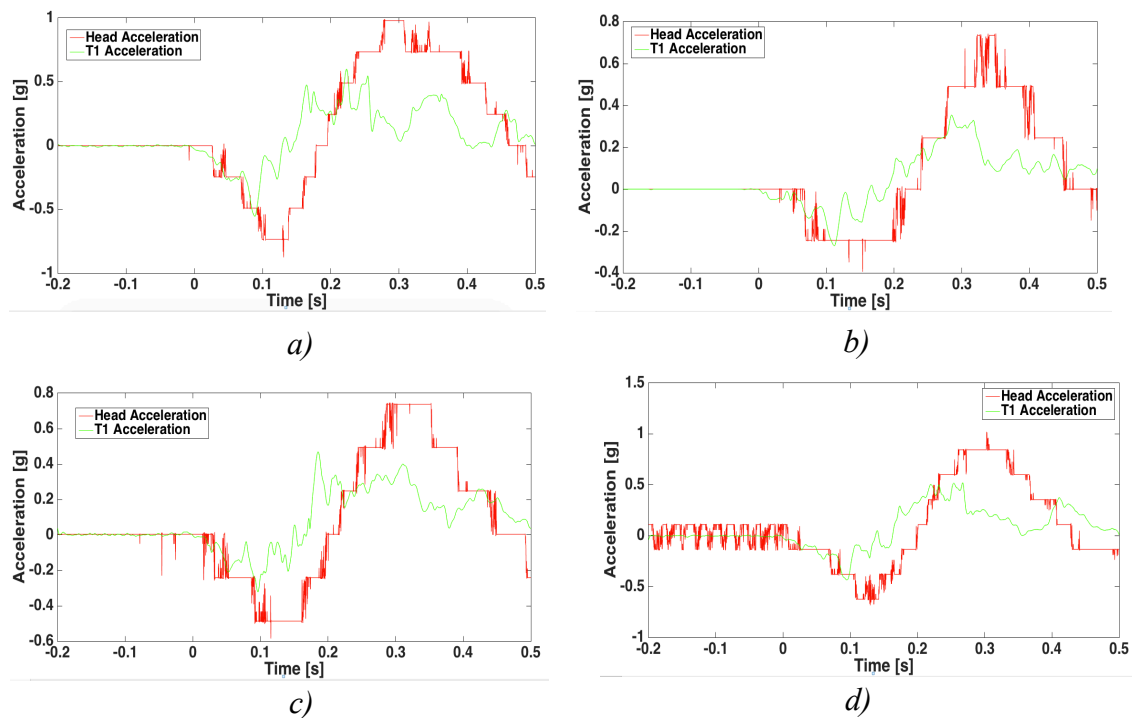
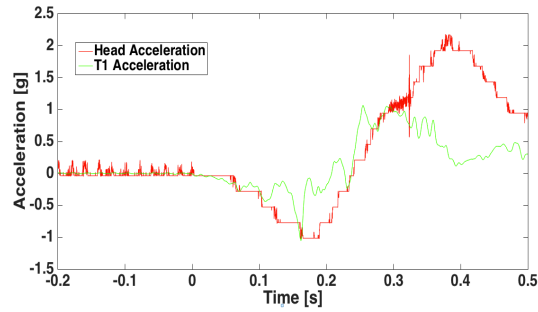


Figure 14.30: H-III6C acceleration signals:

a) seatbelt force 200N b) seatbelt force 370N

c) seatbelt force 544N d) seatbelt force 566N (leaning forward)





e)

Figure 14.31: BioRID50F acceleration signals

- a) seatbelt force 601N      b) seatbelt force 599N  
c) seatbelt force 603N      d) seatbelt force 684N  
e) seatbelt force 614N (leaning forward)

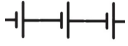
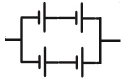
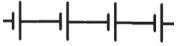
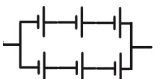
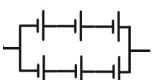
### 14.9.3 $F_x$ , $F_z$ and $MOC_y$ values from static tests

Table 14.22: H-III6C force and moment values

Voltage [V]	Seatbelt force [N]	$F_x$ [kN]	$F_z$ [kN]	$MOC_y$ [Nm]
22	200	0.022	0.007	0.72
22	370	0.014	0.001	0.70
37	544	0.018	0.018	0.99
37 *	566	0.063	0.033	3.48

\*The H-III6C was seated leaning forward

Table 14.23: BioRID50F force and moment values

Voltage [V]	Battery configuration	Seatbelt force [N]	$F_x$ [kN]	$F_z$ [kN]	$MOC_y$ [Nm]
37		601	0.03	0.017	1.77
24		599	0.017	0.027	0.91
50		603	0.023	0.009	1.28
38		684	0.029	0.01	1.58
38*		614	0.032	0.035	2.81

\*The BioRID50F was seated leaning forward (Out of position) with the help of easy tear tap

